

**Neural Correlates of Rhythmic Auditory Stimulation and Rhythmic
Movement: Rate Dependence and Transient to Steady-state Transition**

by

Frederick W. Carver

A Dissertation Submitted to the Faculty of

The Charles E. Schmidt College of Science

In Partial Fulfillment of the Requirements for the Degree of

Doctor of Philosophy

Florida Atlantic University

Boca Raton, Florida

August 2003

UMI Number: 3095021



UMI Microform 3095021

Copyright 2003 by ProQuest Information and Learning Company.

All rights reserved. This microform edition is protected against
unauthorized copying under Title 17, United States Code.

ProQuest Information and Learning Company
300 North Zeeb Road
P.O. Box 1346
Ann Arbor, MI 48106-1346

Neural Correlates of Rhythmic Auditory Stimulation and Rhythmic
Movement: Rate Dependence and Transient to Steady-state Transition

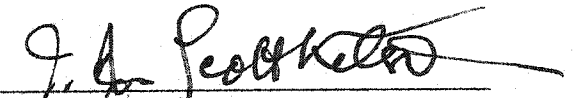
by
Frederick W. Carver

This dissertation was prepared under the direction of the candidate's dissertation co-advisors, Dr. Armin Fuchs and Dr. J. A. Scott Kelso, Program in Complex Systems and Brain Sciences, and has been approved by the members of his supervisory committee. It was submitted to the faculty of The Charles E. Schmidt College of Science and was accepted in partial fulfillment of the requirements for the degree of Doctor of Philosophy.

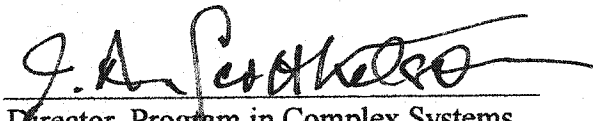
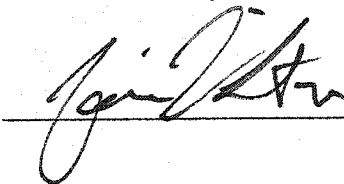
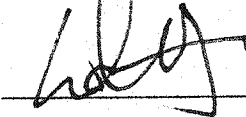
SUPERVISORY COMMITTEE



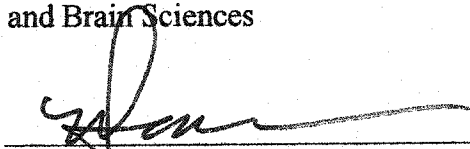
Co-Chairperson



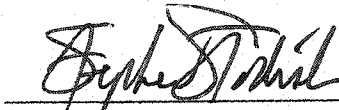
Co-Chairperson



Director, Program in Complex Systems
and Brain Sciences



Dean, The Charles E. Schmidt College of Science



Division of Research and Graduate Studies

18 April, 2003

Date

Acknowledgements

I would like to thank the members of my committee for their advice and assistance with this dissertation. I also wish to express my gratitude for the invaluable guidance from my advisors over the course of my graduate career. Special thanks as well to the entire center family for providing a warm and supportive environment.

Abstract

Author: Frederick W. Carver

Title: Neural Correlates of Rhythmic Auditory Stimulation and
Rhythmic Movement: Rate Dependence and Transient to
Steady-state Transition

Institution: Florida Atlantic University

Dissertation Co-Advisors: Dr. Armin Fuchs and Dr. J. A. Scott Kelso

Degree: Doctor of Philosophy

Year: 2003

The experiments in this dissertation were designed to produce a systematic characterization of the neuroelectric and neuromagnetic correlates of isochronous tone stimulation and simple rhythmic movements over a broad range of rates. The goal was to determine how the cortical representation of rhythm changes with rate, which would provide insight into known rate-dependent differences in perceptual and coordinative abilities. Fundamental transitions in the composition of the auditory and motor responses were hypothesized to occur within the parameter ranges studied here, including the attenuation of major response components and a shift from discrete transient activity at low rates to continuous steady-state activity at high rates. The auditory responses were studied in separate electroencephalography (EEG) and magnetoencephalography (MEG) experiments with stimulation rates ranging from 0.5 to 8Hz. In both studies, a transition

from a transient to a continuous steady-state representation of the tone sequence occurred near 2Hz. In addition, an N1m component of the transient responses disappeared at rates near 8Hz, which may indicate the border beyond which tones are no longer distinct since the response is known to be an index of novelty in the auditory environment. Moreover, in a result important for understanding how evoked activity interacts with activity already present in the cortex, the phase of ongoing 40Hz rhythms is shown to affect the amplitude of the auditory evoked 40Hz response. Rhythmic finger movement was studied using a continuation paradigm in two EEG and MEG experiments at movement rates from 0.5 to 2.5Hz. Major findings included the disappearance of activity associated with movement planning and initiation at rates above 1Hz, suggesting a transition into a steady-state motor response in which there is less direct control of individual movements by the cortex. In addition, the neural correlates of synchronization and continuation were compared, with the results showing a similar cortical organization of metronome-paced and self-paced movements. The attenuation of major response components and the development of continuous steady-state activity within the present parameter ranges indicate rate-dependent changes in the cortical representation of simple rhythms, which are proposed here to relate to known rate-dependent behavioral differences in more complex coordinative environments.

To Priscilla

Table of Contents

| | |
|--|----|
| List of Tables | x |
| List of Figures | xi |
| Introduction | 1 |
| Outline of Experiments | 9 |
| Analysis Techniques | 11 |
| Experiment 1: <i>Spatiotemporal Analysis of the Neuromagnetic Correlates of Rhythmic Auditory Stimulation: Rate Dependence and Transient to Steady-state Transition</i> | 13 |
| 1.1 Introduction | 13 |
| 1.2 Methods | 17 |
| 1.2.1 <i>Subjects</i> | 17 |
| 1.2.2 <i>Procedure</i> | 18 |
| 1.2.3 <i>Data Acquisition</i> | 18 |
| 1.2.4 <i>Data Processing</i> | 19 |
| 1.3 Results: Rate Dependence and Overlap of Long Latency Responses | 21 |
| 1.3.1 <i>Evolution of the Response</i> | 21 |
| 1.3.2 <i>Amplitude of the N1m</i> | 24 |
| 1.3.3 <i>Extent of the N1m in Time and Frequency</i> | 26 |
| 1.3.4 <i>Overlap of Responses to Successive Tones</i> | 33 |
| 1.4 Results: Response Separation using Independent Components Analysis | 37 |

| | | |
|----------------------|---|----|
| 1.5 | Discussion | 41 |
| Experiment 2: | <i>Neuroelectric Activity Associated with Rhythmic Auditory Stimulation: Rate Dependence and the Relationship between Spontaneous and Evoked Activity</i> | 47 |
| 2.1 | Introduction | 47 |
| 2.2 | Methods | 53 |
| 2.2.1 | <i>Subjects</i> | 53 |
| 2.2.2 | <i>Procedure</i> | 53 |
| 2.2.3 | <i>Data Acquisition</i> | 54 |
| 2.2.4 | <i>Data Processing</i> | 54 |
| 2.2.5 | <i>Data Analysis</i> | 55 |
| 2.3 | Results: Rate Dependence and Resonance | 57 |
| 2.3.1 | <i>Evolution of the Response</i> | 57 |
| 2.3.2 | <i>Amplitude of the N1</i> | 60 |
| 2.3.3 | <i>Amplitude of the P2</i> | 61 |
| 2.3.4 | <i>Resonance of the Overall Response</i> | 64 |
| 2.4 | Results: Spontaneous and Evoked Gamma Activity | 70 |
| 2.5 | Discussion | 79 |
| 2.5.1 | <i>Rate Dependence of Response Components</i> | 79 |
| 2.5.2 | <i>Resonance and Response Overlap</i> | 81 |
| 2.5.3 | <i>Spontaneous and Evoked Gamma Activity</i> | 83 |

| | | |
|----------------------|---|-----|
| Experiment 3: | <i>Neuroelectric Activity Associated with Rhythmic Movements: Separation of Overlapping Response Components Using Independent Components Analysis</i> | 86 |
| 3.1 | Introduction | 86 |
| 3.2 | Methods | 91 |
| 3.2.1 | <i>Subjects</i> | 91 |
| 3.2.2 | <i>Procedure</i> | 91 |
| 3.2.3 | <i>Data Acquisition</i> | 92 |
| 3.2.4 | <i>Data Processing</i> | 93 |
| 3.2.5 | <i>Data Analysis</i> | 93 |
| 3.3 | Results | 96 |
| 2.3.1 | <i>Behavior</i> | 96 |
| 2.3.2 | <i>Rate-dependent Evolution of the Response</i> | 96 |
| 2.3.3 | <i>Separate Response Components</i> | 102 |
| 3.4 | Discussion | 107 |
| Experiment 4: | <i>Spatiotemporal Analysis of Neuromagnetic Activity Underlying Rhythmic Movements: Development of the Movement-related Steady-state Response</i> | 114 |
| 4.1 | Introduction | 114 |
| 4.2 | Methods | 118 |
| 4.2.1 | <i>Subjects</i> | 118 |
| 4.2.2 | <i>Procedure</i> | 118 |
| 4.2.3 | <i>Data Acquisition</i> | 119 |
| 4.2.4 | <i>Data Processing</i> | 119 |

| | | | |
|---|------------------------|-------|-----|
| 4.2.5 | <i>Data Analysis</i> | | 120 |
| 4.3 | Results | | 123 |
| 4.3.1 | <i>Behavior</i> | | 123 |
| 4.3.2 | <i>Continuation</i> | | 123 |
| 4.3.3 | <i>Synchronization</i> | | 129 |
| 4.4 | Discussion | | 136 |
| General Discussion | | | 144 |
| Rate Dependence of the Transient Responses | | | 144 |
| Transition into the Steady-state | | | 147 |
| Interaction of Spontaneous and Evoked Activity | | | 150 |
| References | | | 153 |

List of Tables

Chapter 4

| | | |
|-------------|-------|-----|
| 4.1. | | 128 |
|-------------|-------|-----|

Percent of mean variance accounted for by each ICA component

| | | |
|-------------|-------|-----|
| 4.2. | | 136 |
|-------------|-------|-----|

Spatial and temporal correlations between continuation and synchronization components

List of Figures

Chapter 1

| | |
|------|----|
| 1.1. | 20 |
|------|----|

Left: Example of averaged magnetic activity from an N1m response interpolated with a spline of 3rd order and placed over a reconstructed MRI image. White dots represent the positions of the sensors relative to three fiduciary points (nasion, and left and right preauricular points). Light-blue/blue coloring indicates field lines entering the head; in yellow/red regions field lines exit. Right: 2-dimensional polar projection of the same pattern of activity. The nose points to the top of the figure. Bilateral dipolar fields imply activity within both auditory cortices. Sensors colored red were not included in the analyses due to a high noise level.

| | |
|------|----|
| 1.2. | 23 |
|------|----|

Average time series for subject two: one second of data at all stimulation rates from the channel that had the highest overall amplitude in the experiment for this subject. Each time series starts at a tone onset, with dashed lines indicating the onset of succeeding tones. Note that the vertical femto-Tesla scale is different for the columns on the right in order to adjust for the lower amplitudes at higher rates. Hash marks on the horizontal axis indicate 100ms intervals. Black arrows highlight a 150ms subcomponent of the N1m.

| | |
|------|----|
| 1.3. | 25 |
|------|----|

The first mode of the KL decomposition of the peak N1m response patterns at all stimulation rates. The common latency at which the decomposition was performed was determined from the peak response time at the slowest rate. The high λ values beneath each topographic map reflect the large portion of the signal accounted for by the first mode. A linear regression of the amplitudes of the first mode on stimulation ISI revealed high r-squared values. The x-intercepts represent the predicted ISI at which the N1m reaches zero amplitude. The y-axis scale is in arbitrary units produced by the decomposition procedure.

1.4. 28

Results from the cluster analysis procedure applied at all rates and latencies from 35 to 160ms. The top two rows show the patterns corresponding to the cluster centers, and the angle α between them, for all subjects. Below these images are plots showing regions in a latency-rate space where patterns exist that have an angle less than 60° from the cluster centers. The color represents these angles, with shades of blue and red/yellow corresponding to angles from clusters one and two, respectively (see bars at right). A linear interpolation was applied between values at neighboring latencies and rates. Contour lines show the areas within 40° and 20° of the cluster centers (black and white lines, respectively).

1.5. 32

Left: Average topographic maps for 100 and 150ms responses for each subject at a single latency for each response. Rates were included in the average only if they were within the N1m cluster center from figure 1.4. The exact latency used for each average is shown below each map, with the angle α between the spatial patterns indicated above. Right: Time series showing the subpeaks of the N1m at 100 and 150ms at stimulation rates of 0.6Hz (green) and 1.7Hz (blue) from a channel containing a large amplitude N1m response. The separate 150ms response is visible at both rates, but becomes more apparent at the higher rates.

1.6. 36

Average of the projections of the recorded activity from all subjects onto the spatial patterns of their 50ms responses from figure 1.4. Top: An interpolated color image of the projection. The average amplitude of the 50ms response vector is normalized to one, with the maximum amplitude of the projection colored yellow. Any amplitude less than the minimum value on the color scale is colored light blue. The plot is centered at a tone onset, and the borders with the white region on the right and the left indicate the preceding and succeeding tone onsets. The dashed white line at right highlights the 500ms response to the center tone. A dashed line at left tracks the 500ms response to the previous tone, with an arrow indicating the region of interaction between the 500 and 50ms responses. Inset: Amplitudes of the projection at the peak latency of the average 50ms response exhibiting a pronounced peak when the 500ms response interacts with the P1m around 2Hz. Rate is shown on the x-axis, and projection amplitude is on the y-axis. Bottom: Individual plots of P1m amplitudes for all subjects.

| | | |
|------|-------|----|
| 1.7. | | 40 |
|------|-------|----|

ICA decomposition of the N1m response for subjects 2 & 4 at top and bottom, respectively. A single decomposition was performed on the average data from 0 to 320ms latency at the four lowest stimulation rates. The results reveal a separation of the 100 and 150ms components of the N1m. Top: topographic images of the top two modes of the decomposition. Red indicates exiting field and blue is entering field. Bottom: time series of the decomposition at each rate. Tone onset is at left. The red line is the time series of activation for the 100ms component at each rate, and the blue line is the activation pattern for the 150ms response.

Chapter 2

| | | |
|------|-------|----|
| 2.1. | | 59 |
|------|-------|----|

Average time series for subject two: one second of data at all stimulation rates from the channel (Cz) that had the highest overall amplitude in the experiment for this subject. Each time series starts at a tone onset, with dashed lines indicating the onset of succeeding tones. Note that the vertical micro-volt scale is different for the columns on the right in order to adjust for the lower amplitudes at higher rates. Hash marks on the horizontal axis indicate 100ms intervals (the time scale is shown at bottom-right).

| | | |
|------|-------|----|
| 2.2. | | 62 |
|------|-------|----|

The first mode of the KL decomposition of the peak N1 response patterns at all stimulation rates. The common latency at which the decomposition was performed for each subject was determined from the peak response time at the slowest rate. The high λ values beneath each topographic map reflect the large portion of the signal accounted for by the first mode. The y-axis scale is in arbitrary units produced by the decomposition procedure.

| | | |
|------|-------|----|
| 2.3. | | 63 |
|------|-------|----|

The first mode of the KL decomposition of the peak P2 response patterns at all stimulation rates. The common latency at which the decomposition was performed for each subject was determined from the peak response time at the slowest rate. The high λ values beneath each topographic map reflect the large portion of the signal accounted for by the first mode. The y-axis scale is in arbitrary units produced by the decomposition procedure.

2.4a-d. 66-69

KL decomposition applied separately to each stimulation rate for subjects 1-4, respectively. The decomposition was performed on one cycle length of data centered at tone onset. A cycle length for each rate is defined by the inter-stimulus interval. At left for each rate is the spatial mode of the decomposition accounting for the most variance. The eigenvalues are displayed below each mode. Middle: Time series of activation of the top mode, centered at tone onset. A complete single cycle interval of two seconds is shown at 0.5Hz. The same length of time is displayed at all rates, with the time series repeated at higher rates in order to fill out two seconds. Dashed lines indicate tone onsets. Right: Power spectrum for the time series of activation. Green bars indicate the power at the fundamental frequency and higher harmonics in order from left to right (e.g. for a stimulation rate of 1Hz, the bar at left is power at 1Hz, and the succeeding bars are power at 2Hz through 9Hz in order from left to right). The red bar at right highlights frequency doubling of the response by showing the ratio of power at the first harmonic to the fundamental frequency.

2.5. 72

The average mid-latency response for subject 4 at 4.3Hz. One cycle of data is shown centered at tone onset for channel Cz. The raw data was band-pass filtered from 30 to 50Hz prior to averaging. At top and bottom are the topographic patterns of activation at the positive and negative peaks of the response. The positive peak corresponds to mid-latency response Pa, while the negative peak is response Nb.

2.6. 73

ICA mode accounting for the mid-latency response in unaveraged data at 4.3Hz for subject 4. Top: Topographic image of the ICA mode. Red/yellow indicates positive potential distributed throughout the sensors. Middle: Two activation time series of the ICA mode for single tones. Each time series contains gamma oscillations before and after the stimulus. Time is on the horizontal axis centered at tone onset. The vertical axis is amplitude in arbitrary units produced by the decomposition procedure. Bottom: Average of the activation time series showing a gamma response after tone onset with peaks at the same latencies as the mid-latency response in figure 2.5. The mid-latency gamma response makes up the majority of average activity, suggesting that pre-stimulus gamma activity is not phase-locked to the stimulus.

2.7. 75

Top: Phase-sorted time series of the response to each tone for the ICA mode from figure 2.6. The time series are sorted according to the pre-stimulus phase of the gamma

oscillation. Tone onset is indicated by the white dashed line. Amplitude of the response is represented by a red-positive / blue-negative color scale. Pre-stimulus diagonal stripes indicate random phase. Post-stimulus the oscillation is reset to be phase-locked to the stimulus. The lack of activity at bottom-right implies that there is a preferred phase of the pre-stimulus gamma activity for evoking a mid-latency gamma response. Bottom: Average of the single tone-epoch time series, with amplitude in arbitrary units. Tone onset is indicated by the black dashed line.

2.8. 77

Results of the single tone-epoch ICA decomposition for subject 1 at 3.9Hz. Right: Topographic image of the top mode of the decomposition. Top-left: Phase-sorted time series of the ICA mode. The time series are sorted according to the pre-stimulus phase of the gamma oscillation. Tone onset is indicated by the white dashed line. Amplitude of the response is represented by a red-positive / blue-negative color scale. Pre-stimulus diagonal stripes indicate random phase. Post-stimulus the oscillation is reset to be phase-locked to the stimulus. Bottom: Average of the single tone-epoch time series, with amplitude in arbitrary units. Tone onset is indicated by the black dashed line.

2.9. 78

Results of the single tone-epoch ICA decomposition for subject 4 at all stimulation rates. Bottom-right: Topographic image of the top mode of the decomposition. Top-left: Phase-sorted time series of the ICA mode. The time series are sorted according to the pre-stimulus phase of the gamma oscillation. Tone onset is indicated by the white dashed line. Amplitude of the response is represented by a red-positive / blue-negative color scale. Pre-stimulus diagonal stripes indicate random phase. Post-stimulus the oscillation is reset to be phase-locked to the stimulus. Bottom-left: Average of the single tone-epoch time series, with amplitude in arbitrary units. Tone onset is indicated by the black dashed line. Top-right: Phase dependent amplitude of the evoked gamma response. Phase of the pre-stimulus activity is in radians on the vertical axis. Maximum amplitude of the evoked response is on the horizontal axis.

Chapter 3

3.1. 95

- a) Average and standard deviation of relative phase during synchronization in degrees.
- b) Produced rate versus required rate for the continuation phase.

| | |
|----------------|--------|
| 3.2a-d. | 98-101 |
|----------------|--------|

KL decomposition applied separately to each stimulation rate for subjects 1-4, respectively. The decomposition was performed on one cycle of data centered at peak finger flexion. A cycle at each rate is defined by the required inter-response interval. Plotted at left for each rate is the top spatial mode of the decomposition. Eigenvalues are displayed below each mode. At right is the time series of activation of the top mode, centered at the peak of the movement indicated by the dashed line. A complete single cycle interval of two seconds is shown at 0.5Hz. The same length of time is displayed at all rates, with the time series repeated at higher rates in order to fill two seconds. Dashed lines indicate additional movement peaks at higher rates.

| | |
|-------------|-----|
| 3.3. | 105 |
|-------------|-----|

Type I ICA component for all subjects. Left for each subject: Topographic image of the component. Red/yellow represents positive potential; blue/light-blue indicates negative potential. Right-top: Color-coded rate-latency plot of the activation time series of the component at all required movement rates centered at peak flexion, with amplitude in arbitrary units. Bottom: Average of the activation time series across rate shown in red, and an average 1Hz movement profile shown in blue.

| | |
|-------------|-----|
| 3.4. | 106 |
|-------------|-----|

Same as figure 3.3 for the type II component.

Chapter 4

| | |
|-------------|-----|
| 4.1. | 122 |
|-------------|-----|

- a) Average relative phase and standard deviation during synchronization in degrees.
- b) Produced versus required rate and standard deviation for the continuation phase.

| | |
|-------------|-----|
| 4.2. | 125 |
|-------------|-----|

Type I ICA component from the continuation averages for all subjects. Left for each subject: Topographic image of the component. Red/yellow represents exiting field; blue/light-blue indicates entering field. Right-top: Color-coded rate-latency plot of the activation time series of the component at all movement rates. Latency is centered at peak flexion; amplitude is in arbitrary units. Bottom: Average of the activation time series across rate shown in red, and an average 1Hz movement time series shown in blue.

| | | |
|------|-------|-----|
| 4.3. | | 126 |
|------|-------|-----|

Same as figure 4.2 for the type II continuation component.

| | | |
|------|-------|-----|
| 4.4. | | 127 |
|------|-------|-----|

Same as figure 4.2 for the type III continuation component.

| | | |
|------|-------|-----|
| 4.5. | | 131 |
|------|-------|-----|

Same as figure 4.2 for the type I synchronization component.

| | | |
|------|-------|-----|
| 4.6. | | 132 |
|------|-------|-----|

Same as figure 4.2 for the type II synchronization component.

| | | |
|------|-------|-----|
| 4.7. | | 133 |
|------|-------|-----|

Same as figure 4.2 for the type III synchronization component.

| | | |
|------|-------|-----|
| 4.8. | | 134 |
|------|-------|-----|

Same as figure 4.2 for the synchronization N1m component. Latency is centered at tone onset.

Introduction

Rhythms are basic elements of human life, both in terms of how we organize our bodies and how we interact with the world, with examples as far ranging as the beating of the heart, a running gait, and the prosody of speech. Rhythms feature heavily in brain function as well. In addition, human group activities that involve the coupling of auditory and motor rhythms, such as music, marching, and dance, are common to all cultures. In a wide range of behaviors, humans display a clear tendency towards rhythmicity as a means to organize a series of events. Classic examples are our ability to perceive and produce rhythm in poetry and music where the basic elements can be quite complex and the timing between events is relatively variable. In fact, a composer (or performer) can use this tendency to perceive a rhythmic pattern to give expression and tension to a piece of music by varying rhythm beyond our expectations. The development of expectancy is central to both rhythm perception and performance. In order for a drummer to strike at the proper time, he or she must initiate the movement well beforehand. In fact, a common tendency in synchronizing with a metronome is to tap slightly before the event, indicating anticipation rather than reaction (Engström, Kelso, & Holroyd, 1996). So how are rhythmic behaviors organized in the nervous system? Perhaps the simplest mechanism would be an associative or reflex chain where one event in a series triggers the next. However, a large body of research points towards

the existence of higher order representations in which individual elements of the rhythmic sequence are grouped as a whole (see Lashley, 1951; Martin, 1972), although the exact neural mechanism for such a representation is yet to be determined.

Models of rhythmic movements commonly rely on statistical properties of inter-response intervals and linear error correction mechanisms based on the previous response to explain the timing of metronome-paced and self-paced movements (e.g. Vorberg & Wing, 1996; Wing & Kristofferson, 1973). Central to this approach is the presumed maintenance of a temporal interval in memory to which each new interval is compared. However, these models have proven inadequate to explain the full range of dynamic phenomena in rhythmic sensorimotor behavior. For instance, Chen, Ding, and Kelso (1997, 2001) showed that errors in synchronizing with a metronome have long-range correlations, i.e. that the error depends not just on the previous response, but on the entire chain of responses leading up to the present movement. These authors proposed a form of 'dynamic memory' in which timing errors are the result of 'distributed neural processes acting on multiple time scales', instead of (as typically assumed) by a single central clock mechanism. Similar long-range correlations have been observed in a continuation task in which subjects are asked to continue from memory a movement rate that was initiated by synchronization, suggesting that a similar timing mechanism acts in metronome-paced and self-paced movements (Gilden, Thornton, & Mallon, 1995; see also Wing, 1977). Statistical and central clock type models have been proposed for perception of rhythm as well (e.g. Drake & Botte, 1993; Povel & Essens, 1985). However, these models have difficulty accounting for the full range of human abilities to perceive complex rhythmical structures such as found in music. Recently, a dynamical

systems approach to modeling attention to rhythm has proved more successful in capturing key aspects of rhythm perception (Large & Jones, 1999). This approach employs self-sustaining nonlinear oscillators as a model for entraining to rhythms at specific frequencies. Once entrained, the oscillators can reproduce fundamental characteristics of human rhythm perception such as stability in the face of variable stimuli and the formation of periodic expectancies for beat placement.

The dynamic approach to rhythmic and discrete behavior was pioneered in the field of coordination dynamics (see Kelso, 1995), which employs the concepts of self-organization and pattern formation in systems far from equilibrium (Haken, 1977) and the tools of nonlinear dynamical systems. In this field, nonlinear oscillator models have provided a theoretical foundation for the understanding of rhythmic sensorimotor coordination (e.g. Haken, Kelso, & Bunz, 1985; Kelso, DelColle, & Schöner, 1990). A key premise in coordination dynamics is that the collective behavior of a complex system with many nonlinearly interacting components (as in any neuromuscular system) may exhibit its own low dimensional dynamics. Such a system can self-organize into a macroscopic level of organization that can be described in terms of a single collective variable. A classic example is rhythmic bimanual hand coordination, where the dynamics of the system have been shown to be adequately described by the relative phase between the effectors (Kelso, 1984). At movement rates below 2Hz two stable states of bimanual oscillation exist — either in-phase or anti-phase. The anti-phase pattern becomes unstable at higher rates, so that if a subject begins oscillation in an anti-phase pattern they will spontaneously switch to in-phase oscillation with increased movement rate. A similar transition occurs when subjects begin by syncopating a single effector with a

metronome and spontaneously switch to synchronization with increased rate (Kelso et al., 1990). In these experiments movement rate is identified as a control parameter that when systematically varied “drives” the system through a transition in its spatiotemporal dynamics. A transition paradigm is commonly employed in coordination dynamics in order to explore the underlying dynamics of a complex system. Examples of the paradigm include a rate-dependent shift from reaction to anticipation when subjects are instructed to react to metronome beats (Engström et al., 1996), and transitions in categorical speech perception occurring when the time delay between consonants and vowels in simple syllables is reduced (Tuller, Case, Ding, & Kelso, 1994).

If self-sustaining oscillations subserve cortical representations of both rhythm perception and production, then it is natural to expect a certain frequency range across which the oscillations can be maintained. In fact, rhythm perception and rhythmic movement are only possible within frequencies from 0.5 to 10Hz (Fraisse, 1982). The similarity of the frequency range for perception and action suggests a common timing mechanism in the two processes, a hypothesis supported by the fact that both processes have a similar preferred frequency of around 2Hz (Fraisse, 1982).

So what then do we know of the neural correlates of rhythm perception and production? Experiments employing fMRI have revealed a distributed group of cortical and subcortical areas involved in timing behaviors, including the basal ganglia and cerebellum (Jantzen, Steinberg, & Kelso, 2002; Mayville, Jantzen, Fuchs, Steinberg, & Kelso, 2002; Nair, Purcott, Fuchs, Steinberg, & Kelso, 2003; Rao et al., 1997). In addition, a wide body of electroencephalography (EEG) and magnetoencephalography (MEG) literature has revealed transitions in cortical activity associated with the above

mentioned behavioral transitions near 2Hz (Jantzen, Fuchs, Mayville, Deecke, & Kelso, 2001; Kelso et al, 1992; Mayville, Bressler, Fuchs, & Kelso, 1999; Wallenstein, Kelso, & Bressler, 1995), including frequency doubling of the response at a syncope to synchronize transition (Fuchs, Kelso, & Haken, 1992). Recently, some of the observed macroscopic transitions in cortical organization have been successfully modeled with a neural field theory on the level of coupled neural ensembles in the cortex (Jirsa, Friedrich, Haken, & Kelso, 1994; Jirsa, Fuchs, & Kelso, 1998). With rhythmic tone stimulation, large-scale oscillations of cortical potential at low multiples of the stimulation rate have been found at rates above 2Hz, suggesting entrainment of the cortex to the stimulation (Picton, Skinner, Champagne, Kellett, & Maiste, 1987). Most recently, cortical expectancy for tone stimulation has been shown in the form of induced high frequency gamma oscillations occurring pre-stimulus (Snyder & Large, submitted).

Despite these results, much more is left to be understood about the neural correlates of rhythmic auditory stimulation and rhythmic movement, including a detailed determination of the component structure of the cortical response within the rhythmic range of perception and action. The majority of studies of auditory and motor responses in EEG and MEG have employed stimulation and movements separated by several seconds, which are well below the rhythmic range (see for example, Deecke, Grözing, & Kornhuber, 1976; Picton, Hillyard, Krausz, & Galambos, 1974). Cortical responses to stimulation at these rates are termed *transient*, because the activity associated with one event is allowed to die out before the next stimulation occurs. The neurophysiological correlates of stimulation and movement at higher rates are known as *steady-state* responses, and are characterized by continuous activation between events (Regan, 1982,

1989). In the auditory domain, cortical steady-state responses are traditionally studied at stimulation rates above the range perceived as rhythmic (e.g. Galambos, Makeig, & Talmachoff, 1981). The steady-state response to rhythmic movement has been investigated, but typically only at one or two rates at a time (Gerloff et al., 1997, 1998; see Mayville, Fuchs, & Kelso, submitted for an exception).

The goal of this dissertation is to provide a thorough characterization of the neural correlates of rhythmic auditory stimulation and rhythmic movement over a broad range of rates. The intent is to produce a systematic understanding of the cortical representation of rhythm, which in turn can provide insight into the above mentioned behavioral and perceptual differences known to occur at different rates. Four EEG and MEG experiments were performed for this purpose. Each experiment employed a systematic variation of stimulation and movement rate over a parameter range hypothesized to contain a transition from a discrete transient response at low rates to a continuous steady-state response at high rates. The goal was to establish the rate dependence of the transient responses over rates perceived as rhythmic, and to characterize the transition into the steady-state response. Distinct components of the transient responses have been associated with different aspects of the cortical representation of tones and movements. For instance, an N1 component of the auditory response is an index of change in the auditory environment (Näätänen & Winkler, 1999), and a pre-movement Bereitschaftspotential is associated with planning of individual movements (Deecke & Kornhuber, 1978). The question posed here is whether changes in the transient responses occur over the rhythmic rates that may indicate rate-dependent differences in the cortical representation of a rhythmic sequence. A second goal is to determine whether the

continuous steady-state response represents a fundamental reorganization of the response in which transient responses die out and a new continuous oscillation emerges. Such a transition would indicate the disappearance of activity associated with individual tones and movements and the development of a continuous representation of the rhythmic series. In addition, an effort is made here to characterize non-phase locked aspects of the event-related responses in order to determine how evoked activity interacts with ongoing activity in the cortex.

The techniques and tools employed here, EEG and MEG, provide precise millisecond level temporal information about cortical activity. Each technology is primarily sensitive to activity arising from apical dendrites of cortical pyramidal cells aligned perpendicular to the cortical surface, with coactivation of thousands of neurons in an ensemble required to produce an observable level of activity on the order of femtotesla in MEG and microvolts in EEG. MEG is sensitive to the magnetic fields associated with intracellular dendritic currents, whereas EEG picks up electric potentials generated by extracellular return currents. These extracellular currents can be distorted by volume conduction and the process of diffusion through the cerebral spinal fluid, skull, and scalp before reaching the sensors (Nunez, 1981). MEG does not suffer from these problems because of the sensitivity to intracellular currents and the transparency of the skull and surrounding tissues to magnetic fields. However, MEG is primarily sensitive to sources with orientations tangential to the sensors, so responses can be missed that are observable with EEG. Both technologies were employed here because the combination of their different sensitivities provides a more complete picture of the spatiotemporal organization of cortical activity.

As part of the current investigations, new methods will be presented for analyzing large datasets from modern full-head brain imaging systems (61 & 84 channel EEG; 143 channel MEG). Generally up to now traditional EEG and MEG analysis methods have focused on evoked response components in the form of amplitude peaks in averaged single channel time series. One weakness of these techniques is that evoked components can overlap at the sensors, causing a peak in a single channel to be mistaken as a single response, when it actually represents the combination of several. Another disadvantage is the reliance on averaging in order to separate event-related responses from background activity, as this technique requires stationarity of the responses and ignores activity that is not phase-locked to the event. The methods presented here overcome these weaknesses by taking advantage of the spatial information provided by modern high-density sensor arrays. Spatiotemporal analysis techniques such as cluster analysis, Karhunen-Loève decomposition, and independent components analysis are employed for this purpose. The common characteristic of each method is to treat each evoked response component as a characteristic spatiotemporal pattern across all the sensors. This allows for separation of temporally overlapping responses based on their spatial patterns, and for detection of low amplitude responses in averaged and unaveraged data based on coherence across sensors. These methods are further adapted to analyze not only large sensor arrays, but also by the broad parameter ranges in the present studies. The focus is on analyzing all experimental conditions as a whole in order to track the spatiotemporal evolution of response components across a wide range of stimulation and movement rates. For this purpose, data compression techniques are developed for extracting relevant information from large datasets.

Outline of Experiments

Chapter 1 presents an MEG study of the neural correlates of rhythmic auditory stimulation that was collected in Vienna, Austria using a 141 SQUID array full-head system. Each trial in the study consisted of rhythmic tone stimulation at one of twenty-seven stimulation rates from 0.6 to 8.1Hz. Significant findings include discovery of a linear relationship between the amplitude of the dominant N1m component of the evoked response and the rate of stimulation. The response decreases with increased stimulation rate, and is predicted to disappear at a rate of 10Hz. In addition, the continuous steady-state response is shown here to result from overlap between the transient responses to neighboring tones. The steady-state response begins near a stimulation rate of 2Hz.

Chapter 2 presents an EEG study of the neural correlates of rhythmic auditory stimulation. The experiment was performed using our 61 and 84 channel EEG systems, with 23 stimulation rates from 0.5 to 4.9Hz in 0.2Hz steps. The results of the experiment enhance those of the previous MEG study by showing that the onset of the steady-state response near 2Hz is associated with resonance of cortical activity at the stimulation rate. In addition, evoked components not visible in MEG are studied, including the P2 response at 200ms past tone onset, and the mid-latency response, which is a brief 40Hz oscillation occurring just after tone onset. An independent components analysis procedure is used to determine the relationship between the evoked 40Hz response and ongoing 40Hz activity in unaveraged data.

Chapter 3 presents an EEG study of rhythmic movement. A continuation paradigm was used to pace right index finger flexion at 21 movement rates from 0.5 to

2.5Hz in 0.1Hz steps. Each trial began with subjects synchronizing movement with an auditory metronome for 20 tones, after which they continued moving at the required rate for approximately 20 more movements. Averages of the continuation phases were analyzed in order to characterize the rate-dependent evolution of the movement-related response without metronome interference. Results indicate a fundamental reorganization of the cortical response highlighted by the disappearance of activity associated with the planning of individual movements. The movement-related steady-state response at high movement rates is shown to be a simplification of the motor response seen at low rates, caused by a decrease in pre-movement slow-wave activity and the persistence of proprioceptive movement-evoked responses.

Chapter 4 presents an MEG study of rhythmic movement using the same continuation paradigm as in the EEG study. A parameter range of 21 rates from 0.5 to 2.5Hz with 0.1 steps was also employed in this experiment. The results are similar to the EEG study, with the major finding being a reduction of pre- and post-movement activity at high rates. Above 1.5Hz the response primarily consists of the series of movement-evoked responses occurring during and just after the movement. In previous studies, these responses were assumed to have a high degree of spatial and temporal overlap. Here we confirm this hypothesis by using independent components analysis to separate the movement-evoked responses into separate spatiotemporal patterns of activity. In addition, analysis of the synchronization phases of the continuation paradigm reveal the same set of movement-related responses as in continuation, indicating no fundamental differences in the cortical organization of metronome-paced versus self-paced movements.

Analysis Techniques

As mentioned above, the research presented here utilizes a number of spatiotemporal analysis techniques in order to separate evoked responses from overlapping activity in averaged and unaveraged data. Among the most important of these methods are Karhunen-Loève (KL) decomposition and independent components analysis. KL decomposition, which is also known as principal components analysis, is a method for rewriting a spatiotemporal pattern as a sum of spatial basis vectors multiplied by time dependent amplitudes. This is done according to the formula:

$$H_k(t) = \sum_{i=1}^N \xi_i(t) \psi_k^{(i)}(x) \text{ where } k \text{ is the spatial location of each sensor, and } t \text{ is time treated}$$

here as continuous for simplicity of notation. If N is equal to the number of sensors, then the spatiotemporal pattern $H_k(t)$ can be reconstructed exactly. However, the KL decomposition is constructed so that the first $M < N$ vectors will produce the maximum possible reconstruction of the original signal. The spatial vectors $\psi^{(i)}$ are the eigenvectors of the covariance matrix $C_{ij} = \int h_i(t)h_j(t)dt$ where $h_i(t)$ is the time series at sensor location i with the mean removed. The eigenvectors form an orthogonal basis for the dataset that removes second order correlations from the time series.

Independent components analysis (ICA) is similar to KL decomposition in that the goal is to separate the data into a set of fixed spatial patterns with time dependent amplitudes. However, ICA removes higher order correlations, and the spatial patterns are not restricted to being orthogonal to each other. The InfoMax ICA algorithm employed

here uses a single-layer feed forward neural network to separate a dataset into statistically independent components (Bell & Sejnowski, 1995). Given a data matrix x , with each row a time series for a single channel, stochastic gradient ascent is used to find a weight matrix W that maximizes the entropy of outputs u , where $u = Wx_s$ with x_s equal to the sphered input data x ($x_s = Sx$, where $S = 2\langle xx^T \rangle^{-1/2}$). The columns of the inverse matrix $(WS)^{-1}$ are the spatial patterns of the independent components at the sensors, and the rows of the output matrix u are the time series of activation for each component. The InfoMax algorithm was recently extended by Lee, Girolami, and Sejnowski (1999) to achieve optimal separation of both subgaussian and supergaussian components.

**Experiment 1: *Spatiotemporal Analysis of the Neuromagnetic
Correlates of Rhythmic Auditory Stimulation: Rate Dependence and
Transient to Steady-state Transition***

1.1. Introduction

The presentation rate of a series of simple tone or click stimuli is well known to systematically affect the human brain response recorded with electroencephalography (EEG) and magnetoencephalography (MEG). The auditory responses investigated by the majority of studies can be grouped into one of two general categories: transient and steady-state. Transient responses are so-named because they are elicited by a series of tones separated by sufficient time to allow for the neural activity to each tone to return to baseline prior to the onset of the next tone. In addition, a randomized inter-stimulus interval is often employed in this type of study to avoid anticipation by the subject and to minimize the cumulative effect of any overlap of late and early responses across stimulus presentations. Since auditory evoked responses can last for over 300ms (Picton, Hillyard, Krausz, & Galambos, 1974), inter-stimulus intervals (ISIs) on the order of seconds are typically required for these studies. Steady-state responses (SSRs), on the other hand, are recorded at much higher stimulation rates and with constant ISIs, so as to produce continuous activation between successive stimulus events. A large amount of the work on steady-state activity has focused on the 40Hz steady state response, a near sinusoidal response elicited in humans by auditory stimulation near 40 Hz (Azzena et al., 1995;

Galambos, Makeig, & Talmachoff, 1981; Gutschalk et al., 1999; Hari, Hämäläinen, & Joutsiniemi, 1989; Stapells, Linden, Suffield, Hamel, & Picton, 1984). Because of the large amplitude response in human EEG to stimulation at this frequency, this 40 Hz SSR has drawn considerable attention, both as a subject of study and as a research tool, with competing theories having been proposed to explain its origin (see for example Gutschalk et al., 1999; Hari et al., 1989; Pantev, Roberts, Elbert, Roß, & Wienbruch, 1996). Regan (1989) defines the 'ideal steady-state' as a response 'whose constituent frequency components remain constant in amplitude and phase over an infinitely long time period', implying a sustained oscillation at a single frequency or a small group of frequencies. The 40Hz auditory SSR is a classic example of such an ideal response. Here, we will use the more general definition of the SSR given in Regan (1982) since it provides a clearer definition of the border between transient and steady-state activity. By this definition, the transition from a transient to a steady-state response occurs when the ISI becomes short enough to cause overlap between the transient responses to successive tones, thus producing a continuous evoked response. Since transient responses can last over 300ms, the transition from transient to steady-state should occur at stimulation rates between 2 and 5Hz. These rates have not been systematically investigated since they fall between those typically used to evoke transient or steady-state responses. In this experiment we used magnetoencephalography to study the range of stimulation rates containing the hypothesized transient to steady-state transition. Our goal was to determine the onset of the SSR and describe changes in the evoked responses that occur as discrete cortical responses begin to interact.

Compared to the steady-state response, the origin of the transient response is relatively well understood. In EEG and MEG the response consists of a series of electric potentials or neuromagnetic fields that begin soon after tone onset. These were first recorded with EEG, and divided into three response epochs: the so-called early, middle and long latency responses (Picton et al., 1974). The early components, also known as brainstem evoked responses, are subcortical in origin and occur within 10ms of tone onset. These are followed by cortical mid-latency responses (MLRs), which occur between 10 and 50ms. Cortical components that peak after 50ms are referred to as long latency responses (LLRs), and are characterized by longer durations and higher amplitudes than the MLRs. The most prominent long latency response is a negative wave near 100ms, commonly referred to in the EEG literature as the N100 or N1. The term N1m refers to the corresponding magnetic field recorded at a similar latency using MEG. Because of its large amplitude, the N1/N1m complex has received the most experimental attention of the evoked responses (for reviews see Näätänen & Picton, 1987; Woods, 1995). This research has revealed that the N1 consists of several separate components with different latencies and source locations (e.g. Loveless, Levänen, Jousmäki, Sams, & Hari, 1996; for a discussion see Näätänen & Winkler, 1999). The main N1m component, which peaks at around 100ms, is thought to originate in supratemporal auditory cortex along Heschl's gyrus (see Pantev et al., 1995 for specific tonotopy of the response).

Like most long latency responses, the amplitude of the N1 is known to depend on the presentation rate of the auditory stimuli. Several experiments have studied the rate dependency of the N1 response using inter-stimulus intervals on the order of one to

several seconds (Hari et al., 1982; Lü, Williamson, & Kaufman, 1992; Sams, Hari, Rif, & Knuutila, 1993). In general, they report that the amplitude of the N1 decreases with increased presentation rate. However, in these studies the stimulation rates were too slow to allow for a comprehensive investigation of how this amplitude decrease may be related to the transition from a transient to a steady state response. One intention of the current experiment was to study the effect of rate on the N1m over a behaviorally relevant higher range of stimulation rates. For this purpose, and for the purpose of observing the transient to steady-state transition, we used rhythmic tone stimulation from 0.6 to 8.1Hz, a parameter range over which the N1m has not been systematically examined. Based on preliminary EEG work (Carver, Fuchs, Mayville, Davis, & Kelso, 1999), we hypothesized that we would observe the near disappearance of the N1 response within this range of frequencies, which would be at a lower rate than predicted by previous models (Lü et al., 1992). This parameter range is scientifically important not only because it encompasses those rates at which transients become steady states, but also because it contains most of the rates over which isochronous stimuli are perceived as being rhythmic (Fraisse, 1982). In addition, qualitative transitions in the ability of subjects to coordinate rhythmic hand movements with a metronome are also known to occur within this range in both behavior (Kelso, DelColle, & Schöner, 1990) and brain (Fuchs, Kelso, & Haken, 1992; Kelso et al., 1991; Kelso et al., 1992; Mayville et al., 2001; Wallenstein, Kelso, & Bressler, 1995).

The predicted low amplitude of the long latency responses at higher stimulation rates and the potential for interference between responses to successive tones makes it difficult to analyze the auditory responses within the present range of rates. Here we

overcome these problems by employing analysis techniques that take advantage of the high degree of spatial information provided by a full-head 141 sensor MEG system. These methods include principal components analysis (also known as Karhunen-Loève decomposition) and *k*-means cluster analysis. Our results show a linear decrease of the N1m amplitude as the ISI decreases over the range of frequencies, with a predicted disappearance of the response at a stimulation rate between 6 and 10Hz. The N1m attenuation also has effects on the spatiotemporal dynamics of the overall activity from responses close to the N1m, which become apparent as the amplitude of the N1m decreases at higher stimulation rates. We also show the development of interaction between activity elicited by successive tones, which marks the transition point between the transient and steady-state responses. As evidence for this transition, we show interference between the last long latency response at 500ms and the evoked response to the following tone.

1.2. Methods

1.2.1. Subjects

Four subjects (one female and three males) participated in the experiment. Their ages ranged from 26 to 33. All participants reported being right-handed. The experiment was conducted in compliance with all standards of human research outlined in the Declaration of Helsinki as well as by the Institutional Review Board. Informed consent was obtained from each participant prior to MEG recording. All subjects reported normal hearing. Audiometry was not performed.

1.2.2. Procedure

Subjects were seated inside a magnetically shielded room (Vacuum Schmelze, Hanau) with their heads held firmly within the dewar. Auditory stimulation was delivered binaurally through plastic headphones at an individually adjusted volume that each subject reported to be comfortable. Subjects were asked to attend to the auditory stimulation while fixing their gaze at a point two meters in front of them. They were further instructed to minimize all extraneous eye or body movements during the recordings. The experiment consisted of separate trials during which subjects listened to a series of tones presented at a constant rate of stimulation. Each series contained 40 1kHz tones, with each tone lasting for 60ms at a constant amplitude with infinite rise and fall times. Twenty-seven stimulation rates were used in the experiment, ranging from 0.6 to 8.1Hz (see Figure 1.2 for the complete list of rates). Step sizes between rates ranged from 0.1 to 0.8Hz with larger steps at higher rates. Each rate was presented in at least four separate trials, providing a minimum of 160 cycles for averaging. The trial order was randomized across subjects.

1.2.3. Data Acquisition

MEG activity was recorded using a full-head magnetoencephalograph (CTF Inc., Port Coquitlam, BC) comprised of 141 SQuID (superconducting quantum interference device) sensors distributed homogeneously across the scalp. Figure 1.1 (left) shows the approximate locations of the sensors relative to the head of a sample subject. A coordinate system for each subject's head was defined with respect to three fiduciary points: the nasion, and left and right preauricular points. The three-dimensional locations

of these points in the sensor coordinate system were measured prior to each experiment. Conversion to third-order gradiometers was performed in firmware using a set of reference coils (Vrba, Cheung, Taylor, & Robinson, 1999). MEG and stimulus signals were band-pass (0.3-80Hz) and notch filtered (50 and 100Hz – the European line frequency and its harmonic) prior to being digitized at a rate of 312.5Hz.

1.2.4. Data Processing

Separate ensemble averages of single stimulation cycles were calculated for each stimulation rate. Each cycle was centered at tone onset, and the duration was equal to the inter-stimulus interval. The MEG signals were manually inspected for artifacts before averaging, and any cycle with contaminations was discarded. The first two cycles from each trial were also excluded from the final average in order to avoid transients. Topographical mapping of the resulting average evoked fields was performed using a polar projection of the three-dimensional sensor coordinates into two-dimensional space. A spline of 3rd order was used to interpolate activity between sensor positions. Figure 1.1 (right) shows an example of this projection for an N1m response at 100ms latency. Blue coloring in figure 1.1 represents magnetic field lines entering the head, with light blue indicating the strongest radial components of the field. Exiting field lines are indicated by red/yellow coloring, with yellow representing the highest amplitude. As expected for an N1m response, figure 1.1 shows dipolar-like activity patterns over both auditory cortices. Due to a high noise level, 30 sensors at mostly posterior locations were not included in the data analyses (see Figure 1.1 for locations). This left a total of 111

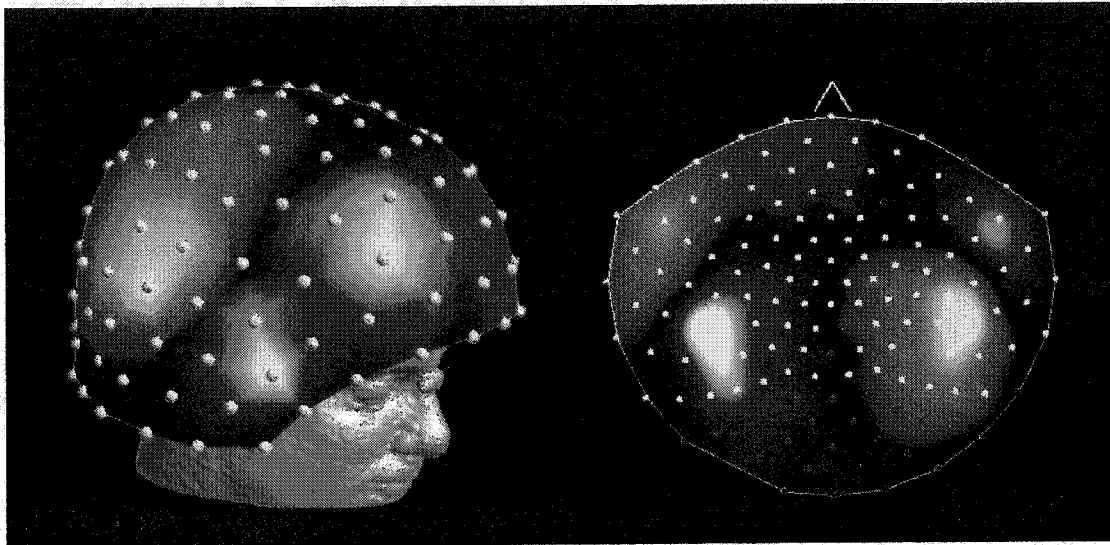


Figure 1.1. Left: Example of averaged magnetic activity from an N1m response interpolated with a spline of 3rd order and placed over a reconstructed MRI image. White dots represent the positions of the sensors relative to three fiducial points (nasion, and left and right preauricular points). Light-blue/blue coloring indicates field lines entering the head; in yellow/red regions field lines exit. Right: 2-dimensional polar projection of the same pattern of activity. The nose points to the top of the figure. Bilateral dipolar fields imply activity within both auditory cortices. Sensors colored red were not included in the analyses due to a high noise level.

channels, but did not create a significant loss of information since most auditory events are seen over frontal, temporal, and central regions.

1.3. Results: Rate Dependence and Overlap of Long Latency Responses

1.3.1. Evolution of the Response

Figure 1.2 shows time series of the averaged auditory evoked responses from subject two. The single channel displayed at all stimulation rates was over right temporal cortex and recorded this subject's highest absolute amplitude of any sensor during the entire experiment. The time series show one second of averaged data starting at tone onset. Predictably, the highest amplitude in the time series occurs during the N1m response at the lowest stimulation rate. As stimulation rate increases, the amplitude of the N1m decreases systematically. In fact, by 2.1Hz the N1m is no longer the most dominant response. At this rate a response at 50ms of opposite polarity has the highest amplitude. Another feature of the rate-dependent N1m evolution is a subpeak of the response near 150ms latency that only appears after the large 100ms peak has begun to reduce (see arrows in the figure). We will show evidence that this represents a separate subcomponent of the N1m. We will also quantify the rate dependence of the N1m and study how the response interacts with temporally adjacent responses. In terms of the overall character of the response, at low stimulation rates magnetic activity returns to base line level before the next tone onset. This is consistent with a transient response to each tone. However, as rate increases above 2Hz, activity is still present at the onset of the next tone. At the higher stimulation rates, the time series show continuous activity between tones, indicative of a steady-state response. We will characterize the rate-

Figure 1.2. Average time series for subject two: one second of data at all stimulation rates from the channel that had the highest overall amplitude in the experiment for this subject. Each time series starts at a tone onset, with dashed lines indicating the onset of succeeding tones. Note that the vertical femto-Tesla scale is different for the columns on the right in order to adjust for the lower amplitudes at higher rates. Hash marks on the horizontal axis indicate 100ms intervals. Black arrows highlight a 150ms subcomponent of the N1m.

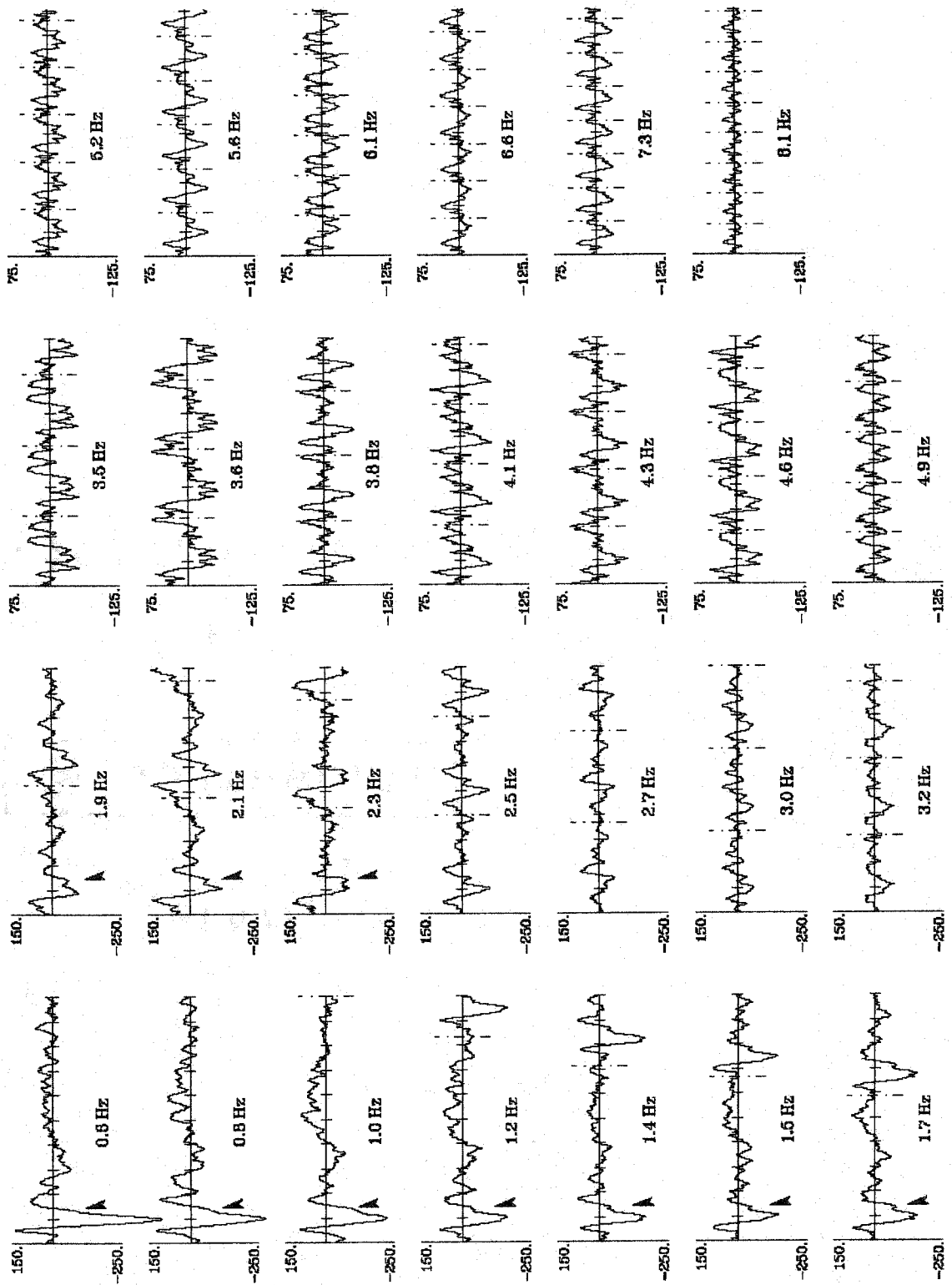


Figure 1.2

dependent transition between the transient and steady-state responses in terms of the onset of overlap between neural activity evoked by successive tones.

1.3.2. Amplitude of the N1m

We first analyzed how the amplitude of the dominant N1m auditory response depends on the rate of stimulation. The latency of the peak of the response was determined by the highest absolute amplitude in any sensor at 0.6Hz, which turned out to be either 99.2 or 102.4ms for all participants – a difference of only one sampling interval. In the following analyses we used these times as an estimate for the latency of the N1m at all stimulation rates because as rate increased the N1m became difficult to distinguish from background activity and neighboring responses (see Figure 1.2). In order to justify the use of one latency at all rates, we checked for any significant shift in latency at stimulation rates up to 2Hz. This frequency was chosen as a cut-off since it was the highest stimulation rate at which the N1m was still identifiable based on amplitude alone. T-tests for each subject revealed that the mean of the latencies between 0.8 and 1.9Hz were not significantly different from the latencies originally determined at 0.6Hz, indicating no temporal shift of the N1m ($t(6) = -2.1, -0.3, 1.5, 0.0$ (two-tailed) for subjects 1-4 respectively). The means for each subject (with SD in parenthesis) were 101.0 (1.71), 98.3 (7.09), 103.8 (8.02), and 102.4 (1.85).

As mentioned earlier, at the higher stimulation rates used in our study the amplitude of the brain signal at 100ms was very low, which made the response difficult to observe in single channels. To overcome this problem, we treated the N1m response as a characteristic spatial pattern of activity based on all good sensors, and tracked the

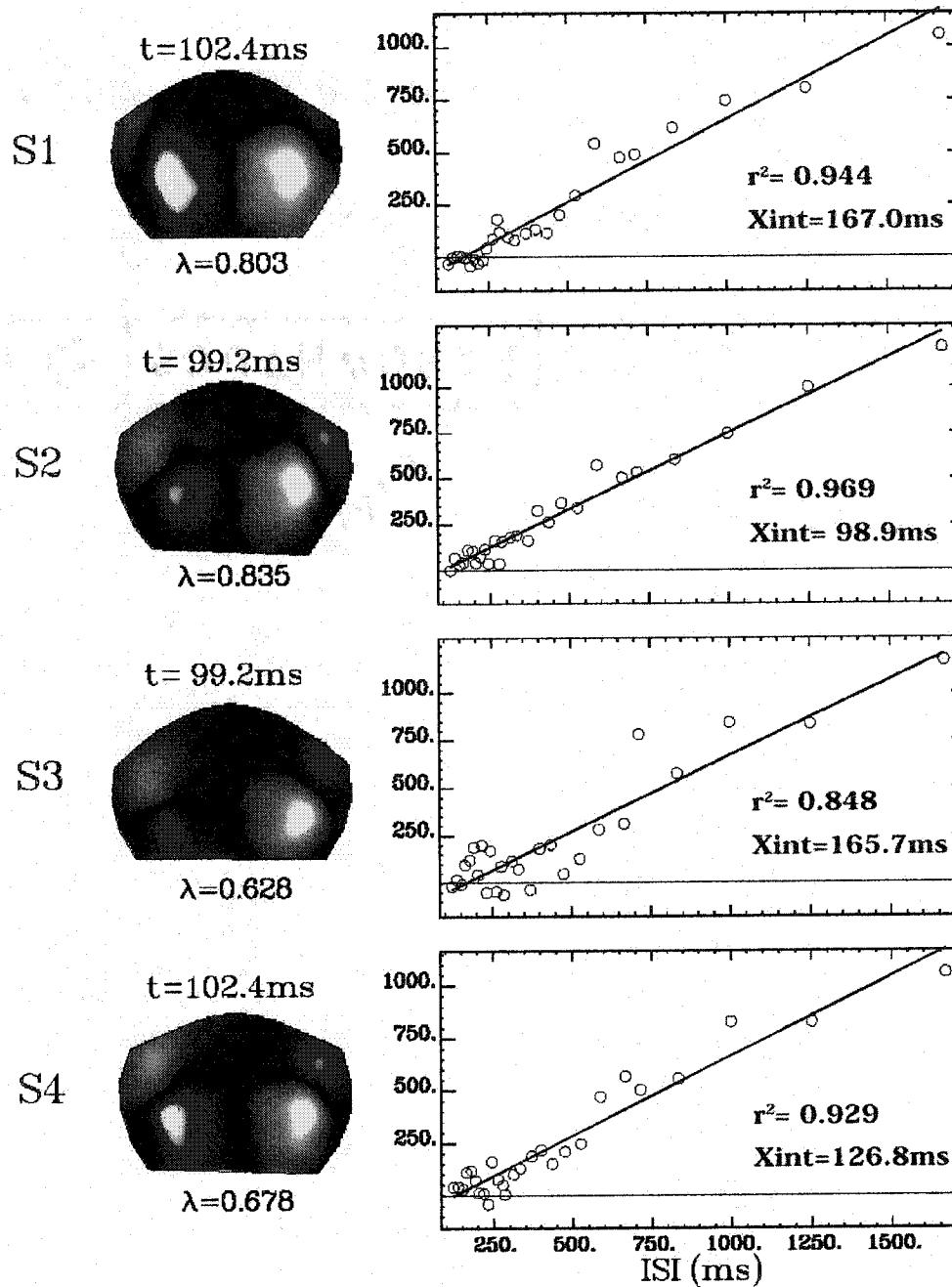


Figure 1.3. The first mode of the KL decomposition of the peak N1m response patterns at all stimulation rates. The common latency at which the decomposition was performed was determined from the peak response time at the slowest rate. The high λ values beneath each topographic map reflect the large portion of the signal accounted for by the first mode. A linear regression of the amplitudes of the first mode on stimulation ISI revealed high r -squared values. The x-intercepts represent the predicted ISI at which the N1m reaches zero amplitude. The y-axis scale is in arbitrary units produced by the decomposition procedure.

amplitude of this pattern across stimulation rate. For this purpose, we applied a Karhunen-Loève (KL) decomposition to the patterns at all stimulation rates at the latencies determined at 0.6Hz (see Fuchs et al., 1992 for a discussion of KL decomposition). Figure 1.3 shows the results of this procedure. For each subject, the first eigenvector of the decomposition captured the spatial pattern of the N1m response (see the topographical maps at left in Figure 1.3). Note from the high eigenvalues (λ) that this mode accounts for more than 80% of the variance in the signal for subjects one and two, and about 65% for subjects three and four.

The amplitude of the response at each stimulation rate was calculated by projecting the spatial pattern from each rate at the determined latency onto the first eigenvector shown at left in figure 1.3. The plot of amplitude vs. inter-stimulus interval to the right of each eigenvector shows a strikingly linear relationship between amplitude and ISI, which is also supported by the high r-squared values obtained through linear regression. At higher stimulation rates, the N1m essentially vanishes. The x-intercept of the linear regression in each case provides a prediction for the ISI at which the response will reach zero amplitude. For each of the four subjects this occurs at an ISI between 98 and 162ms, corresponding to stimulation rates between 6 and 10Hz.

1.3.3. Extent of the N1m in Time and Frequency

At a stimulation rate of 0.6Hz the N1m response has a rise and fall time that extends from approximately 70 to 130ms past tone onset. From the KL analysis we know that the peak amplitude of the response reduced significantly as stimulation rate was increased. We now ask, first, if this reduction is accompanied by a temporal contraction

Figure 1.4. Results from the cluster analysis procedure applied at all rates and latencies from 35 to 160ms. The top two rows show the patterns corresponding to the cluster centers, and the angle α between them, for all subjects. Below these images are plots showing regions in a latency-rate space where patterns exist that have an angle less than 60° from the cluster centers. The color represents these angles, with shades of blue and red/yellow corresponding to angles from clusters one and two, respectively (see bars at right). A linear interpolation was applied between values at neighboring latencies and rates. Contour lines show the areas within 40° and 20° of the cluster centers (black and white lines, respectively).

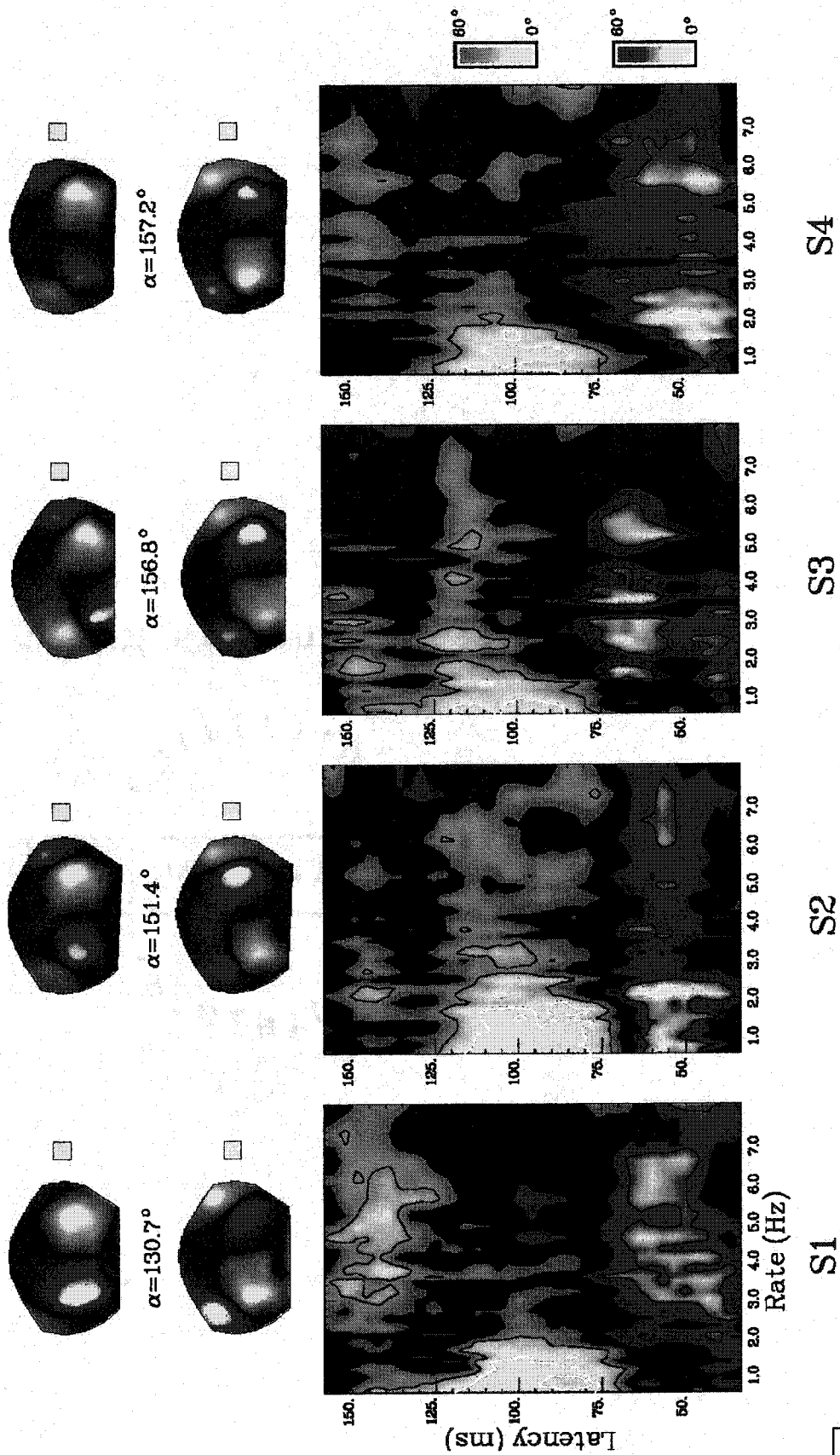


Figure 1.4

of the N1m. In other words, does response duration decrease at higher stimulation rates? And second, if such contraction does occur, is it due to masking by other temporally adjacent responses of opposite polarity that were difficult to observe or suppressed at low stimulation rates?

To accomplish this task, it was necessary to characterize the brain response across a range of latencies as well as stimulation rates. Our goal was to find the region of activity corresponding to the N1m, and to distinguish this from activity associated with neighboring responses. We compared the brain activity between 35 and 160ms from each stimulation rate by compressing the data from each subject into a two-dimensional space with latency and stimulation rate making up the two axes. Each point in this space represents a spatial pattern of magnetic activity recorded at a specific latency and stimulation rate, i.e. a vector in a 111-dimensional space formed by the sensors. In order to find regions of high point density in this space (which correspond to well defined evoked responses in the latency-rate space), we applied a variant of the standard *k*-means clustering algorithm (Aldenderfer and Blashfield, 1984). The *k*-means algorithm finds the centers of regions of high point density (clusters) in the above vector space and assigns points in the neighborhood of these centers to the corresponding clusters. The procedure starts by choosing random initial cluster centers, and then assigning the vectors that are closest to each center to the corresponding cluster. The data within each cluster are then averaged to find the new cluster center. This process is repeated until it becomes stationary (i.e. the cluster membership does not change between iterations). The *k*-means algorithm requires a proximity measure between the objects to be clustered, for which we used the angle α between the high dimensional vectors.

$$\alpha = \arccos \frac{\vec{a} \cdot \vec{b}}{|\vec{a}| |\vec{b}|}, \text{ where } \vec{a} \text{ and } \vec{b} \text{ are 111-dimensional vectors.}$$

The angle measure was chosen as opposed to Euclidean distance because, similar to spatial correlation, it depends only on shape and is independent of amplitude. Thus low and high amplitude patterns of the same shape will be clustered together. By varying the number of clusters from 1 to 7, we determined that two clusters produced the best segmentation of the data for all subjects. Using more than two clusters produced either redundant cluster centers or clusters with very few members. We modified the *k*-means algorithm so that after a few initial iterations only patterns with an angle of less than 45° from the old cluster center were used to calculate the new mean, thereby allowing us to focus on the most dominant activity patterns.

The spatial patterns of the final cluster centers are shown in figure 1.4 (top) for all subjects. Below these patterns are plots of the latency-rate space showing regions of similarity to the cluster centers with stimulation rate on the horizontal axis and latency to tone onset on the vertical axis. Colored are regions of angles less than 60° from the cluster centers, with shades of blue and red/yellow as indicated in the color bars (right) representing clusters one and two, respectively. The colors were interpolated in order to fill out the space. We chose 60° as a threshold because it is less than half the angle between each pair of cluster centers and corresponds to a spatial correlation of 0.5 (see α values in the figure for the angles between the center patterns). The top cluster center for each participant corresponds to the N1m response, with the dipolar structure similar to those from the KL procedure in figure 1.3. Consistent with this characterization, the blue region of similarity to this cluster includes latencies near 100ms, at least for low

stimulation rates. The red region of patterns in the second cluster occurs, in each case, earlier than the first cluster at a latency of about 50ms. The pattern of neuromagnetic activity represented by the second cluster center contains bilateral dipolar fields with a nearly opposite orientation to the N1m. This response more than likely corresponds to the first long latency component known as the P1/P1m in the EEG/MEG literature (Näätänen and Winkler, 1999; Picton et al., 1974) and can also be seen in the single channel time series in figure 1.2. In the literature, the same response has been grouped with the mid-latency components and referred to as the Pb/Pbm or P50/P50m (Mäkelä, Hämäläinen, Hari, & McEvoy, 1994; Yoshiura, Ueno, Iramina, & Masuda, 1996). Here, we will consider it a long latency response and call it the P1m.

The extent of the N1m response in the latency-rate space represents a complex pattern. The response activity near 100ms does reduce at higher rates, although the clustering procedure found regions of similarity to the N1m at latencies other than 100ms. The most prominent activity appears near 150ms in the latency-rate plots of figure 1.4. Each subject shows coherent horizontal bands proximal to the first cluster at this latency. Since this activity is most coherent at higher frequencies, it could represent a latency shift of the N1m from 100 to 150ms. Figure 1.5 shows topographical images of the activity patterns at 100 and 150ms latencies for each subject. These were generated by averaging the data from all stimulation rates that clustered with the N1m at these latencies. The results show that for each subject the 150ms response has a spatial pattern differing by 30° or more from the main response at 100ms for three of the four subjects. Because of this difference, the activity at 150ms likely represents a separate response instead of a temporal shift of the 100ms response. Evidence for a separate response is

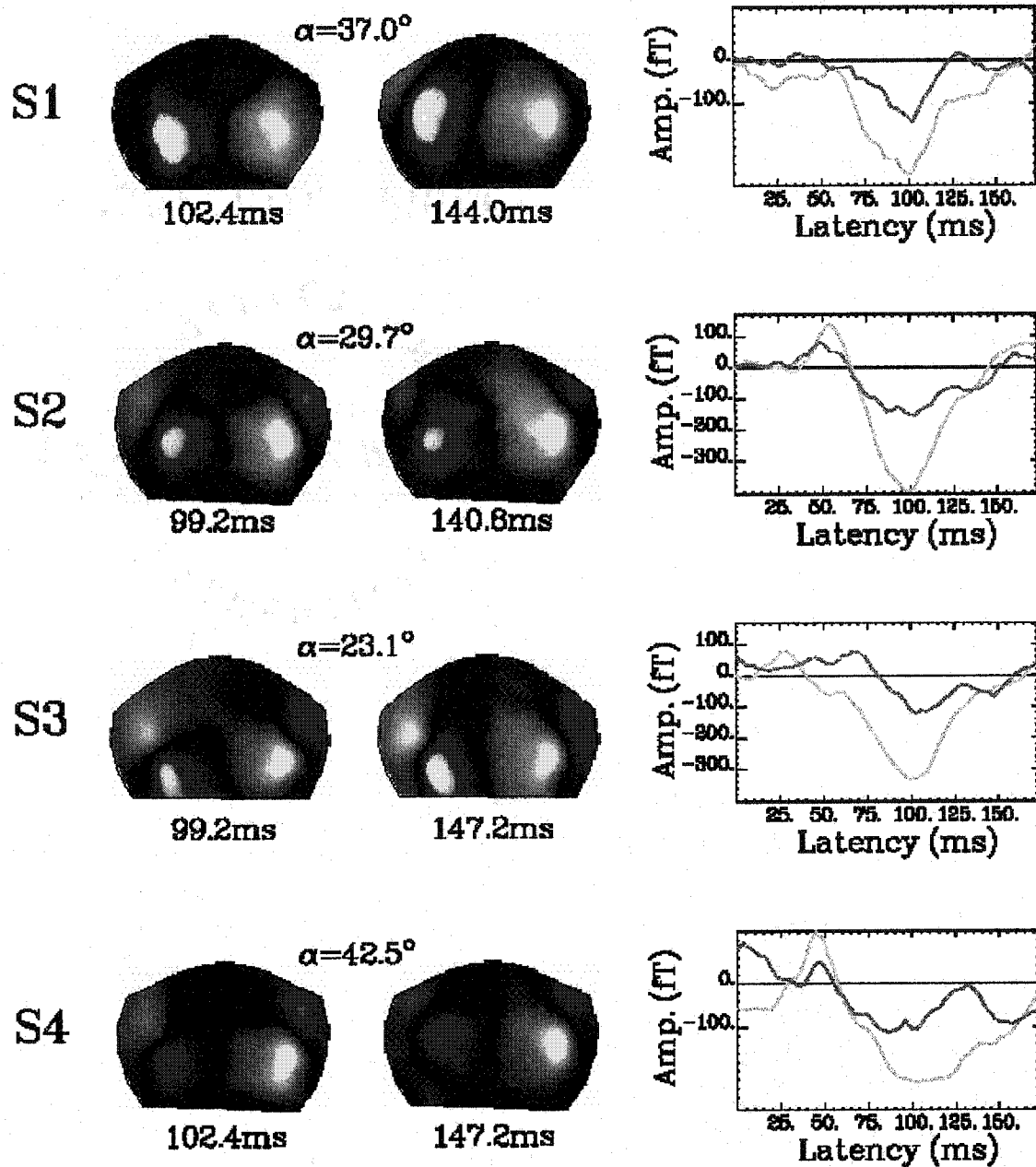


Figure 1.5. Left: Average topographic maps for 100 and 150ms responses for each subject at a single latency for each response. Rates were included in the average only if they were within the N1m cluster center from figure 1.4. The exact latency used for each average is shown below each map, with the angle α between the spatial patterns indicated above. Right: Time series showing the subpeaks of the N1m at 100 and 150ms at stimulation rates of 0.6Hz (green) and 1.7Hz (blue) from a channel containing a large amplitude N1m response. The separate 150ms response is visible at both rates, but becomes more apparent at the higher rates.

further enhanced by the single channel time series shown at right. For each subject, data are plotted at stimulation rates of 0.6 and 1.7Hz from a channel exhibiting both a large N1m and a 150ms response. At 0.6Hz the main N1m deflection extends up to 150ms, but at 1.7Hz the response has diminished in both amplitude and temporal extent. At the higher frequency there is a distinct separate peak near 150ms which exists alongside the dominant 100ms response. This peak is also evident at lower rates (arrows in Figure 1.2), suggesting that the main N1m component partially obscures the response at lower stimulation rates. This may explain why the clustering procedure shows little evidence of a separate 150ms response at lower rates.

Earlier we hypothesized that a rate-dependent reduction in the temporal extent of the 100ms response would reveal other responses that were not clearly visible at low stimulation rates. This is apparent for the N1m subcomponent discussed previously, but is also true for the earlier P1m response. In the latency-rate plots of subjects one, three, and four, this response is either not apparent at the lower stimulation rates, or only occurs for a few milliseconds. As the temporal extent of the N1m reduces at higher rates, the 50ms response extends into latencies previously occupied by the N1m. The increased temporal extent of the 50ms response may indicate that the high amplitude 100ms response masked the P1m at lower stimulation rates.

1.3.4. Overlap of Responses to Successive Tones

How is the response to a given stimulus influenced by the response to the previous tone? Since the first major response in each subject is the P1m at 50ms latency, we searched for evidence of late responses from the previous tone interfering with this

response. We studied this interference by using a projection of the entire dataset onto the spatial pattern of the 50ms response. This proved to be a useful means of data compression by providing a single measure of similarity or dissimilarity to the P1m, thus emphasizing long latency responses that could positively or negatively interfere with the response. The measure also took full advantage of the high degree of spatial information available from all the sensors, which allowed for observation of low amplitude long-latency responses that were difficult to observe in single channels. Figure 1.6 shows the average results for all subjects. The projection amplitudes A are from the formula

$$A = \frac{\vec{a} \cdot \vec{b}_{ij}}{\vec{a} \cdot \vec{a}}, \text{ where } \vec{a} \text{ is the vector representing the spatial pattern of the P1m, and } \vec{b} \text{ is}$$

the spatial pattern of activity recorded at latency i and stimulation rate j . The spatial pattern of the P1m used as a reference is from the clustering results shown in figure 1.4. The color plot in figure 1.6 shows the average of the projection data from all subjects at all stimulation rates. The intent is to show the evolution and onset of response overlap. Projection amplitudes are represented by a color scale, with colors interpolated between neighboring latencies and rates. Positive amplitudes are plotted in red/yellow indicating a high degree of similarity to the P1m; negative amplitudes are colored blue and indicate dissimilarity. The plot is centered at tone onset, with a full inter-stimulus interval presented before and after the tone at all but the very slow rates. Borders with the white regions at the left and the right indicate the previous and next tone onsets. After the center tone onset, the P1m and N1m appear as red and blue vertical stripes. The N1m appears as a negative deflection since the spatial pattern of the response is nearly opposite in polarity to the P1m (see Figure 1.4). Several other long latency responses follow the

Figure 1.6. Average of the projections of the recorded activity from all subjects onto the spatial patterns of their 50ms responses from figure 1.4. Top: An interpolated color image of the projection. The average amplitude of the 50ms response vector is normalized to one, with the maximum amplitude of the projection colored yellow. Any amplitude less than the minimum value on the color scale is colored light blue. The plot is centered at a tone onset, and the borders with the white region on the right and the left indicate the preceding and succeeding tone onsets. The dashed white line at right highlights the 500ms response to the center tone. A dashed line at left tracks the 500ms response to the previous tone, with an arrow indicating the region of interaction between the 500 and 50ms responses. Inset: Amplitudes of the projection at the peak latency of the average 50ms response exhibiting a pronounced peak when the 500ms response interacts with the P1m around 2Hz. Rate is shown on the x-axis, and projection amplitude is on the y-axis. Bottom: Individual plots of P1m amplitudes for all subjects.

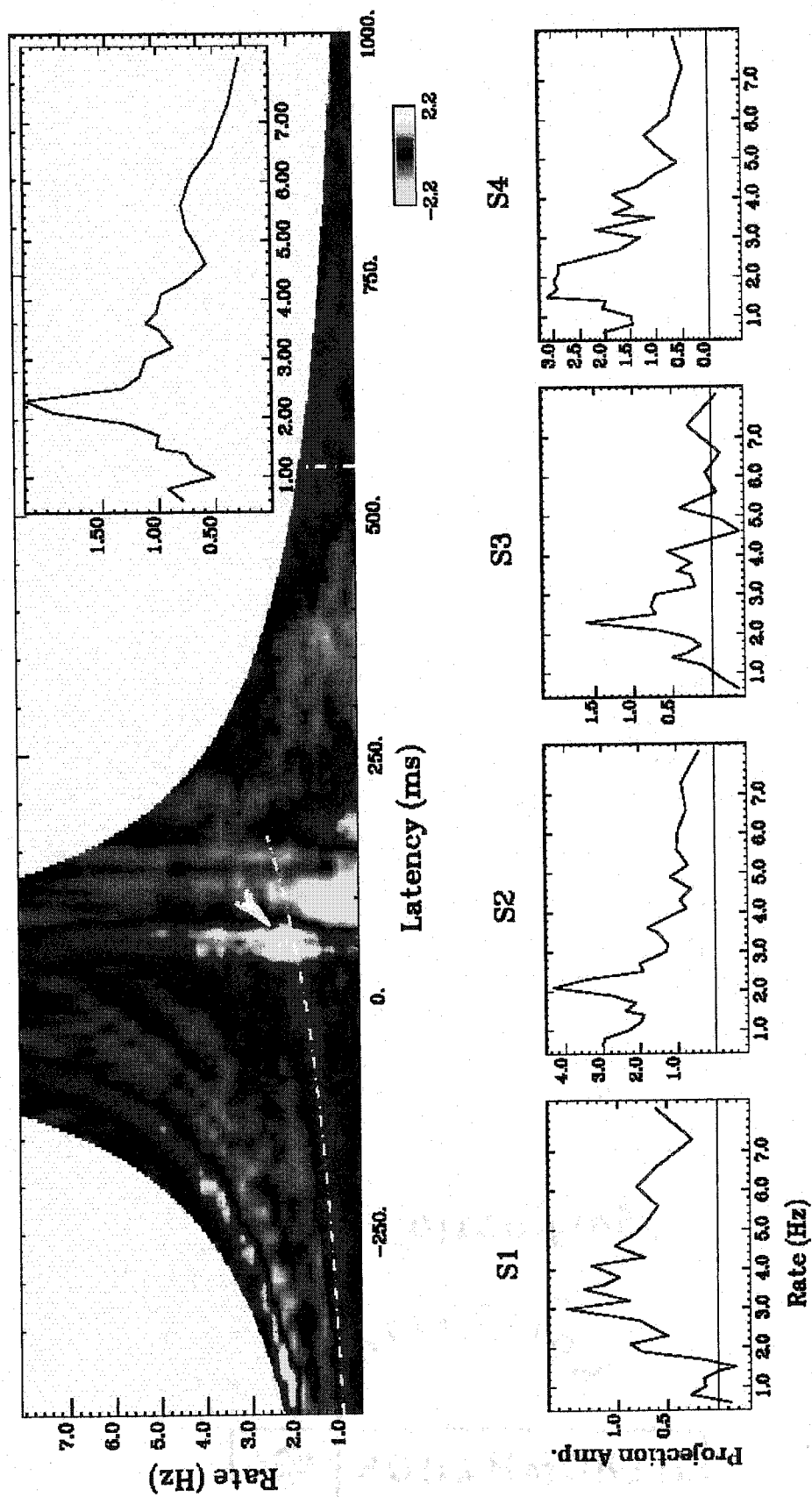


Figure 1.6

N1m, including a broad region of positivity beginning near 500ms, indicating a response pattern spatially similar to the P1m. The same long latency responses are seen emanating from the previous tone onset at left. A dashed line tracks the previous 500ms response. As stimulation rate increases to 2Hz, activity still present from the previous tone begins to overlap with the response to the central tone. When the 500ms response overlaps the P1m, the spatially similar responses enhance each other. This is indicated by the increase in projection amplitude within the region of interaction (see arrow in the figure).

The inset plot at top in figure 1.6 highlights the affect of response overlap on the P1m. The graph shows the amplitude of the projection at the peak latency of the average P1m as a function of stimulation rate. This amplitude peaks around 2Hz, where the 500ms response has maximum overlap with the P1m. The plots at bottom show the individual P1m amplitudes for each subject. All subjects show a spike in P1m amplitude near 2Hz, representing the maximum of the response in three out of four subjects. For the subjects who show a P1m response at all rates (2 & 4) the amplitude spike appears to interrupt a general trend of rate-dependent reduction of the response. In the color plot, the region of interaction between the 500ms response and the P1m also reveals a slight latency increase of the P1m and a delayed onset of the N1m. This implies that the constructive interference between the spatially similar 500ms and P1m responses also coincides with destructive interference with the dissimilar N1m.

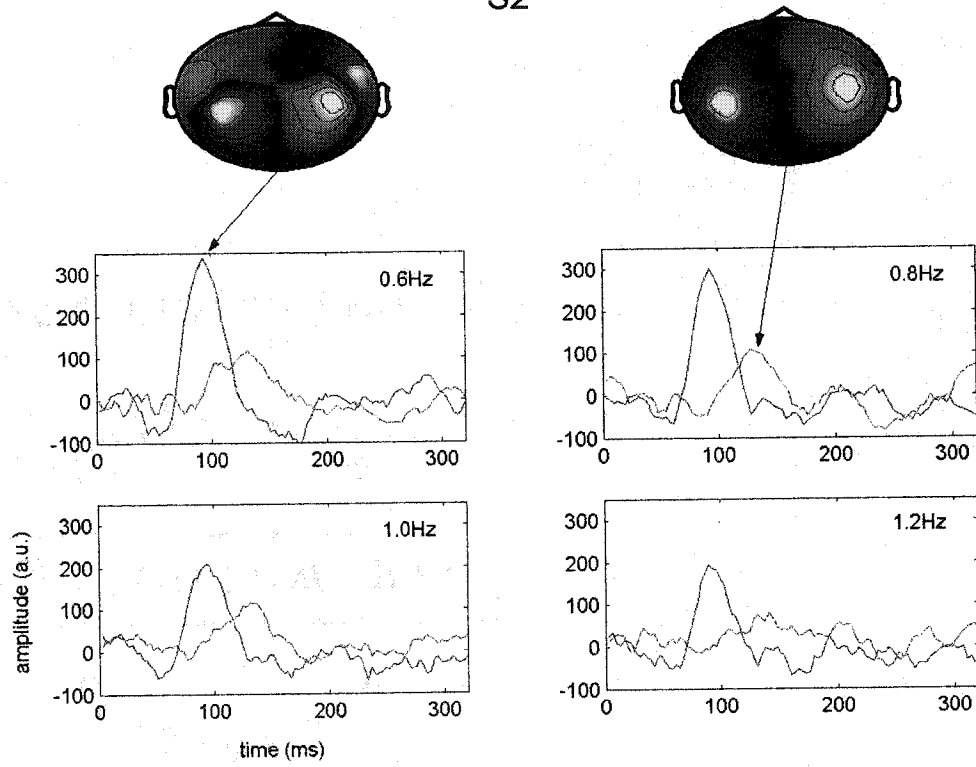
1.4. Results: Response Separation using Independent Components Analysis

In figure 1.5 we provided evidence for an N1m subcomponent peaking at 150ms latency. This response only became apparent as a separate subcomponent after the rate-

dependent reduction of the main N1m response at 100ms. The single channel time series in figure 1.5 indicates that the 150ms component is not clearly distinct from the main response at low rates, but becomes a separate deflection as the main response reduces. The possibility still exists that the response only develops at high rates, and does not exist as a response separate from the N1m at the low rates. In this section, we employ an independent components analysis (ICA) procedure (Makeig et al., 2002) to determine if the 150ms response represents a process independent from the main N1m response at the lowest stimulation rates when the main N1m component still has a large amplitude. The procedure uses the InfoMax algorithm from Bell and Sejnowski (1995) to separate the multi-channel signal into statistically independent time series, each with a distinct and constant spatial pattern at the sensors. We performed the ICA decomposition on the lowest four stimulation rates of 0.6, 0.8, 1.0, and 1.2Hz. The average data from 0 to 320ms latency at each rate were grouped together and the ICA decomposition performed on all the data at once. Prior to implementing the ICA decomposition, a KL decomposition of the data was used to reduce the dimension of the vector space. This procedure created a smaller set of virtual sensors by projecting the original time series onto the vector space formed by the top modes of the decomposition. The ICA procedure was effective at separating a 150ms subcomponent of the N1m in 2 out of 4 subjects (subjects 2 & 4). The results are shown in figures 1.7, which presents the two modes accounting for the most variance in the original data for each subject. The spatial patterns of each mode at the sensors are shown at top. Below these patterns are the associated time series of each mode, shown in red and blue at each rate. For each subject, the mode at left captures the main N1m component. The spatial pattern is similar to that

Figure 1.7. ICA decomposition of the N1m response for subjects 2 & 4 at top and bottom, respectively. A single decomposition was performed on the average data from 0 to 320ms latency at the four lowest stimulation rates. The results reveal a separation of the 100 and 150ms components of the N1m. Top: topographic images of the top two modes of the decomposition. Red indicates exiting field and blue is entering field. Bottom: time series of the decomposition at each rate. Tone onset is at left. The red line is the time series of activation for the 100ms component at each rate, and the blue line is the activation pattern for the 150ms response.

S2



S4

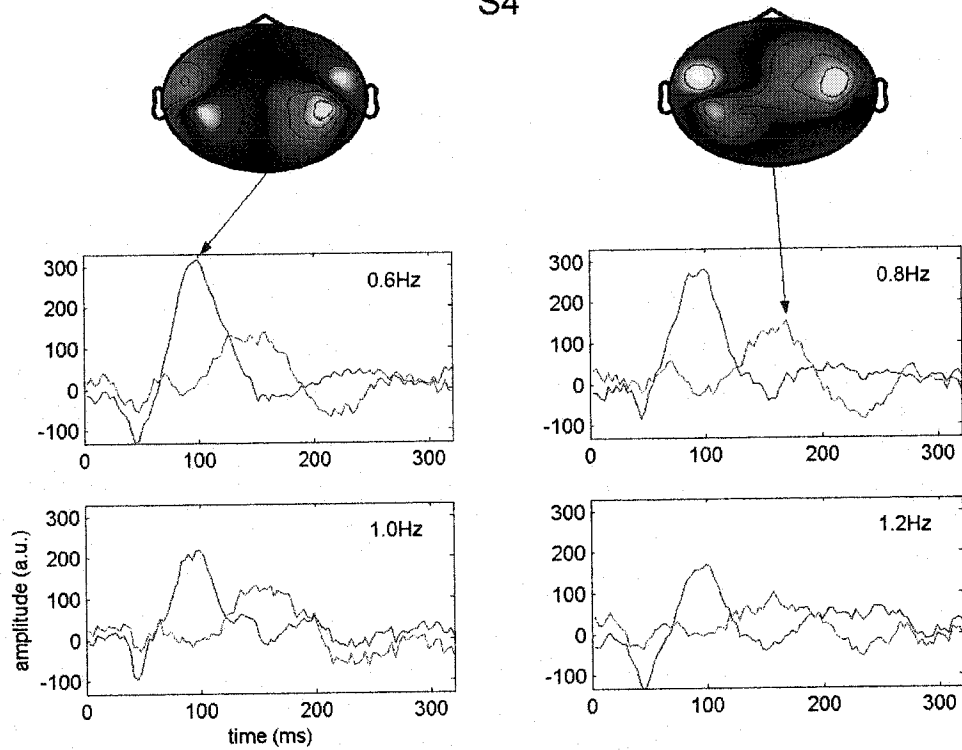


Figure 1.7

obtained in the prior analyses, and the time series exhibits a clear peak at 100ms latency. The second mode represents a response peaking at 150ms for all rates, with a time series that overlaps with the main N1m component. In the previous analyses (figure 1.4 & 1.5), the 150ms response was only observable because it did not reduce as quickly as the main N1m, and so became obvious at higher rates. Here we show that the 150ms subcomponent is an independent process even at low stimulation rates when the main N1m response is still strong. These results highlight the utility of ICA for finding previously unobservable or inseparable responses in MEG.

1.5. Discussion

The intention of this experiment was to characterize the cortical auditory response to rhythmic stimuli within a parameter range that is relevant for studies of perception and behavior. The relatively simple yet systematic design used in this study may serve as a basis for more complex studies in areas such as music and speech perception and sensorimotor coordination. Several studies have investigated the rate dependency of the N1m at rates slower than used in this experiment (Lü et al., 1992; Mäkelä et al., 1993; Sams et al., 1993). Among these, Lü et al. (1992) used ISIs covering the range from 0.8 to 16 seconds. In contrast to the linear dependence found here, Lü et al. (1992) modeled the ISI dependency of the main component with a function of the form $A(1 - e^{-(t-t_0)/\tau})$, with amplitude A , ISI t , time of decay onset t_0 , and lifetime τ . This function becomes asymptotic at high ISIs, accounting for the fact that the amplitude increase levels off at ISIs above 10s. Sams et al. (1993) used a similar exponential function to model the rate dependence of the N1m using ISIs ranging from 0.75 to 12 seconds. Here, we found that

the N1m is linearly dependent on inter-stimulus interval over the range of stimulation rates from 0.6 to 8.1Hz. The linear dependence of the N1m in the present experiment should not be surprising, however, since the ISIs used here are in the linear range of the previous exponential models, before the function approaches an asymptote at high ISIs.

One of the predictions of the Lü et al. (1992) exponential model of the N1m is that the component disappears at an ISI equivalent to the duration of the stimulus. Thus, the evoked response is considered refractory with respect to tone offset. To our knowledge, our experiment is the first to test this prediction at ISIs shorter than the 0.8s used in Lü et al. (1992). For all subjects the N1m disappears at higher ISIs than the tone offset at 60ms, and in fact for three of the subjects the ISI is more than twice that value (Figure 1.3). It is possible, however, that the increase of the zero amplitude times was due to interference from the 50ms response. The present results (Figure 1.4) show that the 50ms response for three of our subjects eventually extends very close to 100ms. These data suggest that as the N1m reduces in amplitude, the 50ms response may become a greater part of the signal at 100ms and thus interfere with the remaining low amplitude N1m. Interference from activity originating from the previous tone could also have caused difficulty in observing the N1m at higher stimulation rates. Overlap between responses to successive tones was present in all subjects at stimulation rates above 2Hz.

In an EEG study using five stimulation rates from 0.5 to 10Hz, Erwin and Buchwald (1986) found that the 50ms P1 response reduces in amplitude with increased stimulation rate. For the subjects showing a P1m at all rates in figure 1.6, the response is also attenuated by increasing rate, although the general pattern is interrupted by a large amplitude spike near 2Hz from interference with the spatially similar 500ms response to

the previous tone. Obtaining an accurate model of the rate dependence of the P1m over this range of stimulation rates is made difficult by this potential for interference. One possible method for overcoming this problem is the maximum length sequence (MLS) method employed by Picton, Champagne, and Kellett (1992). The MLS consists of a specially constructed sequence of inter-stimulus intervals designed to average out the effect of response overlap. Using this method, the authors confirmed that the P1 is attenuated by increasing rate. Besides interference from previous responses, the P1m may also be affected by overlap from the large amplitude N1m response at low stimulation rates. This was apparent in the results of the clustering procedure (Figure 1.4) in at least three subjects. Interference from either the N1m or activity induced by the previous tone may explain why some studies report an increase rather than a decrease of P1m amplitude with increased stimulation rate (see for example Alain, Woods, & Ogawa, 1994).

In the present study, a 150ms response was also obscured by the main N1m component at low stimulation rates. Because of its temporal and spatial proximity to the N1m, this response is best described as a subcomponent of the main N1m response. Multiple subcomponents of the N1/N1m have been observed in previous EEG and MEG studies at latencies ranging from 75 to 170ms (for reviews see Näätänen and Picton, 1987; Woods, 1995). Some of the studies of N1m rate dependence report a secondary N1m response, although none at a latency of 150ms (Lü et al., 1992; Sams et al., 1993). Mäkelä et al. (1993) found that as stimulation rate increased to 1Hz, a single source was no longer adequate to model the N1m. This coincides with the pattern of emergence observed here in which a second component became apparent at higher rates. However,

no studies of N1m rate dependence have used rates in the range of the present study. Although not a study of rate dependence, Loveless et al. (1996) used pairs of stimuli in a similar range of ISIs as studied here and found a similar N1m subcomponent. The authors used ISIs ranging from 70 to 500ms, and showed that the last tone in the pair produced separate N1m components at 100 and 150ms. As shown here, the second component was significantly stronger at shorter ISIs.

By the definition used here, the onset of overlap between the transient responses to successive tones marks the beginning of the continuous steady-state response (Regan, 1982). Here we found this onset at a stimulation rate of 2Hz. The steady-state response, however, is traditionally recorded at much higher stimulation rates (~10-80Hz). As reported earlier, at 40Hz the steady-state response forms a near sinusoidal oscillation at the stimulation frequency, which is a much simpler response than the time series found here at 2Hz (see Figs. 1.2 & 1.6). The source of the high frequency steady-state response is still under debate, with argument centering on whether the response results from overlap of transient responses, or phase locking of ongoing cortical rhythms, or some combination of the two (Azzena et al., 1995). Due to their rate dependence, long latency responses are not considered to make up a large part of the response (Hari et al., 1989). This contrasts with the onset of the low frequency SSR seen here, which comes in the form of overlapping long latency responses. The SSR can also be thought of as an oscillatory response that has a resonant frequency near 40Hz (Galambos et al., 1981). Using amplitude modulation of a simple tone, Picton, Skinner, Champagne, Kellett, & Maiste (1987) showed that the SSR actually has two resonant regions – one from 20 to

50Hz, and another from 2 to 5Hz. Based on these results, it may be possible to divide the steady-state response into distinct low and high frequency regimes.

Several studies have recorded mid-latency responses at stimulation rates from 8 to 10Hz to test the idea that the 40Hz response results from overlap of these responses (Azzena et al., 1995; Gutschalk et al., 1999; Hari et al., 1989). The rates used here bordered this range and provided strong evidence that LLRs from previous tones could exist within the latency range of the mid-latency response to the present tone (between 10 and 50ms). We show evidence for a 150ms N1m subcomponent that is observable up until 8.1Hz (Figure 1.4). At a stimulation rate of 8Hz, a 150ms response lands precisely at 25ms past the next tone onset. Therefore, this response could interact with the MLRs recorded at these rates, and cause discrepancies when trying to account for the 40Hz response by simple summation. If residual LLRs can be seen at 8.1Hz, then the possibility exists that long latency responses contribute to the SSR at 40Hz as well. In accordance with this idea, Santarelli et al. (1995) found responses in the latency range of the LLRs after the last click of a 40Hz click train, suggesting that long latency responses are evoked by each click.

The present results suggest several issues for future study. Among these is determining the characteristics of the observed activity at 500ms past tone onset. Standard transient responses, recorded with long randomized ISIs, typically do not contain a coherent response at such a long latency (Picton et al., 1974). Possibly, 500ms activity only occurs during rhythmic stimulation. One method to clarify this issue would be to present stimuli with slightly variable ISIs. If the 500ms response is induced by rhythmic stimuli only, it should disappear with enough variability in the tone sequence.

The present experiment could also be repeated, but with a slightly higher range of ISIs. The 500ms response might disappear as the ISI increases beyond the theoretical limit of rhythm perception. Fraisse (1982) reports that this upper limit is near 1800ms, which is close to the longest ISI used in this experiment. Future work might also determine if the onset of continuous activity between tones near 2Hz has any significance for the processing of auditory information. Results from previous behavioral studies suggest that this possibility may deserve further investigation (see Gura, 2001). For example, if subjects tune a metronome to a tempo that sounds the most natural, they consistently prefer a rate very close to 2Hz (Fraisse, 1982). In addition, the just noticeable difference between two different rates of isochronous tone stimulation is lowest within a region centered at 2Hz (Drake and Botte, 1993). Auditory stimulation at 2Hz is significant in sensorimotor coordination experiments as well. When subjects flex their index finger between successive tones (syncopate), they find the task increasingly difficult as the stimulation rate is increased. Beyond a critical point they spontaneously switch to synchronizing movement with the metronome (Kelso et al., 1990). In unpracticed subjects, this transition typically occurs at movement rates approaching 2Hz (but see Jantzen, Fuchs, Mayville, Deecke, & Kelso, 2001). The change from a transient to a steady-state response occurs when discrete cortical activity overlaps to form a continuous sensory/perceptual representation. The aforementioned perceptual and behavioral phenomena may well be linked to this qualitative transition in the nature of the auditory response.

**Experiment 2: Neuroelectric Activity Associated with Rhythmic
Auditory Stimulation: Rate Dependence and the Relationship between
Spontaneous and Evoked Activity**

2.1. Introduction

Cortical activity associated with auditory stimulation is traditionally divided into two types: transient and steady-state (Regan, 1982, 1989). Transient responses are elicited by brief tones separated by intervals on the order of seconds, which allows the cortical activity associated with each tone to return to baseline before the next stimulus. Steady-state responses, on the other hand, are elicited by fast auditory stimulation in which tones or clicks are separated by tens of milliseconds. This produces continuous activity in the cortex that is difficult to associate with a specific event. The discrete vs. continuous nature of these two types of responses has led to different approaches when analyzing their neural correlates with electroencephalography (EEG) and magnetoencephalography (MEG). Transient responses are typically treated as a series of separate response components, each defined by an amplitude peak at a particular latency in the evoked potential or magnetic field (e.g. Picton Hillyard, Krausz, & Galombos, 1974). In contrast, for steady-state responses the continuous oscillatory nature of the response is emphasized, and analysis is performed in the frequency domain (e.g. Picton, Skinner, Champagne, Kellett, & Maiste, 1987). Here we seek to characterize the cortical response to rhythmic tone stimulation within a parameter regime that contains the border

between the discrete transient and continuous steady-state responses. For this purpose, we performed an EEG experiment with 23 separate stimulation rates from 0.5 to 4.9Hz, with 0.2Hz steps. We hypothesized that this parameter range would contain the transient to steady-state transition based on an earlier MEG experiment where we found the border near 2Hz (Carver, Fuchs, Jantzen, & Kelso, 2002).

The current parameter range is not only important because it is the transition zone between the two major types of auditory evoked responses; this range also contains rates significant for our understanding of perception and sensorimotor coordination (e.g. Drake & Bertrand, 2001; Engström, Kelso, & Holroyd, 1996; Large, Fink & Kelso, 2002; Repp, 2001). Stimulation rates from 0.5 to 4.9Hz covers much of the range over which an isochronous series of tones are perceived as a rhythm, and within this range, rates near 2Hz are commonly reported to be a preferred rhythm when subjects are asked to tune a metronome to their liking (Fraisse, 1982). Also near 2Hz, subjects are able to better distinguish between two series of tones at slightly different rates (Drake & Botte, 1993). When subjects are asked to syncopate with a rhythmic tone sequence, they find the task increasingly difficult with increased rate, and beyond a certain rate spontaneously switch to synchronization (Kelso, DelColle, & Schöner, 1990). In unpracticed subjects, this occurs at rates near 2Hz. These phenomena suggest that the transition from a discrete transient response to a continuous steady-state response is meaningful for perception and behavior and deserves further investigation. Because we will be observing evoked responses over the border region between transient and steady-state activity, we will apply analysis techniques suited for both kinds of responses. As is typical for studies of transient evoked responses, we will characterize the rate dependence of separate response

subcomponents at set latencies past tone onset. We will also observe the global oscillatory nature of the response in the frequency domain as is usually done in investigations of the steady-state response.

In EEG the transient response consists of a series of distinct peaks of the electrical potentials occurring at different latencies after tone onset (Picton et al., 1974). These are traditionally divided into three response epochs: the so-called early, middle, and long latency responses. The early components, also known as brainstem-evoked responses, are subcortical in origin and occur within 10ms of tone onset. These are followed by cortical mid-latency responses (MLRs), which consist of a series of fast oscillations of the electric potential between 10 and 60ms. Cortical components that peak after 60ms are referred to as long latency responses (LLRs), and are characterized by longer durations and higher amplitudes than the MLRs. The most prominent long latency response is a negative wave near 100ms, commonly referred to in the EEG literature as the N100 or N1 (for review see Näätänen & Picton, 1987). The term N1m refers to the corresponding peak in MEG. Most of the peaks recorded in EEG correspond to peaks at similar latencies in the neuromagnetic field amplitude in MEG, although certain responses, such as the P2 at 200ms latency, are better seen with EEG than MEG. Previous experiments have demonstrated that the amplitude of some, but not all, of the transient auditory evoked responses depend on stimulation rate (e.g. Erwin & Buchwald, 1986). Because of its large amplitude, the rate dependence of the N1 has received a considerable amount of experimental attention (for review see Näätänen & Winkler, 1999). Several studies have shown that the amplitude of this response reduces systematically in both EEG (Hari, Kaila, Katilla, Toumisto, & Varpula, 1982; Hari et al.,

1987) and MEG (Lü, Williamson, & Kaufman, 1992; Sams, Hari, Rif, & Knuutila, 1993) as stimulation rates increase. However, the fastest stimulation rate in these studies was 0.8Hz, which is at the low end of the rates used here. In our recent MEG study, we extended this work by revealing a systematic decrease of the N1m response amplitude at rates up to 8.1Hz (Carver et al., 2002). A linear dependence of the N1m amplitude on inter-stimulus interval was observed, and the response was predicted to reach zero amplitude at ISIs between 100 and 150ms. Part of the purpose of the present experiment was to characterize the rate-dependent evolution of the corresponding N1 response in EEG. We hypothesized that we would observe a similar pattern of rate dependence as in the MEG experiment. Previous work has shown that the N1 represents a reaction to change in the auditory environment; in fact, an N1 is also elicited by the offset of a tone if the tone duration is long enough (Hari et al., 1987). Attenuation of the N1 across the present range of rates could thus imply that the primary percept of the tone sequence is transitioning from that of a series of discrete events, to each tone being part of a rhythmic whole. In addition to the N1, we investigated the rate dependence of the neighboring P2 response at 200ms latency. This response has received relatively little experimental attention, largely because it is strongly suppressed in MEG. Hari et al. (1982) showed that the N1 and P2 responses have a similar pattern of rate dependence up to a rate of 1Hz, suggesting that they are part of the same process in the auditory response. Here we extend these results to higher stimulation rates.

In our recent MEG experiment, we revealed that the transient response extends up to 500ms after tone onset. At a stimulation rate of 2Hz the responses to successive stimuli overlapped, which lead to a continuous steady-state response. Commonly

recorded at stimulation rates above 10Hz, the steady-state response (SSR) is qualitatively different from the transient response because it is characterized by continuous activation between stimuli (Regan, 1982). According to a definition given in Regan (1989), the SSR must also exhibit periodicity at low multiples of the stimulation rate. The most prominent SSR is elicited by a 40Hz click train, which produces a resonant response in the cortex at the stimulation rate (Galambos, Makeig, & Talmachoff, 1981). The 40Hz SSR has received a considerable amount of experimental attention (Azzena et al., 1995; Gutschalk et al., 1999; Hari, Hämäläinen, & Joutsiniemi, 1989); however, this is not the only resonant frequency of the auditory SSR. Picton et al. (1987) used amplitude modulation of a continuous tone to show resonance of the SSR at low multiples of the stimulation rate at rates from 30 to 50Hz. In addition, they discovered resonant activity across a lower frequency range from 2 to 5Hz. The latter range covers the higher end of the stimulation rates in the present experiment, although our experiments differ in that we use discrete tone stimulation instead of amplitude modulation of a pure tone. Despite this difference, we hypothesized that we would observe resonance of the evoked response at rates of 2Hz and above in the current experiment. This would indicate the beginning of steady-state activity as defined by Regan (1989), and would compliment the results of our previous MEG experiment (Carver et al., 2002).

The origin of the 40Hz SSR has been the subject of considerable debate in the literature (cf. Hari et al., 1989; Pantev, Roberts, Elbert, Roß, & Wienbruch, 1996). One possibility is that it results from linear summation of the transient responses to successive tones, which at this stimulation rate overlap to form a continuous 40Hz oscillation. The mid-latency responses would make up the majority of the transient response at these

rates, since the long-latency responses are believed to have disappeared by 40Hz (Hari et al., 1989; but see Santarelli et al., 1995). When band-pass filtered around 40Hz, the early part of the transient response forms a brief 40Hz oscillation, sometimes referred to as the transient gamma-band response (Roß, Picton, & Pantev, 2002). Analysis of single trial data in EEG and MEG has revealed that the amplitude of the evoked gamma response may depend on the amplitude of pre-stimulus gamma activity (Başar, Rosen, Başar-Eroglu, & Greitschus, 1987; Pantev et al., 1991). Work in other perceptual modalities has further shown that evoked oscillatory activity may not be spontaneously generated, but instead represents a phase resetting of ongoing pre-stimulus oscillations in the same frequency band (Makeig et al., 2002; Tesche & Karhu, 2000). Here we search for similar evidence for the auditory evoked gamma-band response. We use independent components analysis (ICA) to study the relationship between evoked and ongoing gamma activity in unaveraged data. The ICA algorithm is the same as employed by Makeig et al. (2002) to reveal that a visual evoked alpha-band response (~10Hz) is generated by resetting of ongoing alpha activity. ICA works to separate a mixed signal at the sensors into statistically independent spatiotemporal components, each with a fixed spatial pattern of activity at the sensors. We hypothesized that ongoing and evoked gamma activity would be captured by the same independent component based on studies by Sukov and Barth (1998, 2001) that showed a common source for each type of oscillation in the auditory cortex of rats.

2.2. Methods

2.2.1. Subjects

Four male subjects, all of whom reported to be right-handed, participated in the experiment. Their ages ranged from 21 to 30. The experiment was conducted in compliance with all standards of human research outlined in the Declaration of Helsinki as well as by the Institutional Review Board. Informed consent was obtained from each participant prior to EEG recording. All participants reported normal hearing.

2.2.2. Procedure

The experiment was performed in the Human Brain and Behavior Laboratory at the Center for Complex Systems and Brain Sciences. Auditory stimulation was delivered binaurally through either plastic headphones or a single speaker placed in front of the subject. The volume was set at a level that the subjects reported to be comfortable. Subjects were asked to attend to the auditory stimulation while fixing their gaze on an 'X' placed on the wall two meters in front of them. They were further instructed to minimize all extraneous eye or body movements during each trial. The experiment consisted of separate trials during which subjects listened to a series of tones presented at a constant rate of stimulation. Each series contained 50 1kHz tones, with each tone lasting 60ms with zero rise and fall times. Twenty-three stimulation rates were used in the experiment, ranging from 0.5 to 4.9Hz, in 0.2Hz steps. Separate trials at each rate were repeated four times for subjects 1 and 2 and three times for the remaining subjects, thus providing either 150 or 200 tone stimulation cycles for averaging. The trial order was randomized for each subject. The experiment lasted approximately 2 hours.

2.2.3. *Data Acquisition*

EEG activity was recorded using two separate systems. A 61-channel system with Grass 12A5 amplifiers (Grass-Telefactor, West Warwick, RI) was used for subjects one and two. The EEG activity from the remaining two subjects was recorded with an 84-channel Manscan system (Sam Technology, Inc., San Francisco, CA). In each case, electrodes were placed on the scalp according to a modified 10/20 International System of Electrode Placement. The 61-channel system employed a left mastoid reference during recording. The data were later rereferenced using an average of the left mastoid and electrode T8 in order to remove lateral bias. The Manscan system used left and right mastoid electrodes as an average reference during the recording. Regardless of recording system, digitization was performed at 256Hz. Either immediately before or after the experiment a Polhemus Isotrack II (Colchester, VT) was used to record the 3D location of each electrode, plus three fiduciary points: the nasion, and left and right preauricular points. The fiduciary points were used to create a subject specific 3D coordinate system for the electrode locations.

2.2.4. *Data Processing*

The EEG signals were manually inspected before averaging, and any cycle with eye-blink or movement artifacts was discarded. Each cycle was centered at tone onset, and the duration was equal to the inter-stimulus interval for each rate. Separate ensemble averages of single stimulation cycles were calculated for each stimulation rate. Prior to averaging, the raw signals were band-pass filtered from 0.1 to 50Hz. The first two cycles

from each trial were excluded from the final average in order to avoid transients. Topographical mapping of the resulting event-related potentials was performed by a polar projection of the three-dimensional sensor coordinates into two-dimensional space. A spline of 3rd order was used to interpolate activity between sensor positions. For each subject several channels were excluded in the final analyses due to a high noise level.

2.2.5. Data Analysis

In order to determine the rate dependence of the N1 and P2 response components we used a Karhunen-Loève (KL) decomposition procedure (also known as principal components analysis) to separate each component from background activity. The decomposition was performed on the neural activity patterns of each component at all stimulation rates. The activity patterns for each component were taken from all channels at a single common latency past tone onset at each stimulation rate. This latency was determined by finding the time at which the component reached maximum amplitude in any channel at the rate of 0.5Hz. The slowest stimulation rate was used for this purpose because each component exhibited the highest absolute amplitude at this rate. The KL decomposition was then applied to the group of activity patterns from all rates in order to find the main direction of variance for each component in the vector space formed by the sensors. In other words, the procedure was used to find the eigenvector of the decomposition with the largest eigenvalue, which would represent the dominant spatial activity pattern of the response. The associated amplitudes of the eigenvector at each stimulation rate were then used to characterize the rate-dependent evolution of the component. After performing this procedure for both components, we compared the

resulting spatial patterns of the N1 and P2 by finding the angle between the patterns in the vector space formed by the sensors.

KL decomposition was also utilized to search for evidence of resonance of the overall response at harmonics of the stimulus frequency. In this procedure, the decomposition was performed separately at each rate. One cycle of data was used for this purpose, with the time series centered at tone onset and lasting the length of the inter-stimulus interval. Before KL decomposition, the data were smoothed with a fourth order Savitzky-Golay filter in order to remove high frequency oscillations that were not the subject of this analysis. A power spectrum of the time series of the top eigenvector of the decomposition was used to determine if the overall response had begun to resonate at low multiples of the stimulation rate.

In order to test the hypothesis that the 40Hz mid-latency oscillation is related to ongoing gamma activity occurring pre-stimulus, we used an independent components analysis (ICA) procedure to analyze unaveraged data at each stimulation rate. Analysis of unaveraged data was necessary because any ongoing 40Hz activity would presumably not be phase-locked to the stimulus and so would not appear in averaged data. For this task, we employed ICA Toolbox software (Makeig et al., 2002). This software employs the InfoMax algorithm from Bell and Sejnowski (1995) to separate the multi-channel signal into statistically independent time series, each with a distinct and constant spatial pattern at the sensors. Before ICA decomposition, the unaveraged time series at individual stimulation rates were band-pass filtered from 30 to 50Hz in order to isolate ongoing and evoked gamma activity. In addition, KL decomposition was utilized to reduce the dimension of the data. This was done by projecting the raw data onto the

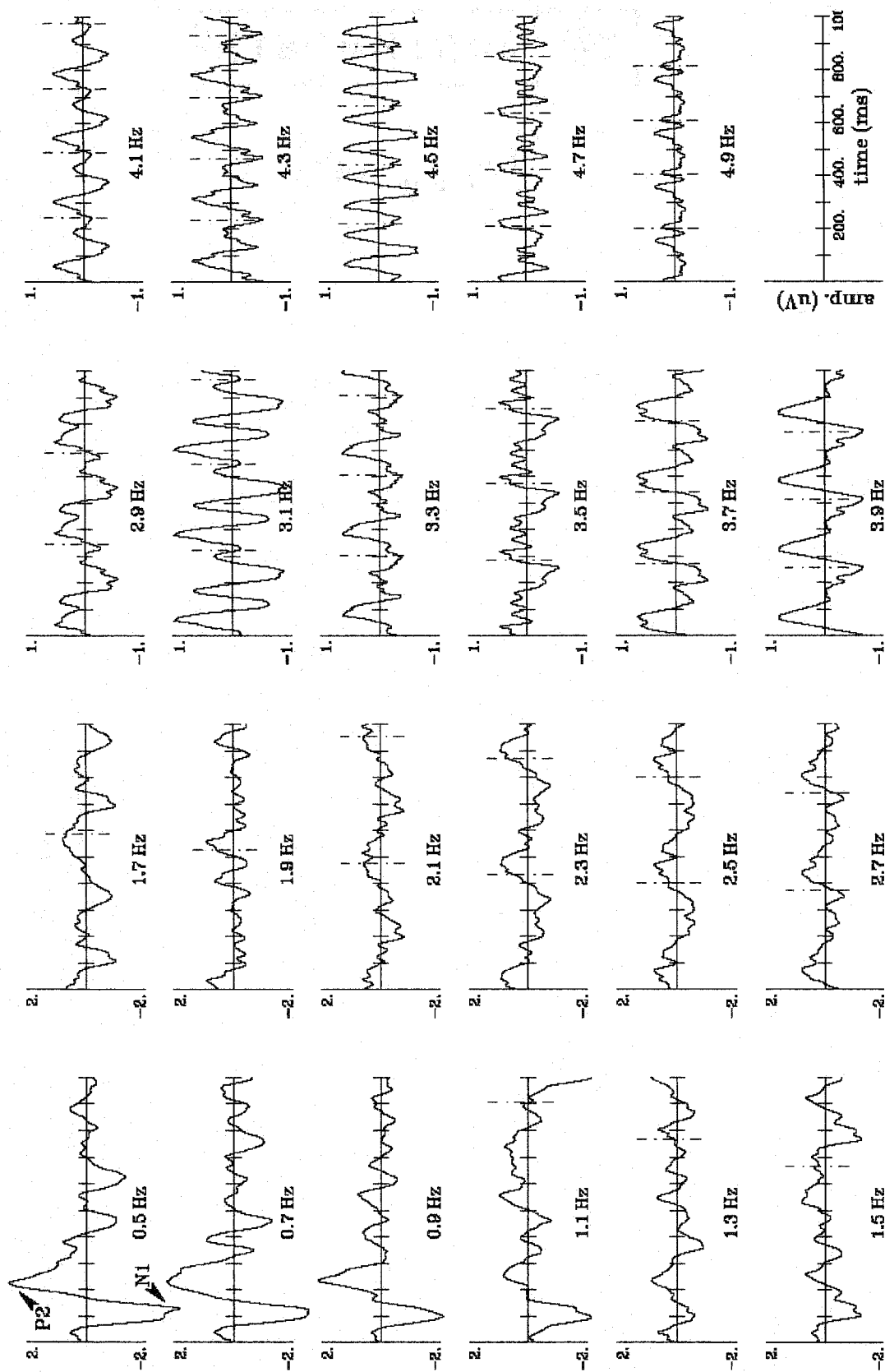
orthogonal vector space formed by the top ten eigenvectors of the decomposition. Because the ICA algorithm attempts to produce as many independent components as there are sensors, the reduction of the space to ten dimensions avoided degenerate solutions caused by an overestimation of the number of independent components. After ICA decomposition, the original data were projected onto the ICA spatial modes, and the modes placed in the order of mean variance accounted for in the original time series. The activation time series of each mode were averaged around tone onset in order to determine which mode captured the mid-latency response. In order to observe the relationship between the evoked gamma response and the phase of ongoing activity, we sorted the activation time series of the mid-latency mode by pre-stimulus phase. We used a latency of 10ms post-stimulus as the border between pre and post stimulus activity in order to account for the time it takes auditory evoked activity to reach the cortex (Picton et al., 1974). The phases of the pre-stimulus gamma oscillations were determined with a complex filter at the peak frequency of the gamma response over three cycles of oscillation.

2.3. Results: Rate Dependence and Resonance

2.3.1. Evolution of the Response

The rate-dependent evolution of the auditory response is shown in figure 2.1, which presents the averaged auditory evoked responses from a single channel (Cz) at all rates for a single subject (subject 2). At the slowest stimulation rate (0.5Hz), the largest response is a negative potential deflection peaking at 100ms past tone onset. This is the evoked response component referred to as the N1/N100 in previous studies of transient

Figure 2.1. Average time series for subject two: one second of data at all stimulation rates from the channel (Cz) that had the highest overall amplitude in the experiment for this subject. Each time series starts at a tone onset, with dashed lines indicating the onset of succeeding tones. Note that the vertical micro-volt scale is different for the columns on the right in order to adjust for the lower amplitudes at higher rates. Hash marks on the horizontal axis indicate 100ms intervals (the time scale is shown at bottom-right).



auditory responses (Picton et al., 1974). As stimulation rate increases, the amplitude of this response component systematically decreases. In fact, by 2.1Hz the component is no longer apparent as a negative deflection. The second largest amplitude component in this channel is a positive deflection around 200ms latency, corresponding to the response typically labeled the P2 or P200. The P2 decreases in amplitude with increased stimulation rate in a manner similar to the N1, and has also vanished by 2.1 Hz. At low stimulation rates positive and negative deflections in the average response continue after 200ms, although beyond 600ms no response shows a consistent polarity and latency across more than one rate. This is consistent with the pattern of a transient response, where the activity evoked by each tone reduces to near baseline before the next tone. At stimulation rates beyond 1.9Hz brain activity is continuously present between tone onsets, which is symptomatic of a steady-state response. Between 2.1 and 2.7Hz, the response appears to follow a slow potential oscillation at the stimulation rate. Other rhythmic patterns emerge at higher rates, including an oscillation at three times the stimulus rate at 3.1Hz, and twice the stimulus rate at 4.5Hz.

2.3.2. Amplitude of the N1

Figure 2.1 revealed a systematic reduction of the auditory evoked N1 component with increased stimulation rate for a single subject. Here we present the results of the KL decomposition procedure used to provide a more precise characterization of the rate dependence of the N1. Figure 2.2 shows the results of this procedure for all subjects. At left are the spatial patterns of the N1 and the eigenvalues of the decompositions, the latter showing that the pattern makes up over 85% of the variance in all subjects at the

specified latency. Light blue color in the spatial pattern indicates negative potential. At right is the amplitude of the response vector at all stimulation rates in arbitrary units produced by the KL procedure. The horizontal line indicates zero amplitude. As expected, the highest amplitude is at the lowest stimulation rate (0.5Hz). As stimulation rate increases from 0.5 to 2Hz, there is a systematic decrease in the amplitude of the N1. After 2Hz the amplitude pattern is noisier but near zero for all subjects.

2.3.3. *Amplitude of the P2*

Figure 2.3 presents the results of the same KL procedure applied to the 200ms P2 component of the evoked response. For all subjects, at least 80% of the variance at the selected latency is accounted for by the top mode of the decomposition. As above, the latency of the P2 was chosen at the time of maximal amplitude in any sensor at a stimulation rate of 0.5Hz. This rate showed the highest amplitude P2 in all subjects, with peak latency ranging from 203 to 227ms. The P2, while opposite in polarity to the N1, has a spatial pattern similar to the earlier component (the angles between the spatial patterns of the N1 and P2 are 164.4°, 159.4°, 167.7°, & 158.2° for subjects 1-4, respectively). The component reaches a maximum at frontal and central channels, with the peak at a location similar to each subject's N1. The amplitude of the response also exhibits a pattern of rate dependence similar to the N1, with the amplitude systematically decreasing from 0.5 to 2Hz. After 2Hz the amplitude of the component varies around zero.

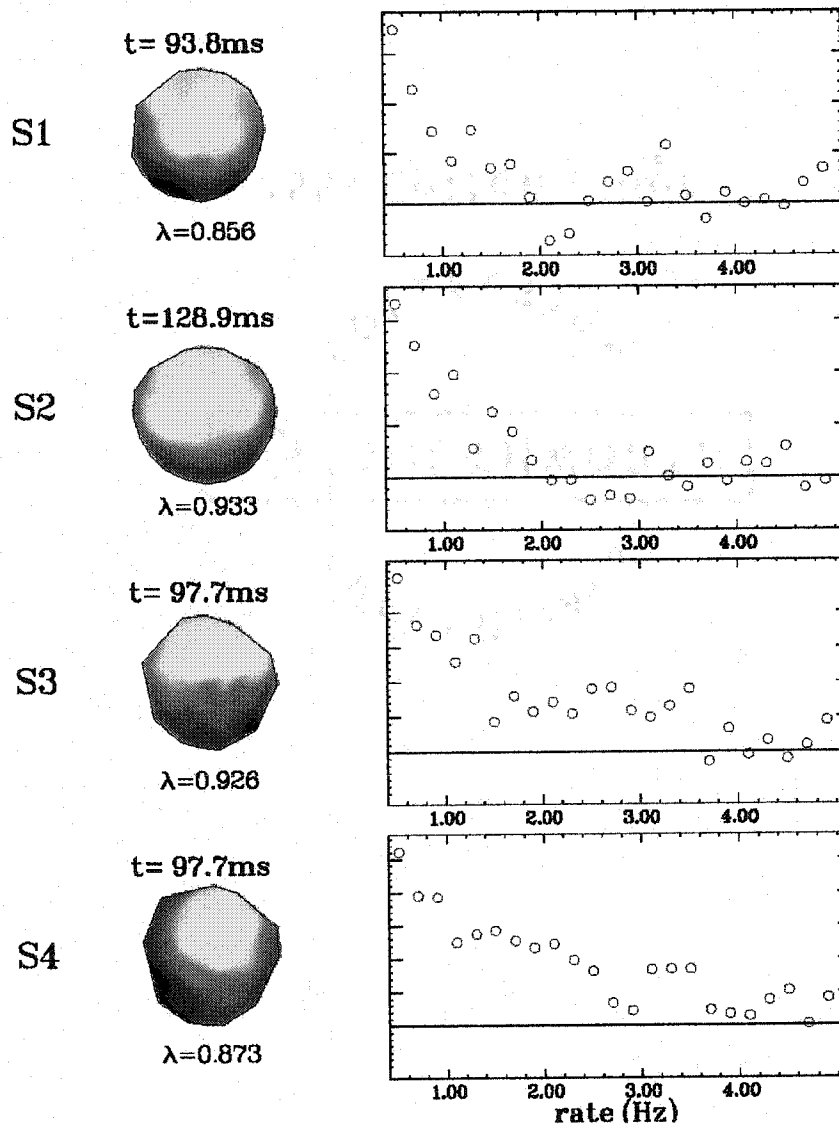


Figure 2.2. The first mode of the KL decomposition of the peak N1 response patterns at all stimulation rates. The common latency at which the decomposition was performed for each subject was determined from the peak response time at the slowest rate. The high λ values beneath each topographic map reflect the large portion of the signal accounted for by the first mode. The y-axis scale is in arbitrary units produced by the decomposition procedure.

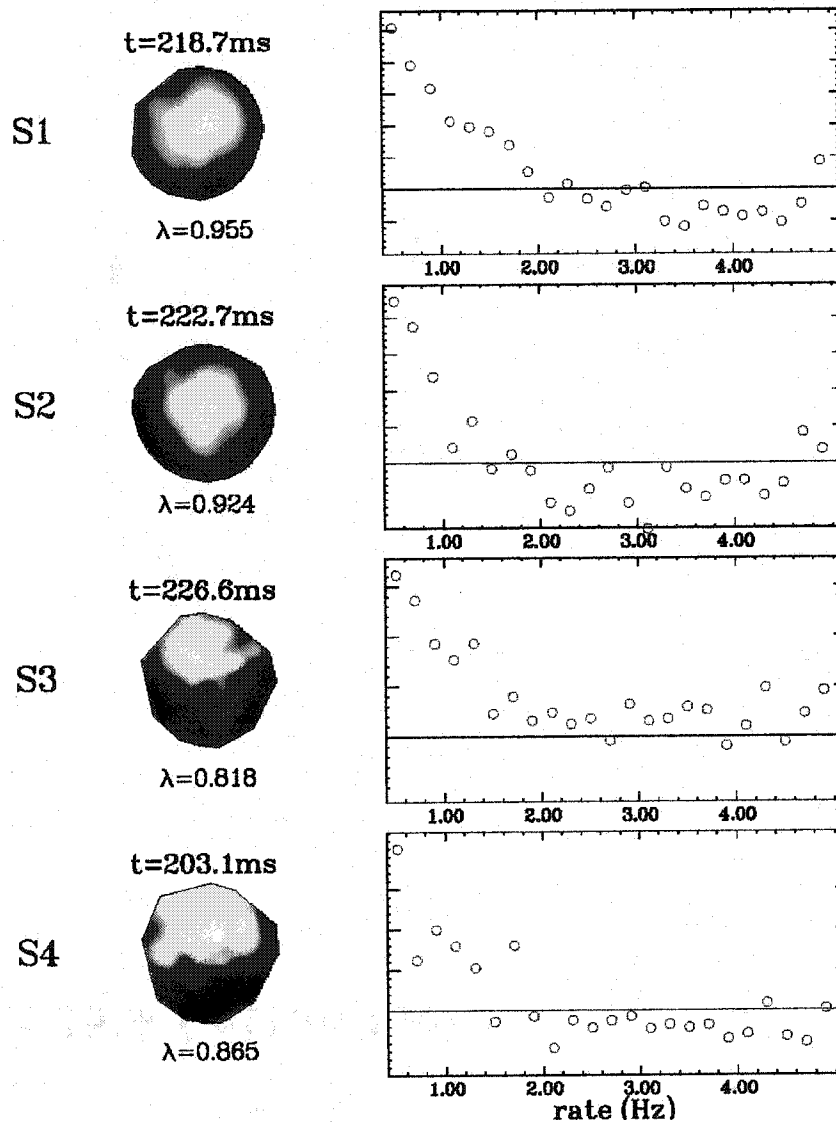


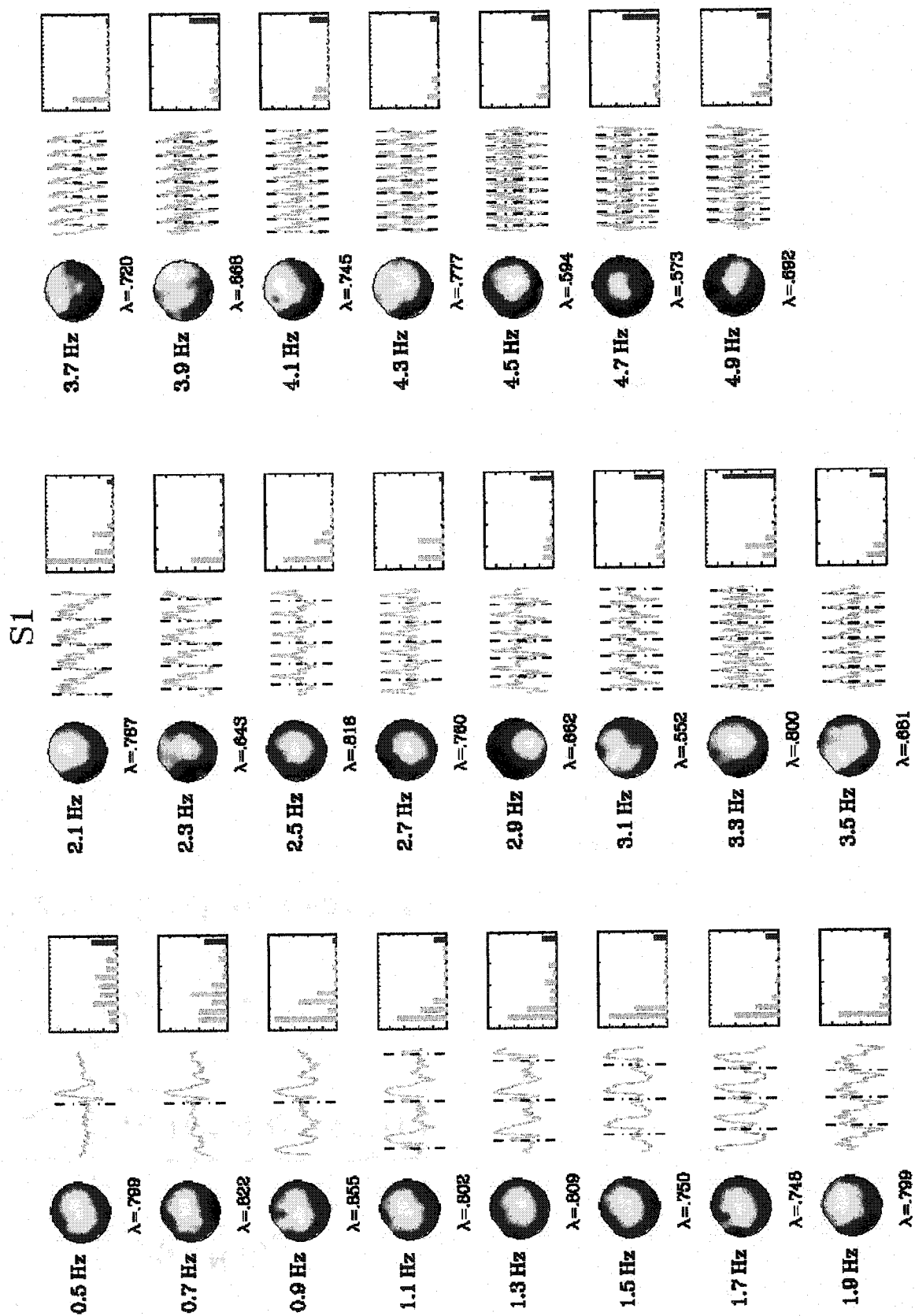
Figure 2.3. The first mode of the KL decomposition of the peak P2 response patterns at all stimulation rates. The common latency at which the decomposition was performed for each subject was determined from the peak response time at the slowest rate. The high λ values beneath each topographic map reflect the large portion of the signal accounted for by the first mode. The y-axis scale is in arbitrary units produced by the decomposition procedure.

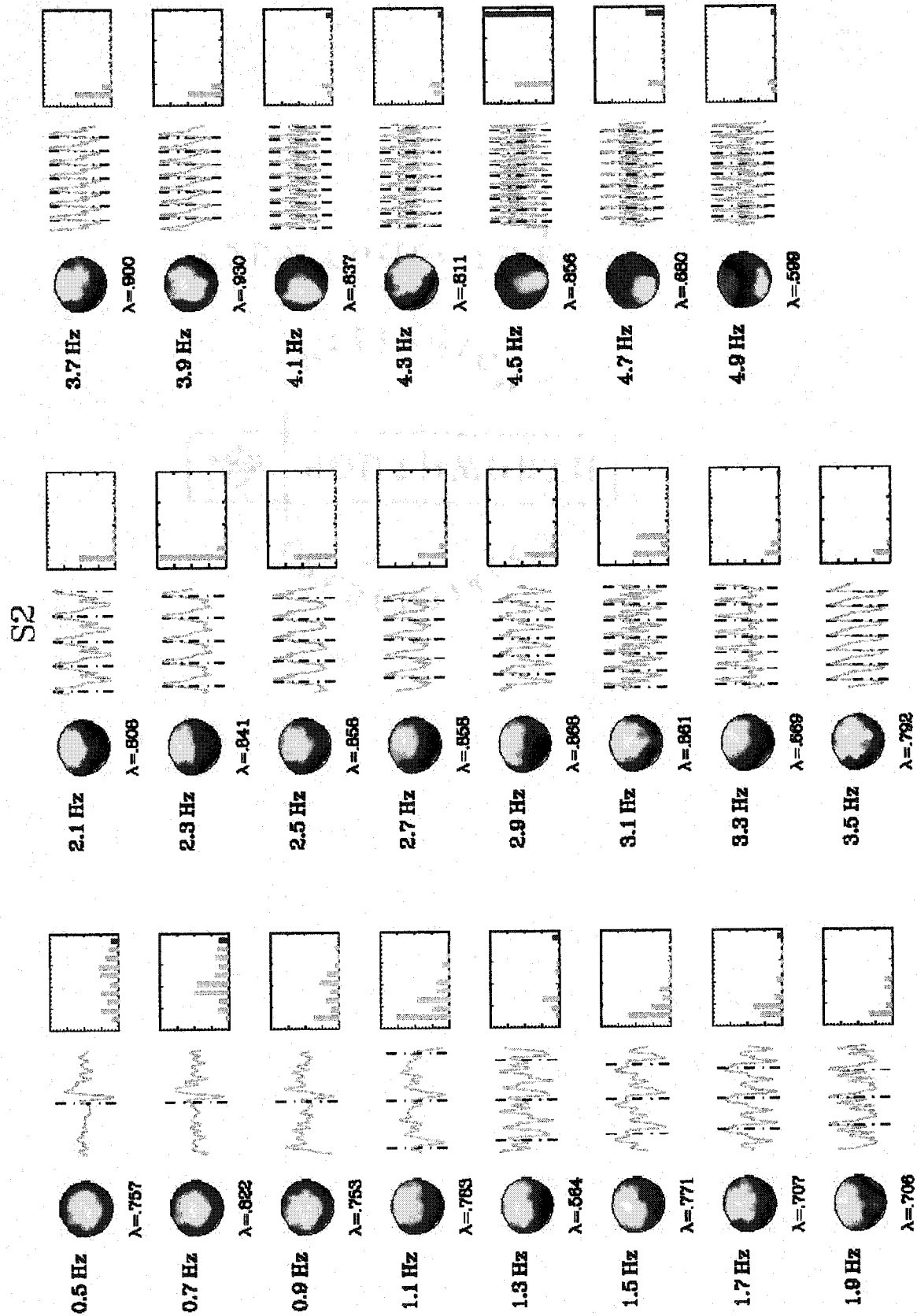
2.3.4. *Resonance of the Overall Response*

Figure 2.1 showed slow wave potential oscillations at the fundamental and higher frequencies for stimulation rates above 2Hz at Cz. The intent of the following analyses was to search for evidence of resonances at harmonics of the stimulus frequency across the entire sensor array. For this purpose the KL procedure was used to analyze the spatiotemporal evolution of the evoked response at each rate for one cycle of averaged data centered at tone onset. Figures 2.4a-d present the results for subjects 1-4, respectively. The spatial modes of the decomposition accounting for the largest variance at each rate are displayed along with their eigenvalues. The modes account for over 50% of the variance at each rate, with the majority over 80%. Shown to the right of each spatial pattern (or eigenvector) is the time series of activation of the pattern for an interval of two seconds for all rates. At far right for each rate is a power spectrum performed on the single cycle time series. The fundamental frequency is at left, with higher harmonics shown in order from left to right. The red bar at right shows the ratio of the second to the fundamental frequency, which is meant to highlight frequency doubling of the response.

At low rates in all subjects the top mode primarily captures the variance associated with the N1/P2 complex, as should be expected given their large amplitude at these rates. This is reflected in both the spatial pattern and time series of the dominant mode, and is a result of the near opposite spatial patterns of the N1 and P2 responses in each subject (see angle measures in section 2.3.3), which allows both patterns to be expressed by a single spatial mode. The power spectrum of the time series at low stimulation rates shows a complex response spread across a wide range of frequencies.

Figures 2.4a-d. KL decomposition applied separately to each stimulation rate for subjects 1-4, respectively. The decomposition was performed on one cycle length of data centered at tone onset. A cycle length for each rate is defined by the inter-stimulus interval. At left for each rate is the spatial mode of the decomposition accounting for the most variance. The eigenvalues are displayed below each mode. Middle: Time series of activation of the top mode, centered at tone onset. A complete single cycle interval of two seconds is shown at 0.5Hz. The same length of time is displayed at all rates, with the time series repeated at higher rates in order to fill out two seconds. Dashed lines indicate tone onsets. Right: Power spectrum for the time series of activation. Green bars indicate the power at the fundamental frequency and higher harmonics in order from left to right (e.g. for a stimulation rate of 1Hz, the bar at left is power at 1Hz, and the succeeding bars are power at 2Hz through 9Hz in order from left to right). The red bar at right highlights frequency doubling of the response by showing the ratio of power at the first harmonic to the fundamental frequency.





S3

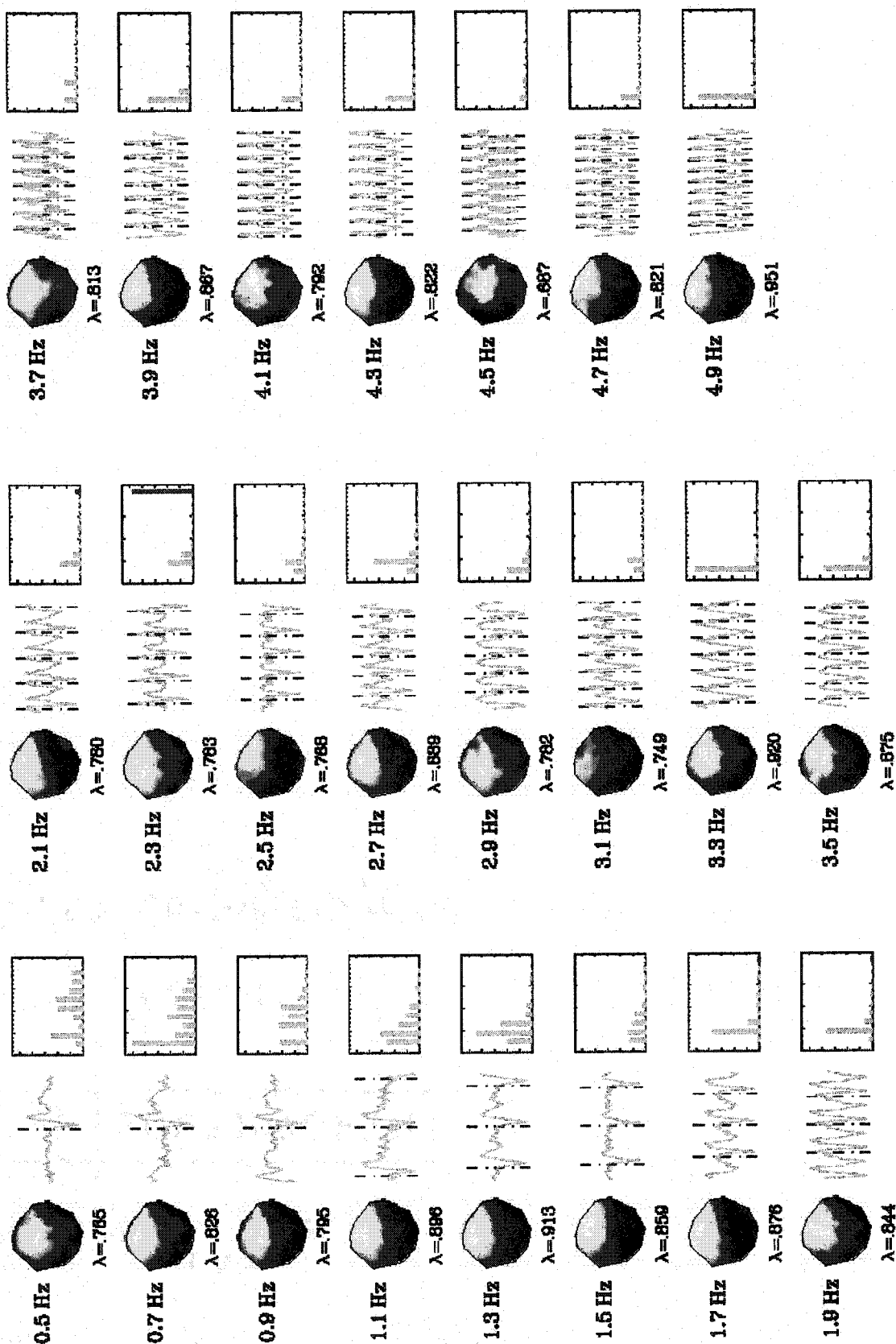


Figure 2.4c

S4

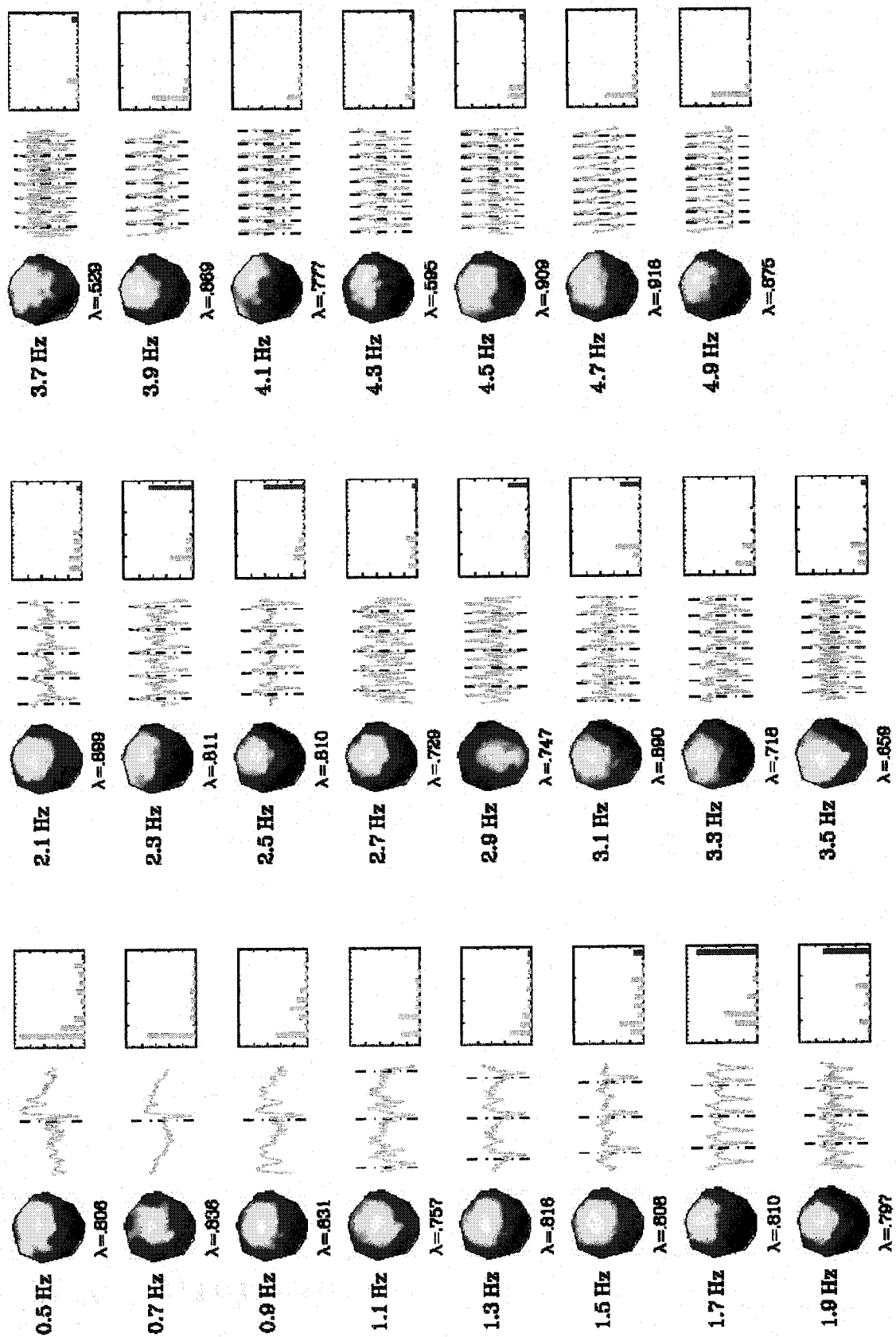


Figure 2.4d

The evolution of the response at higher rates presents a variable picture across subjects, although a common trend does emerge. As was evident in the single channel time series from figure 2.1, at rates above 2Hz the overall response shows continuous activity between tones, which implies that the time between tones is insufficient for the activity elicited by each tone to reach baseline before the next tone onset. In addition, a rhythmic resonant type response emerges at rates above 2Hz at low multiples of the stimulation rate. For subject 1 (figure 2.4a), the spatial pattern of the dominant mode shifts to frontal channels at 1.9 and 2.1Hz. This is accompanied by the onset of a rhythmic response with power concentrated mostly at the fundamental frequency (i.e. the rate of stimulation). At higher rates, the time series contain a larger portion of oscillation at twice the fundamental. A similar pattern of increased power at the fundamental and frontal shift of activity near 2Hz is repeated for subject 2 in figure 2.4b. This subject further shows a strong frequency doubling effect at 4.5Hz, accompanied by a posterior shift in activity. Considering that 9Hz is in the alpha frequency range, the frequency doubling could relate to residual occipital alpha activity (see figure 2.1). Subject 3 exhibits oscillation at twice the fundamental around 2Hz (figure 2.4c). Resonance at the fundamental occurs at rates of 3Hz and above. Likewise, for subject 4 frequency doubling also occurs near 2Hz, and resonance at the fundamental begins at higher rates.

2.4. Results: Spontaneous and Evoked Gamma Activity

In this section, we test the hypothesis that the 40Hz mid-latency oscillation is related to spontaneous gamma activity occurring pre-stimulus. Figure 2.5 presents an example of the mid-latency response for subject 4 at a stimulation rate of 4.3Hz. The

average time series is from a single channel (Cz), which was band-pass filtered between 30 and 50Hz. After stimulus onset (time zero), the channel displays a brief oscillation at 40Hz with peaks at times consistent with the MLR. The maximum positive amplitude occurs near 30ms, which is a peak traditionally termed Pa in EEG (Picton et al., 1974). At top in figure 2.5 is the spatial pattern of the Pa component. The activity pattern is a broad positive deflection with similar amplitude at all sensors. The largest negative deflection, traditionally termed Nb, is plotted at bottom. The spatial pattern displays distributed activation across all the sensors similar to the previous Pa component. The similarity of these two patterns implies that the mid-latency response represents a single pattern of coherent oscillation across the entire sensor array.

In order to assess whether this gamma oscillation relates to spontaneous or ongoing gamma activity we applied ICA decomposition to the unaveraged data for the same subject and rate as in figure 2.5 (subject 4 at 4.3Hz). After decomposition, the resulting spatiotemporal modes were placed in order of variance accounted for in the original data. Figure 2.6 shows the mode of ICA decomposition capturing the most variance (68% of the total). The spatial pattern of the decomposition exhibits a distributed pattern of coherent activation at all the sensors, similar to the average pattern in figure 2.5. The plot at center in figure 2.6 displays sample activation time series for the top ICA mode across two stimulation cycles. Each time series contains a significant amount of gamma oscillation occurring both pre and post stimulus. At bottom in figure 2.6 is a plot of the average of the time series at all the stimulation cycle epochs. The pattern of temporal activation revealed in the average is nearly identical to the average pattern in figure 2.5, which indicates that the ICA decomposition has captured the

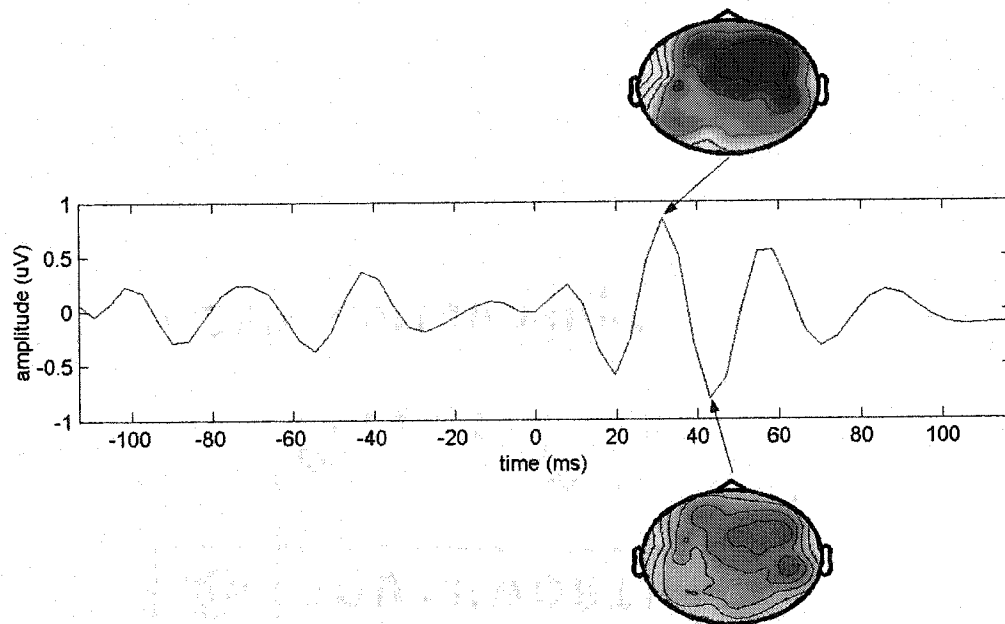


Figure 2.5. The average mid-latency response for subject 4 at 4.3Hz. One cycle of data is shown centered at tone onset for channel Cz. The raw data was band-pass filtered from 30 to 50Hz prior to averaging. At top and bottom are the topographic patterns of activation at the positive and negative peaks of the response. The positive peak corresponds to mid-latency response Pa, while the negative peak is response Nb.

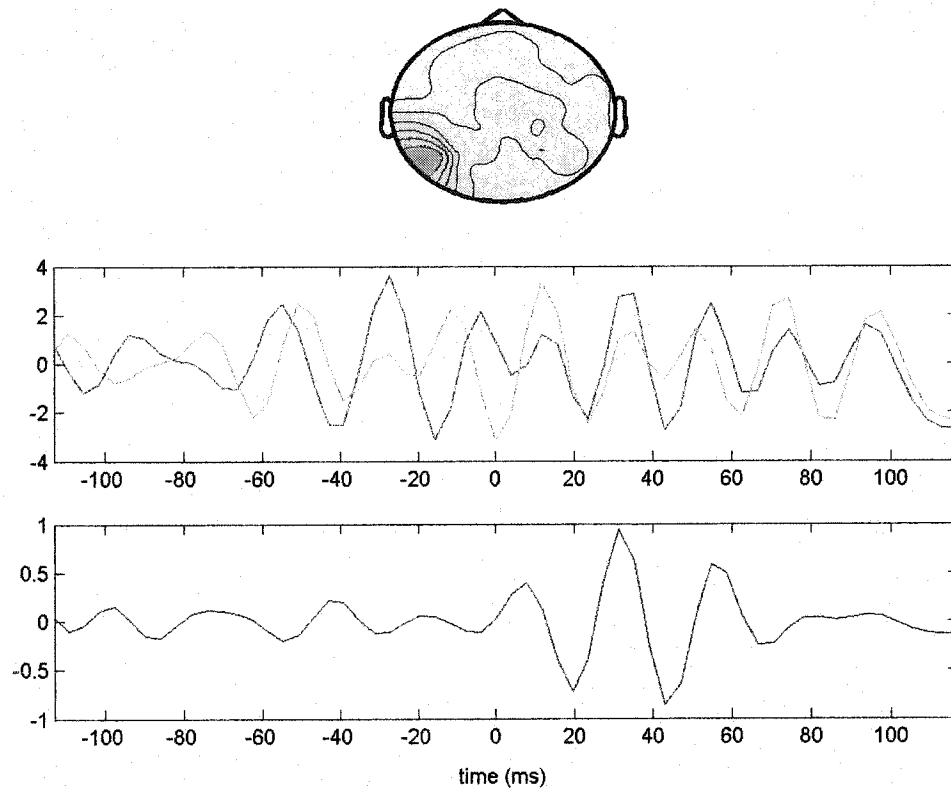


Figure 2.6. ICA mode accounting for the mid-latency response in unaveraged data at 4.3Hz for subject 4. Top: Topographic image of the ICA mode. Red/yellow indicates positive potential distributed throughout the sensors. Middle: Two activation time series of the ICA mode for single tones. Each time series contains gamma oscillations before and after the stimulus. Time is on the horizontal axis centered at tone onset. The vertical axis is amplitude in arbitrary units produced by the decomposition procedure. Bottom: Average of the activation time series. The average shows a gamma response after tone onset with peaks at the same latencies as the mid-latency response in figure 2.5. The mid-latency gamma response makes up the majority of average activity, suggesting that pre-stimulus gamma activity is not phase-locked to the stimulus.

spatiotemporal activation pattern of the mid-latency response. In the plot at center, the two unaveraged time series display synchronized oscillations at the same phase as the average mid-latency response after stimulus onset. However, the amplitude of the ongoing oscillation does not change, which could indicate that the evoked gamma response represents a phase resetting of ongoing gamma activity. This idea was tested by sorting the activation time series associated with each tone by the phase of the pre-stimulus gamma activity. The results of the phase sorting are presented in figure 2.7. The figure shows a 156ms window centered at tone onset, with sorted tone-epochs on the vertical axis. Amplitude is represented by a red-positive blue-negative color scale. Most tone-epochs show strong gamma oscillations at all latencies, with similar amplitudes pre- and post-stimulus. The pre-stimulus activity has an even distribution of phases of the gamma oscillation (tilted lines), while post-stimulus, the oscillation shows a single phase with amplitude maxima vertically aligned with the mid-latency response. This supports the idea that the mid-latency response represents a phase resetting of the ongoing gamma oscillation, instead of a pure evoked response unrelated to background activity. Additionally, the amplitude of the post-stimulus oscillation does not appear to be consistent across phase. At bottom-right in the plot, the amplitude of the mid-latency response is attenuated for a broad range of phases, indicating that there may be a preferred phase range for eliciting an evoked response, with the largest amplitude response occurring when stimulation reaches the cortex near the positive peak of the ongoing oscillation.

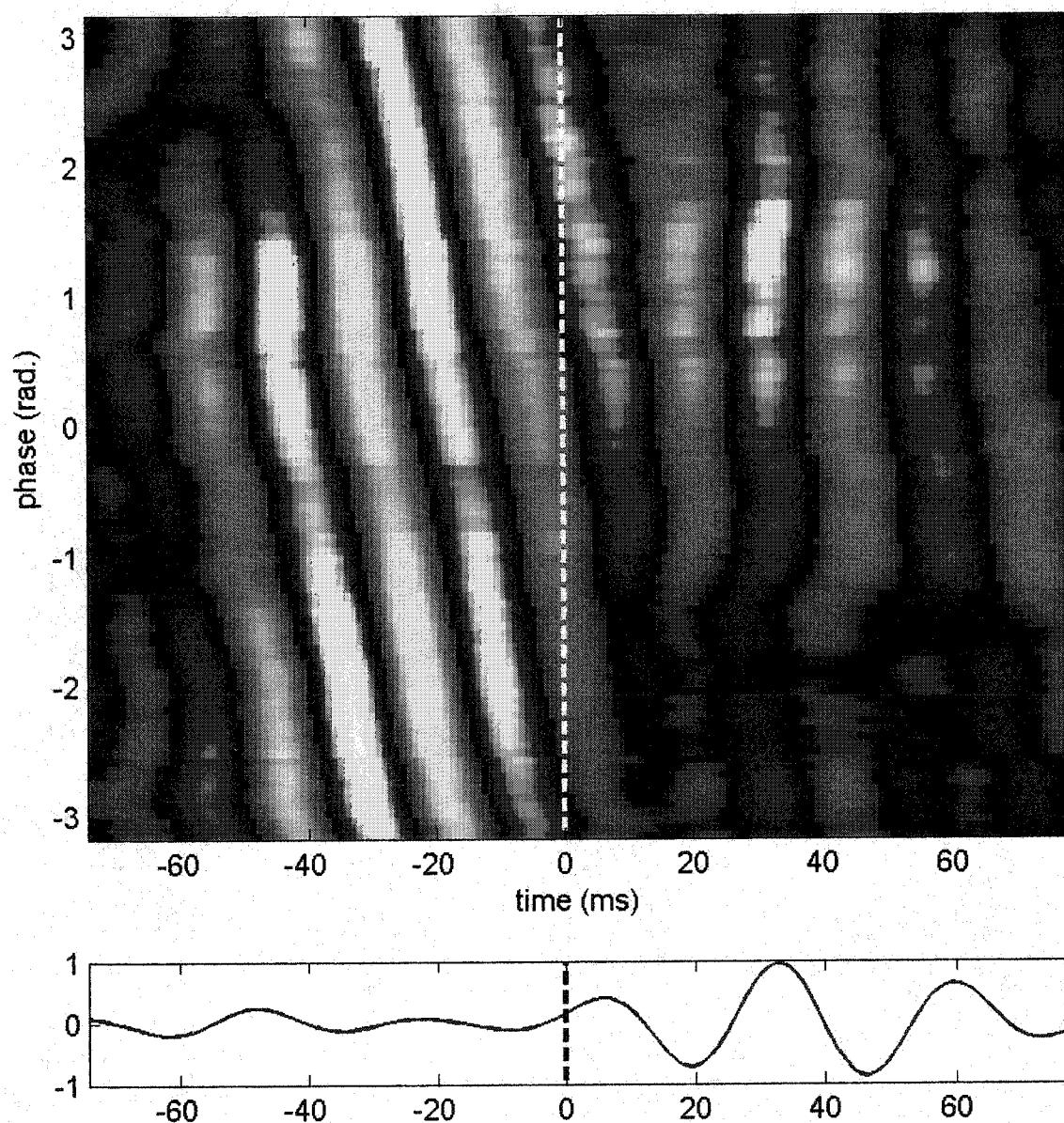


Figure 2.7. Top: Phase-sorted time series of the response to each tone for the ICA mode from figure 2.6. The time series are sorted according to the pre-stimulus phase of the gamma oscillation. Tone onset is indicated by the white dashed line. Amplitude of the response is represented by a red-positive / blue-negative color scale. Pre-stimulus diagonal stripes indicate random phase. Post-stimulus the oscillation is reset to be phase-locked to the stimulus. The lack of activity at bottom-right implies that there is a preferred phase of the pre-stimulus gamma activity for evoking a mid-latency gamma response. Bottom: Average of the single tone-epoch time series, with amplitude in arbitrary units. Tone onset is indicated by the black dashed line.

Figure 2.8 presents the same phase resetting plot for a different subject (subject 1). In this case, the ICA decomposition was performed at a rate of 3.9Hz. The results of the decomposition are similar to those of the previous subject; the spatial pattern of the mode accounting for the most variance (31% of total) is a distributed coherent oscillation across all the sensors, and the average time series of the mode, shown at bottom, captures the evoked gamma response. In addition, the phase-sorted plot reveals a similar pattern of phase resetting of the ongoing gamma oscillation.

Subject 4 displayed a strong mid-latency response at all rates in this experiment. To test whether the phase resetting pattern is consistent across all rates, we applied the ICA decomposition procedure to the entire set of raw data for this subject. The raw tone-epochs from all rates were grouped together and a single ICA decomposition applied to the entire dataset. In order to have a similar proportion of data from each rate, a 200ms window of data was used from each tone, with the data centered at tone onset. Figure 2.9 presents the results of the ICA procedure. The top mode of the decomposition captured 54% of the original variance. The spatial pattern of the mode at bottom-right shows a pattern of distributed activation similar to the decompositions performed at single rates. To the left of this pattern is the average of all tone-epochs, which, as expected, displays a pattern of activation consistent with the mid-latency response. Above this average is the phase-sorted plot for all the single tone-epochs. As in the previous figures, the pre-stimulus phase distribution is random. Post-stimulus, the oscillation is reset to be phase-locked to the stimulus. The post-stimulus activity also displays an apparent amplitude dependence on the phase of the pre-stimulus activity. The plot at right displays the pre-stimulus phase / post-stimulus amplitude relationship. The horizontal axis indicates

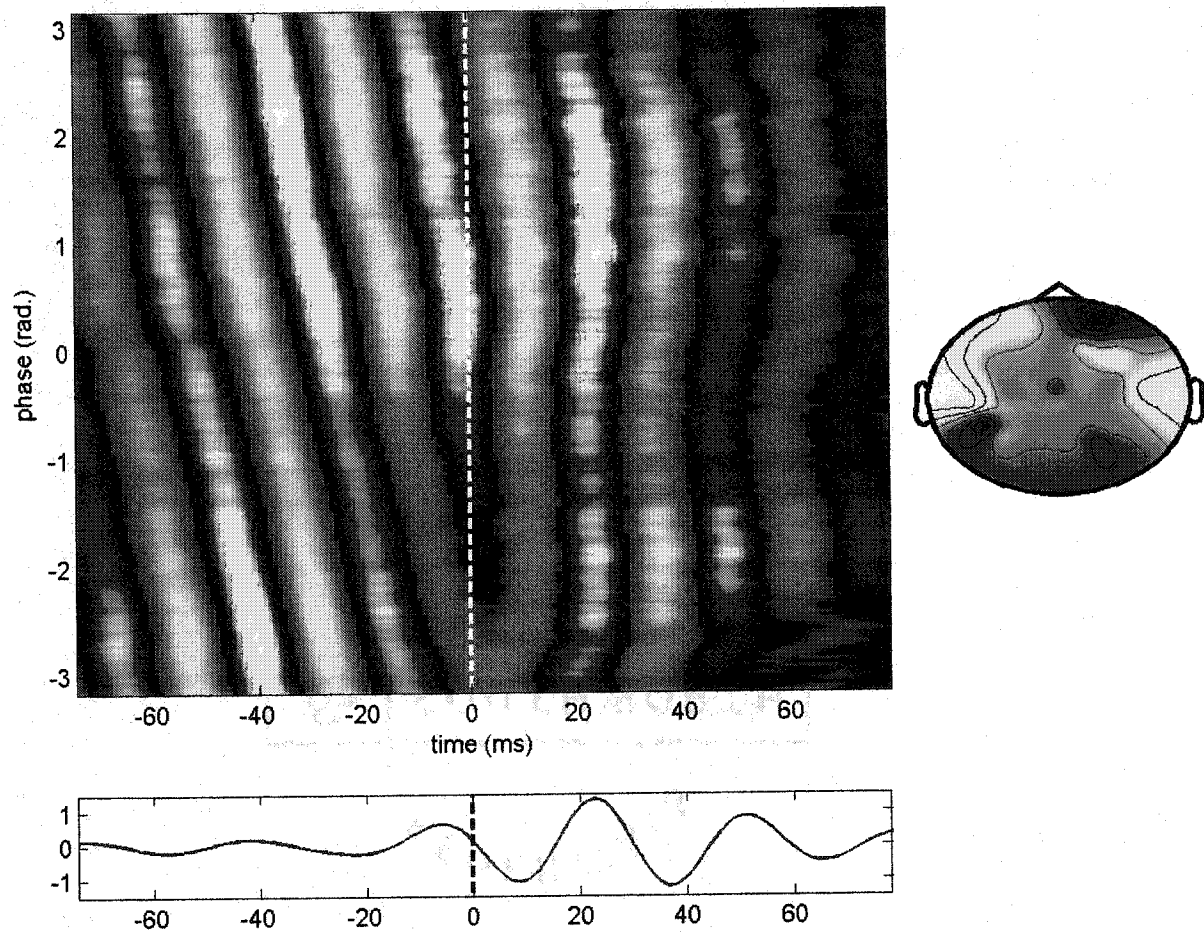


Figure 2.8. Results of the single tone-epoch ICA decomposition for subject 1 at 3.9Hz. Right: Topographic image of the top mode of the decomposition. Top-left: Phase-sorted time series of the ICA mode. The time series are sorted according to the pre-stimulus phase of the gamma oscillation. Tone onset is indicated by the white dashed line. Amplitude of the response is represented by a red-positive / blue-negative color scale. Pre-stimulus diagonal stripes indicate random phase. Post-stimulus the oscillation is reset to be phase-locked to the stimulus. Bottom: Average of the single tone-epoch time series, with amplitude in arbitrary units. Tone onset is indicated by the black dashed line.

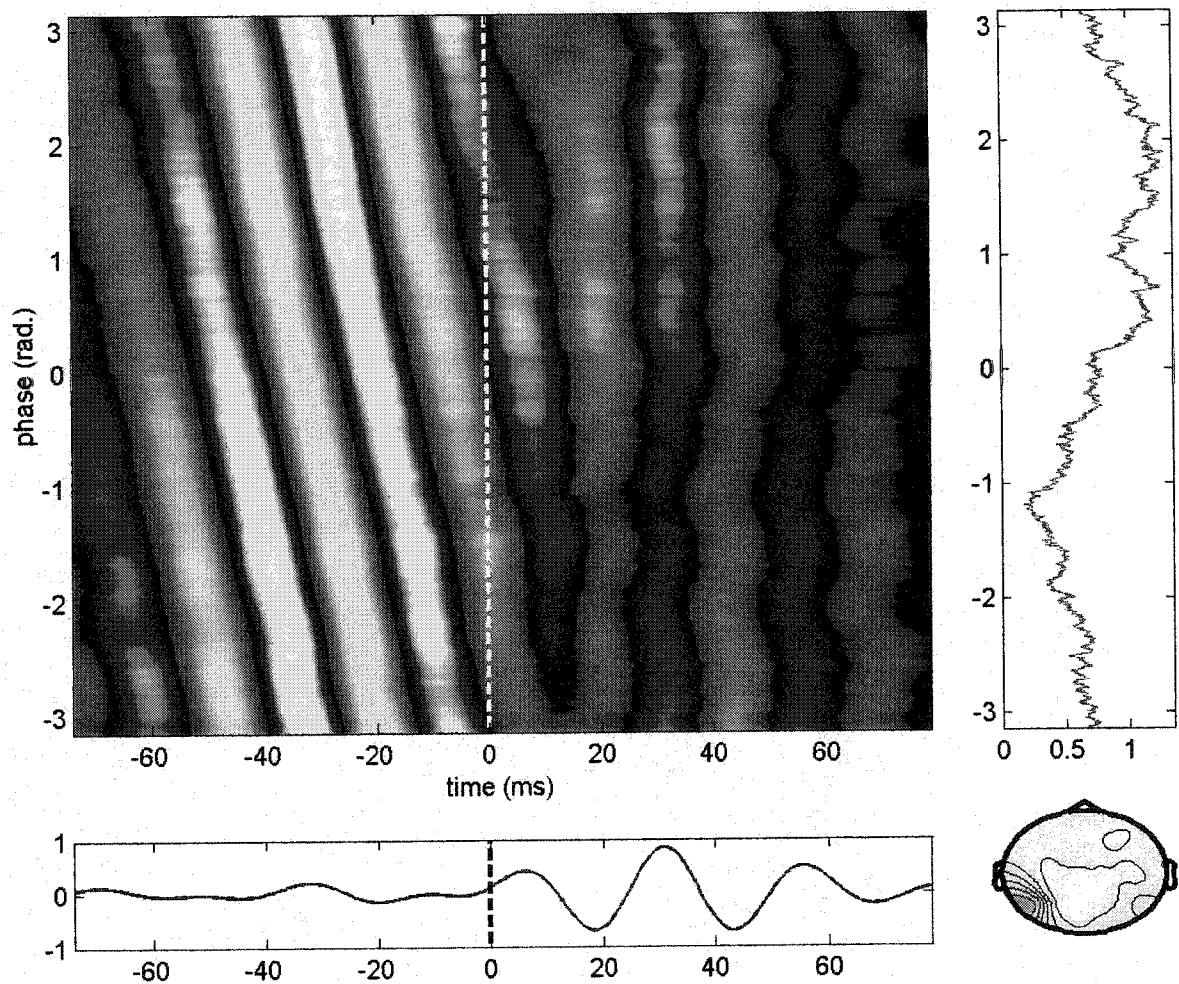


Figure 2.9. Results of the single tone-epoch ICA decomposition for subject 4 at all stimulation rates. Bottom-right: Topographic image of the top mode of the decomposition. Top-left: Phase-sorted time series of the ICA mode. The time series are sorted according to the pre-stimulus phase of the gamma oscillation. Tone onset is indicated by the white dashed line. Amplitude of the response is represented by a red-positive / blue-negative color scale. Pre-stimulus diagonal stripes indicate random phase. Post-stimulus the oscillation is reset to be phase-locked to the stimulus. Bottom-left: Average of the single tone-epoch time series, with amplitude in arbitrary units. Tone onset is indicated by the black dashed line. Top-right: Phase-dependent amplitude of the evoked gamma response. Phase of the pre-stimulus activity is in radians on the vertical axis. Maximum amplitude of the evoked response is on the horizontal axis.

amplitude of the evoked gamma response for each phase of the pre-stimulus oscillation. The phase scale is the same as for the color plot at left. Amplitude of the evoked response at each phase was determined by searching for the maximum positive and negative amplitudes of the response after 10ms latency. We used the average of the absolute amplitudes of the positive and negative peaks as an estimate of response amplitude. The results confirm a phase / amplitude relationship. For phases above 0 radians, the amplitude of the evoked response is greater than for phases below 0 radians. Referring back to the color plot, this phase relationship implies that stimulation at or just after the positive peak of the ongoing oscillation produces the maximum amplitude response.

2.5. Discussion

2.5.1. Rate Dependence of Response Components

One goal of this experiment was to characterize the rate dependence of N1 and P2 components of the averaged auditory evoked response over a broad range of rhythmic stimulation rates. For the N1 this is the first experiment to study the rate dependence of the response at stimulation rates higher than 1Hz. Previous studies using EEG have employed ISIs on the order of seconds (Hari et al., 1982; Hari et al., 1987), and do not cover the parameter range perceived to be rhythmic. These studies have shown that the amplitude of the N1 decreases systematically with increased ISI. Additionally, the response amplitude becomes asymptotic as ISI increases above 10 seconds (Hari et al., 1982). More recently, experimenters have concentrated on the corresponding N1m component observed with MEG (Mäkelä et al., 1993; Sams et al., 1993). The rate

dependence of the N1m was modeled by Lü et al. (1992) using an exponential function of the form $A(1 - e^{-(t-t_0)/\tau})$, with amplitude A , ISI t , time of decay onset t_0 , and lifetime τ . According to this model, the response should disappear at an ISI equal to the length of the stimulus. Thus, the N1m is considered refractory with respect to tone offset. Our previous MEG experiment of rhythmic auditory stimulation was the first to test this prediction at rates above 1Hz (Carver et al., 2002). We found an earlier than expected disappearance of the response at ISIs near 150ms. Here we also show a systematic decrease of the N1 with increased stimulation rate. However, the response tapers out near a rate of 2Hz, which is far earlier than the rate predicted by Lü et al. (1992) and the rate found in our previous MEG study. A possible explanation of this discrepancy is the different sensitivities of the two recording technologies. Past research utilizing both EEG and MEG in auditory recordings indicates that for slower rates there is a significant difference between the rate dependence of the N1 and N1m (Hari et al., 1982). The authors suggest that the difference may originate from multiple source contributions to the N1 and the fact that MEG is insensitive to radial components (Huotilainen et al., 1998; Virtanen, Ahveninen, Ilmoniemi, Näätänen, & Pekkonen, 1998). It is known that multiple sources contribute to the N1/N1m, with more components apparent in EEG as opposed to MEG (for a review see Woods, 1995). Possibly, the difference in N1 rate dependence seen here is a product of contributions from additional sources. In addition, we revealed in the previous MEG work that 2Hz marks the onset of the continuous steady-state response. Here the onset of the SSR is associated with resonance of the overall response at low multiples of the stimulation rate. This phenomenon may also prevent observation of the N1 response at rates above 2Hz.

The study by Hari et al. (1982) is one of the few to discuss the rate dependence of the P2. Most of the more current work on the rate dependence of auditory response components has exclusively used MEG because of its presumed advantage for source localization (Mäkelä et al., 1993; Sams et al., 1993). However, this technology is poor for investigating the P2, because the component typically is not apparent in MEG recordings. Hari et al. (1982) showed that the P2 exhibits a similar pattern of rate dependence as the N1 for stimulation rates below 1Hz. The present results confirm that a similar pattern exists for higher rates as well. The response amplitude falls off systematically as stimulation rate increases to 2Hz. At higher rates, just as with the N1, the component tapers off to a negligible amplitude. The similar rate dependence of the N1 and P2 suggests that they are part of the same process in the cortical auditory response, and may best be considered as a single biphasic component.

2.5.2. Resonance and Response Overlap

In our previous MEG experiment we observed that the transition from a transient to a steady-state response began near 2Hz (Carver et al., 2002). Here we reveal that rates of 2Hz and above are associated with an increase in resonant activity of the entire response at low multiples of the stimulation rate (figures 2.4a-d). For the MEG experiment we used the Regan (1982) definition of the border between the transient and steady-state response. By this definition, the transition occurs when discrete transient responses begin to overlap to form continuous activity between tones. However, some authors use a more strict definition of the steady-state response, namely that the SSR is continuous evoked activity that is phase-locked to the stimulus at low multiples of the

stimulation rate (Galambos et al., 1981; Regan, 1989). In this definition, the primary steady-state response occurs at a stimulation rate of 40Hz, since stimulation at this rate elicits a clear resonant response in the cortex at the stimulus frequency. However, Picton et al. (1987) demonstrated that this is not the only rate of stimulation that produces resonant activity in the cortex. The authors used amplitude modulation of a simple tone to drive the auditory response and found two resonant regions of stimulation: one from 20 to 50Hz, and the other from 2 to 5Hz. The second region coincides with the range of rates over which we found resonant activity elicited by rhythmic tone stimulation. Therefore, by either definition of the steady-state response, i.e. overlapping transient responses or resonance at low multiples of the stimulation rate, we have shown that the steady-state response begins near a stimulation rate of 2Hz. The association between response overlap and resonance at low multiples of the fundamental is likely not coincidental. As long latency responses begin to overlap, they presumably would interact with each other and cause a fundamental transition in the nature of the auditory response. In our earlier MEG experiment, we demonstrated the effect of response overlap on the early part of the long latency response (Carver et al., 2002). The interaction between the evoked responses to successive tones was associated with a significant increase in the amplitude of the P1m response at 60ms latency.

The direct perceptual and behavioral consequences of the onset of the steady-state response are potentially far reaching. The onset of overlap between the auditory traces of each tone marks the beginning of a continuous perceptual representation of the ongoing auditory activity. This may be related to subjects marking 2Hz as a preferred frequency of rhythmic stimulation when they are asked to tune a metronome to their liking (Fraisse,

1982). In addition, subjects are better able to distinguish small changes in tempo near a stimulation rate of 2Hz (Drake & Botte, 1993). Such results led Drake and Bertrand (2001) to label rates near 2Hz as a 'zone of optimal processing' for rhythm perception. These findings suggest that the onset of resonant activity in the cortex marks a period of perceptual resonance as well. Auditory stimulation at 2Hz also marks a transition point in the ability of subjects to syncopate with a series of tones (Kelso et al., 1990). Near this rate subjects spontaneously switch to a synchronized mode of coordination. This may also be related to the beginning of continuous resonant activity in the cortex, since at 2Hz the cortical representation of the movement may begin to entrain with the auditory evoked response. We also show that 2Hz is associated with the disappearance of the N1 in EEG. The N1 is thought to be a reaction to change in the auditory environment (Näätänen & Winkler, 1999), and so the attenuation of the component may reflect a rate beyond which the tones are primarily perceived as part of a rhythmic whole instead of discrete events in time. These relationships between brain and behavior are potentially significant for our understanding of the correlation between observed EEG activity and perception, and should be further investigated.

2.5.3. Spontaneous and Evoked Gamma Activity

In Makeig et al. (2002) the ICA procedure employed here was used to analyze the relationship between spontaneous cortical oscillations and activity evoked by a visual stimulus in EEG. The authors demonstrate that evoked alpha oscillations (~10Hz) are generated by phase resetting of ongoing alpha activity, although the post-stimulus activity only tended toward a certain phase while all phases were still present. This is in contrast

to the present results, which show nearly all post-stimulus gamma oscillations reset to the same phase. Tesche and Karhu (2000) found anticipatory phase resetting of a 7Hz theta rhythm in the hippocampus using MEG. The authors employed a method known as signal space projection to analyze the raw signals, which is distinct from ICA in that it assumes a set of sources prior to signal decomposition. Taken together, these results challenge the traditional view that evoked responses are unrelated to ongoing cortical activity. Increasingly, researchers are suggesting that evoked activity results from alteration of ongoing cortical dynamics, which implies that averaging of evoked responses produces a significant loss of information by attenuating non phase-locked activity (Başar, 1980; Brandt, Jansen, & Carbonari, 1991; Jirsa & Kelso, 2000; Snyder & Large, submitted).

The perceptual correlates of the phase resetting behavior observed here should be further investigated. For instance, Tiitinen et al. (1993) demonstrated that attending to auditory stimuli increased the amplitude of the evoked gamma response. If the evoked response is generated by phase resetting of ongoing activity, then the Tiitinen et al. (1993) results may imply that increased jitter in the post-stimulus phase produces a smaller average. Synchronized gamma activity has been linked to binding of cortical areas in perceptual and perceptuomotor tasks (Başar-Erglu, Strüder, Schürmann, Stadler, & Başar, 1996; Bressler, Coppola, & Nakamura, 1993; Gray & Singer, 1989; Sauvé, 1999; Talon-Baudry, Bertrand, Delpuech, & Pernier, 1996). The phase resetting behavior seen here could act as a means to synchronize gamma activity across disparate areas of cortex. Here the phase resetting occurred at a latency when thalamic input is known to be reaching the cortex. If cortical areas receiving simultaneous thalamic input are all reset

to the same phase of the gamma oscillation, it would provide a fast mechanism to synchronize gamma activity in separate areas of cortex.

The relationship between gamma phase resetting and the 40Hz steady-state response also deserves further investigation. Because spontaneous and evoked gamma oscillations were captured by the same ICA spatial mode, we assumed that they arose from the same source locations. This assumption is supported by recent findings from intracortical recordings in rats (Sukov & Barth, 1998, 2001). The authors showed that the peak of both evoked and spontaneous auditory gamma oscillations arise from a ventrotemporal region on the border of primary and secondary auditory cortex. If spontaneous and evoked gamma oscillations arise from the same location, then it is reasonable to hypothesize that the same phase resetting behavior would be observed when evoked gamma responses begin to overlap and interact at fast stimulation rates. In this study we revealed that the maximum amplitude evoked response occurs when stimulation comes at or just after the peak of the spontaneous oscillation. If this behavior also occurs when evoked responses overlap, then resonance of the steady-state response at certain stimulation rates could be explained by the phase of the evoked gamma response at which activity related to a new stimulus reaches the cortex.

**Experiment 3: Neuroelectric Activity Associated with Rhythmic
Movements: Separation of Overlapping Response Components Using
Independent Components Analysis**

3.1. Introduction

Studies of rhythmic movement commonly find rate-dependent transitions in coordinative abilities and distinct behaviors associated with specific ranges of movement rates. For instance, when subjects perform rhythmic bimanual coordination in an anti-phase pattern, they spontaneously switch to in-phase oscillation with increased rate (Haken, Kelso, & Bunz, 1985; Kelso, 1984). Such transitions typically occur at rates around 2Hz. A similar transition occurs when subjects are asked to flex their index finger between metronome beats, i.e. syncopate. As stimulation rate is increased subjects find the task more and more difficult, and beyond a critical point they spontaneously switch to a movement pattern synchronized with the metronome (Kelso, DelColle, & Schöner, 1990). Again, the transition typically happens at movement rates approaching 2Hz. Additionally, at rates of 1Hz and higher subjects show a strong preference for synchronizing with a metronome despite having been instructed to react (Engström, Kelso, & Holroyd, 1996). Even without coordinative constraints, subjects show differential behaviors across rhythmic movement rates; for example, when asked to tap at a natural pace, subjects consistently prefer movements near a rate of 2Hz (Fraisse, 1982).

Studies of the neural correlates of sensorimotor coordination have observed significant alterations in ongoing cortical dynamics associated with behavioral transitions in EEG (Mayville, Bressler, Fuchs, & Kelso, 1999; Wallenstein, Kelso, & Bressler, 1995) and MEG (Fuchs, Kelso, & Haken, 1992; Jantzen, Fuchs, Mayville, Deecke, & Kelso, 2001; Kelso et al, 1992). However, the neurophysiological basis for such transitions remains unclear. With the current experiment we seek an understanding of the rate-dependent variation of electrical potentials generated by simple self-paced rhythmic movements, which may provide insight into behavioral transitions in more complex coordinative tasks. A continuation paradigm is commonly employed in studies of self-paced rhythmic movement in order to obtain movements at set rates without metronome interference (e.g. Ivry & Keele, 1989; Rao et al., 1997; Wing & Kristofferson, 1973). Each trial in a continuation paradigm begins with a synchronization phase in which subjects synchronize some aspect of a rhythmic movement, such as a finger tap on a computer key, with an auditory or visual metronome. This is followed by a continuation phase in which the metronome ceases and subjects are required to continue moving at the same rate. Here we employ the paradigm in an electroencephalography (EEG) study of cortical activity associated with self-paced rhythmic movements at rates ranging from 0.5 to 2.5Hz in 0.1Hz steps. A systematic investigation of a wide parameter range was employed in order to observe how the neural organization of rhythmic movement changes with increased movement rate. In a recent magnetoencephalography (MEG) study, Mayville et al. (submitted) employed a continuation paradigm over the same parameter range as here and observed a rate-dependent decrease in pre-movement activity associated with motor planning. This suggested that at higher rates movements

were no longer individually planned and controlled as discrete units, but were instead continuously monitored as part of a sustained oscillation. Here we seek similar evidence in EEG for such a qualitative transition in the cortical activity patterns associated with self-paced movements.

Cortical activity patterns associated with voluntary finger movements have been well documented in the EEG and MEG literature (e.g. Cheyne & Weinberg, 1989; Deecke, Grözing, & Kornhuber, 1976). However, the majority of these experiments used movements separated by several seconds, which is well outside the rhythmic range employed here. In EEG, such movements are preceded by a slow-wave negative potential over central electrodes known as the readiness potential or Bereitschaftspotential (BP). This deflection can start a second or more before EMG onset, and is thought to derive from sources involved in the preparation for movement such as the supplementary motor area (SMA) and pre-motor cortex (PMC) (Deecke & Kornhuber, 1978; Praamstra, Stegman, Horstink, & Cools, 1996). Relative contributions from motor planning areas may vary depending on task condition and difficulty, with SMA related more to internally generated movements, and PMC related to sensory-guided movements (Schubatz, Friederici, & von Cramon, 2000). The end of the BP is marked by a motor potential (MP) just before movement onset, which is thought to relate to the outgoing motor command from primary motor cortex (Barrett, Shibasaki, & Neshige, 1986). Following the BP/MP complex is a series of positive and negative peaks in the cortical potential beginning just after movement onset. These peaks are traditionally referred to as movement-evoked potentials because they relate to proprioceptive and cutaneous feedback from the movement. The first movement-evoked

potential is the most consistently observed of the evoked responses, with peak latencies ranging from 50 to 100ms after movement onset (Shibasaki, Barrett, Halliday, & Halliday, 1980). Two additional movement-evoked potentials follow the first, although these are not reported in all studies. A similar series of movement-evoked fields, with peaks at the same latencies as the movement-evoked potentials, are observed in MEG (Cheyne & Weinberg, 1989; Hoshiyama et al., 1997). A recent MEG study by Kelso et al. (1998) showed a correspondence between the first movement-evoked field and proprioceptive features of the movement by demonstrating a tight coupling of the activation profile of the response and velocity of finger movement. Taken together, the entire sequence of cortical activity associated with a single movement can last well over a second. Because the interval between each movement will be less than one second at movement rates beyond 1Hz, we hypothesized that we would observe a significant modification of the movement-related response within the current parameter range, possibly associated with overlap of successive evoked responses.

Experiments recording motor-related activity with faster movement rates than in studies of voluntary movements typically use a metronome to pace movement (e.g. Jantzen et al., 2001; Mayville et al., 1999). In an EEG experiment employing metronome-paced finger flexion, Gerloff et al. (1997) found a continuous steady-state response to rhythmic movement at a rate of 2Hz, which consisted of a motor potential 57ms before EMG onset and a post movement potential 93ms after EMG onset. Similar results were found with a second MEG study that used a self-paced movement near 2Hz (Gerloff et al., 1998). Here we seek to understand how the steady-state response at 2Hz relates to activity recorded in studies of voluntary movement with longer inter-response

intervals. At rates of 1Hz and above the activity associated with successive movements may begin to overlap as the movements come closer together. In addition, sources apparent at low rates may disappear, which would imply that the steady-state response results from the development or recruitment of new source contributions at higher rates. With the current experiment we investigate the rate-dependent evolution of the motor-related response from slow movements at 0.5Hz to relatively fast movements at 2.5Hz. This will provide insight into the origin of the movement-related steady-state response by producing a systematic characterization of the transition from discrete transient activity at low rates to continuous steady-state activity at high rates.

Previous studies have reported a large amount of temporal overlap between activation arising from different sources during the movement-related response in EEG (e.g. Cheyne, Weinberg, Gaetz, & Jantzen, 1995). Temporal overlap can lead to spatial overlap of activity patterns at the sensors, which makes it difficult to determine the spatiotemporal characteristics of separate evoked response components. Here we overcome this problem by applying spatiotemporal analysis techniques that take advantage of the high degree of spatial information provided by a full-head electrode array to separate response components from each other and from background activity. Karhunen-Loève decomposition is employed to determine the dominant spatiotemporal pattern of the event-related responses. The results indicate a transition from slow to fast potential oscillations with increased movement rate. Using independent components analysis it is discovered that this transition results from differences in the rate dependence of overlapping components of the movement-related response. A slow-wave component

drops out at high rates, whereas a fast-wave component is found to be relatively independent of the pace of movement.

3.2. Methods

3.2.1. Subjects

Four male subjects, all of whom reported to be right-handed, participated in the experiment. A small number of subjects were used because of the large datasets involved and a desire to analyze subject's responses on an individual basis. The experiment was conducted in compliance with all standards of human research outlined in the Declaration of Helsinki as well as by the Institutional Review Board. Informed consent was obtained from each participant prior to EEG recording. No subject reported motor or hearing deficits.

3.2.2. Procedure

The experiment was performed in the Human Brain and Behavior Laboratory at the Center for Complex Systems and Brain Sciences. Auditory stimulation (1kHz tones, 60ms duration) was delivered binaurally through either plastic headphones or a single speaker placed in front of the subject, with the volume set at a level that the subject reported to be comfortable. Subjects were asked to perform the task while fixing their gaze on an 'X' placed on the wall two meters in front of them. They were further instructed to minimize all extraneous eye or body movements during the trials. Movement was recorded in the form of pressure changes in an air pillow placed beneath the right index finger. Subjects were instructed to synchronize right index finger flexion

with the auditory metronome for twenty pacing tones and to continue flexing their finger at the same rate after the tones stopped until they heard a long beep indicating the end of the trial. The time span for the continuation phase was the same as for the pacing. Subjects were asked to maintain contact with the pillow throughout the synchronization and continuation phases of each trial. The trials were conducted at rates from 0.5 to 2.5Hz in 0.1Hz steps, with trial order randomized for each subject. Each rate was presented in five separate trials, thus providing approximately 100 continuation movements for averaging. The experiment lasted approximately 2 hours.

3.2.3. Data Acquisition

EEG activity was recorded using two separate systems. A 61-channel system with Grass 12A5 amplifiers (Grass-Telefactor, West Warwick, RI) was used for subjects one and two. The EEG activity from the remaining two subjects was recorded with an 84-channel Manscan system (Sam Technology, Inc., San Francisco, CA). In each case, a modified 10/20 International System of Electrode Placement was used to distribute electrodes on the scalp. The 61-channel system employed a left mastoid reference during recording. The data were later rereferenced using an average of the left mastoid and electrode T8 in order to remove lateral bias. The Manscan system uses left and right mastoid electrodes as an average reference during the recording. Regardless of recording system, digitization was performed at 256Hz. A Polhemus Isotrack II (Colchester, VT) was used to record the 3D location of each electrode, plus three fiduciary points: the nasion, and left and right preauricular points. The fiduciary points were used to create a

3D coordinate system for the electrode locations. Movements were recorded using a pressure sensitive pillow, and were digitized along with the EEG signal at 256Hz.

3.2.4. Data Processing

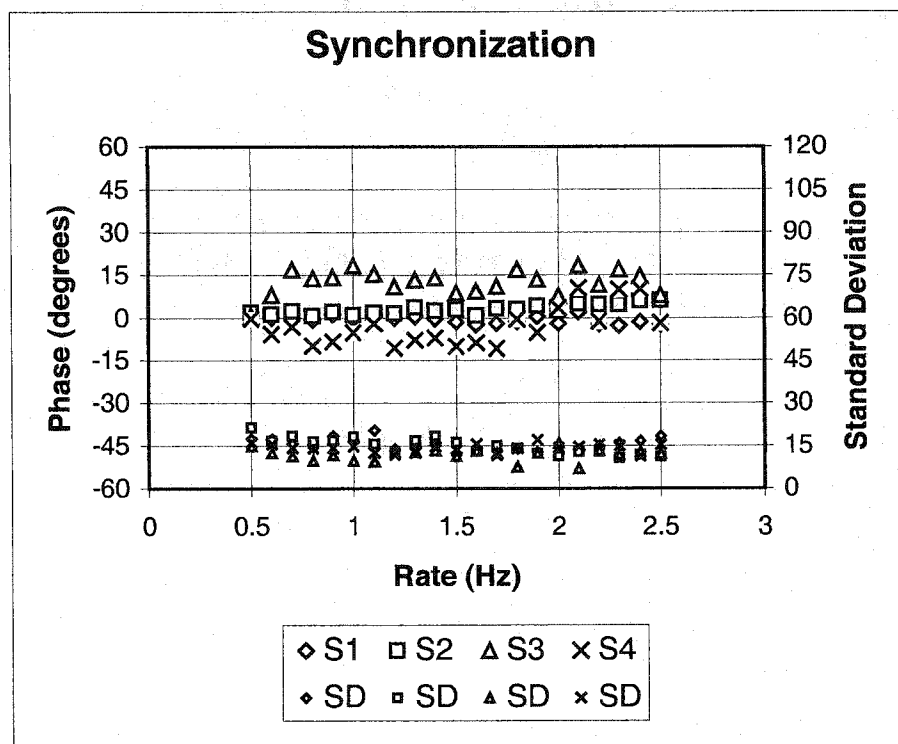
Averages of movement-related neural activity were produced for the continuation phases at each stimulation rate. Before averaging, the times of peak finger flexion for each movement were analyzed to determine if the subject continued movement at the required rate in the continuation phase of each trial. The inter-response intervals (IRIs) of the movements were examined, and movements with IRIs deviating by more than two standard deviations from the mean IRI were not included in the final average. Each movement cycle for averaging was centered at peak movement amplitude, and the duration of the cycle was equal to the required inter-response interval. The raw signals were band-pass filtered from 0.1 to 50Hz prior to averaging. In addition, the EEG signals were manually inspected for eye-blink or movement artifacts, and any cycle with contaminations was discarded. The first two movements in the continuation phase from each trial were excluded from the final averages in order to avoid transients. Topographical mapping of the resulting event-related potentials was performed by a polar projection of the three-dimensional sensor coordinates into two-dimensional space. A spline of 3rd order was used to interpolate activity between sensor positions.

3.2.5. Data Analysis

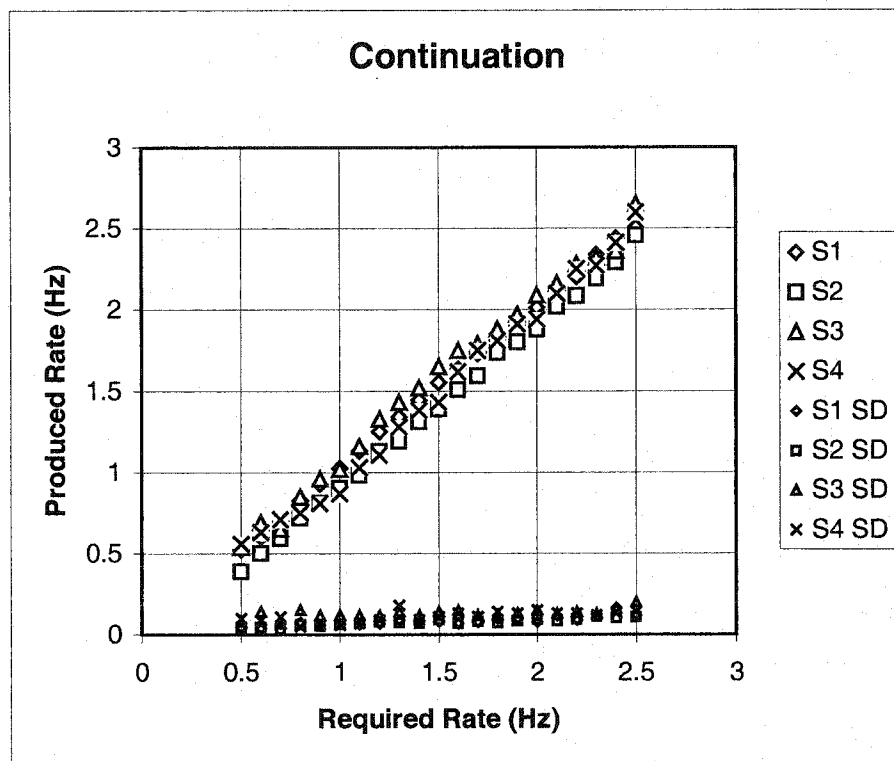
In order to characterize the rate-dependent evolution of the movement-related response a Karhunen-Loève (KL) decomposition procedure was used to find the main

directions of variance. The decomposition was performed on a single cycle of averaged data at each rate to find the eigenvector of the decomposition with the largest eigenvalue, which represents the dominant spatial activity pattern of the response at the sensors. Each fixed spatial pattern has an associated time series of activation over the movement cycle. Before KL decomposition, the data were smoothed using a fourth order Savitzky-Golay filter to remove high frequency oscillations that were not the subject of this analysis.

In order to separate the movement-related response into distinct spatiotemporal patterns, an independent components analysis (ICA) procedure (Makeig et al., 2002) was used to analyze the average data across all stimulation rates. The procedure uses the InfoMax algorithm from Bell and Sejnowski (1995) to separate the multi-channel signal into statistically independent time series, each with a distinct spatial pattern at the sensors. For each subject, the continuation averages at each rate were concatenated and analyzed together as a single dataset. The ICA algorithm was applied to the dataset in order to track the evolution of separate response components across movement rates. One of the assumptions of the InfoMax algorithm is that there are as many independent components in the data as there are sensors. This can be an overestimation of the number of sources contributing to the evoked response if the number of sensors is relatively large compared to the number of time points. In order to avoid this problem, KL decomposition was applied to the datasets to reduce the dimension of the sensor space. The top few modes of the decomposition were then used as an orthogonal basis for the data, and new time series in each principal direction were found by projecting the original data onto the new basis. The resulting ICA decompositions for each subject produced



a) Average and standard deviation of relative phase during synchronization in degrees.



b) Produced rate versus required rate for the continuation phase.

several components that related to residual noise in the averaged data, determined by lack of temporal consistency across stimulation rate and by spatial patterns that suggested eye movement and muscle artifacts as well as occipital alpha activity. We discuss here only those types of the remaining motor-related components that were found in all subjects. The percent of variance accounted for by each component was estimated by calculating the mean variance of the component and dividing by the mean variance in the original data.

3.3. Results

3.3.1. Behavior

Figure 3.1 presents the average performance of each subject during the synchronization and continuation phases at each rate. All subjects were able to synchronize with the auditory metronome at all rates, producing an averaged phase relation with the metronome of 20 degrees or less (figure 3.1a). Figure 3.1b shows the mean and standard deviation of the actual rate produced during the continuation phase at each required rate. All subjects produced a mean movement rate close to that required, indicating that they were able to perform the continuation task.

3.3.2. Rate-dependent Evolution of the Response

Presented here are the results of the KL decomposition procedure used to determine the dominant pattern of the movement-related response during the continuation phase at each stimulation rate. Figures 3.2a-d show the results of the analysis for subjects 1-4, respectively. The spatial modes of the decomposition accounting for the largest

Figures 3.2a-d. KL decomposition applied separately to each stimulation rate for subjects 1-4, respectively. The decomposition was performed on one cycle of data centered at peak finger flexion. A cycle at each rate is defined by the required inter-response interval. Plotted at left for each rate is the top spatial mode of the decomposition. Eigenvalues are displayed below each mode. At right is the time series of activation of the top mode, centered at the peak of the movement indicated by the dashed line. A complete single cycle interval of two seconds is shown at 0.5Hz. The same length of time is displayed at all rates, with the time series repeated at higher rates in order to fill two seconds. Dashed lines indicate additional movement peaks at higher rates.

S1

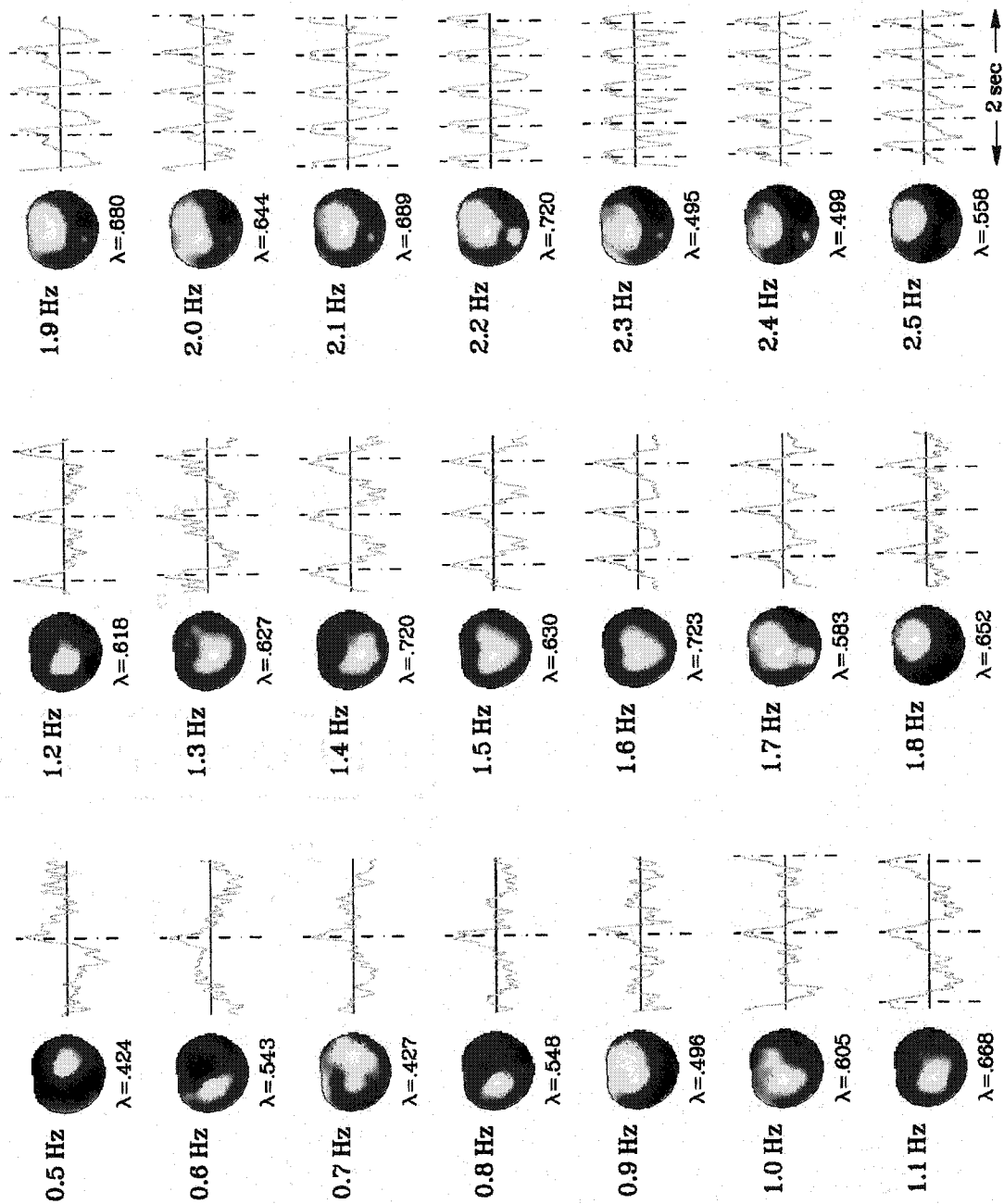


Figure 3.2a

S2

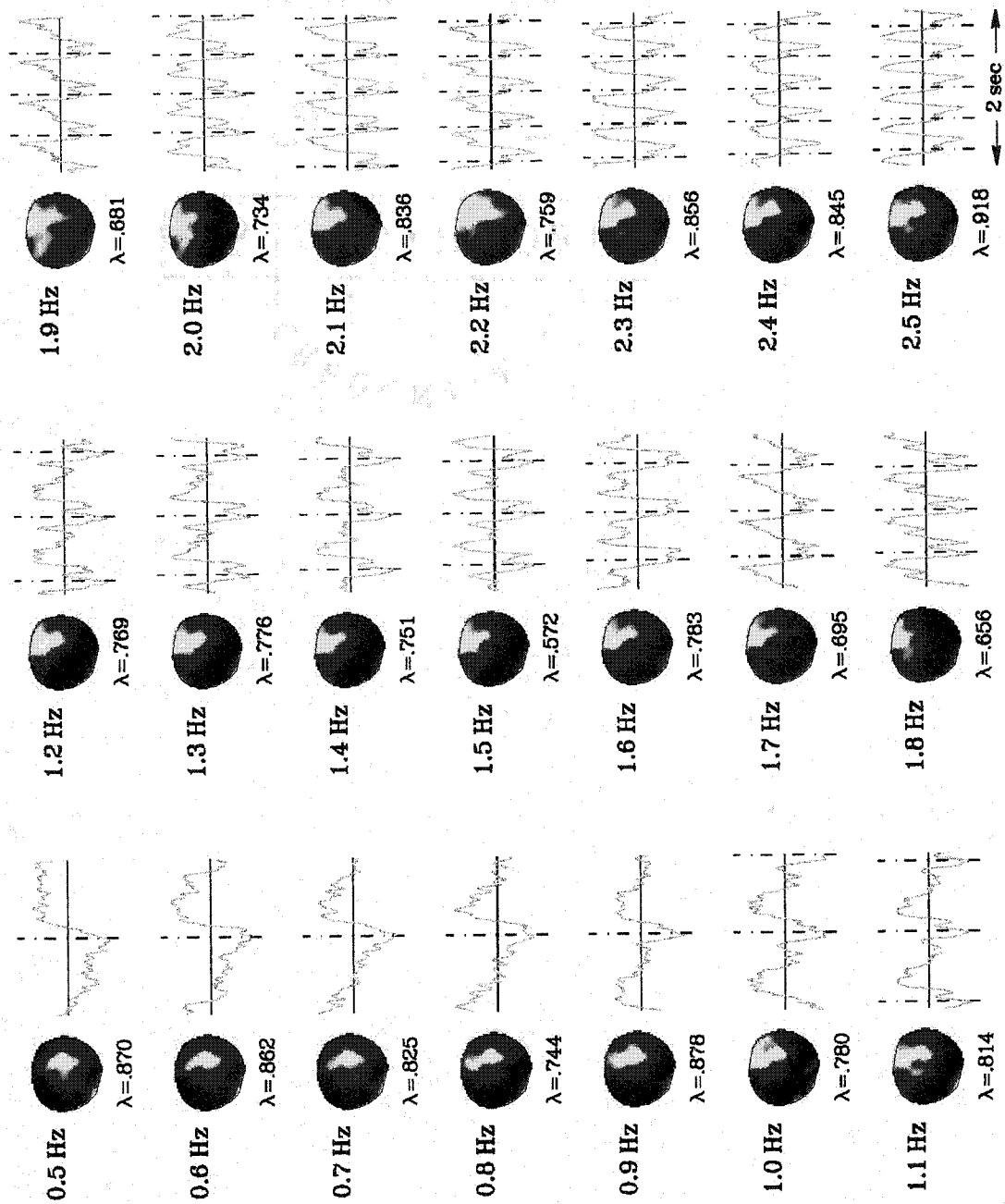


Figure 3.2b

S3

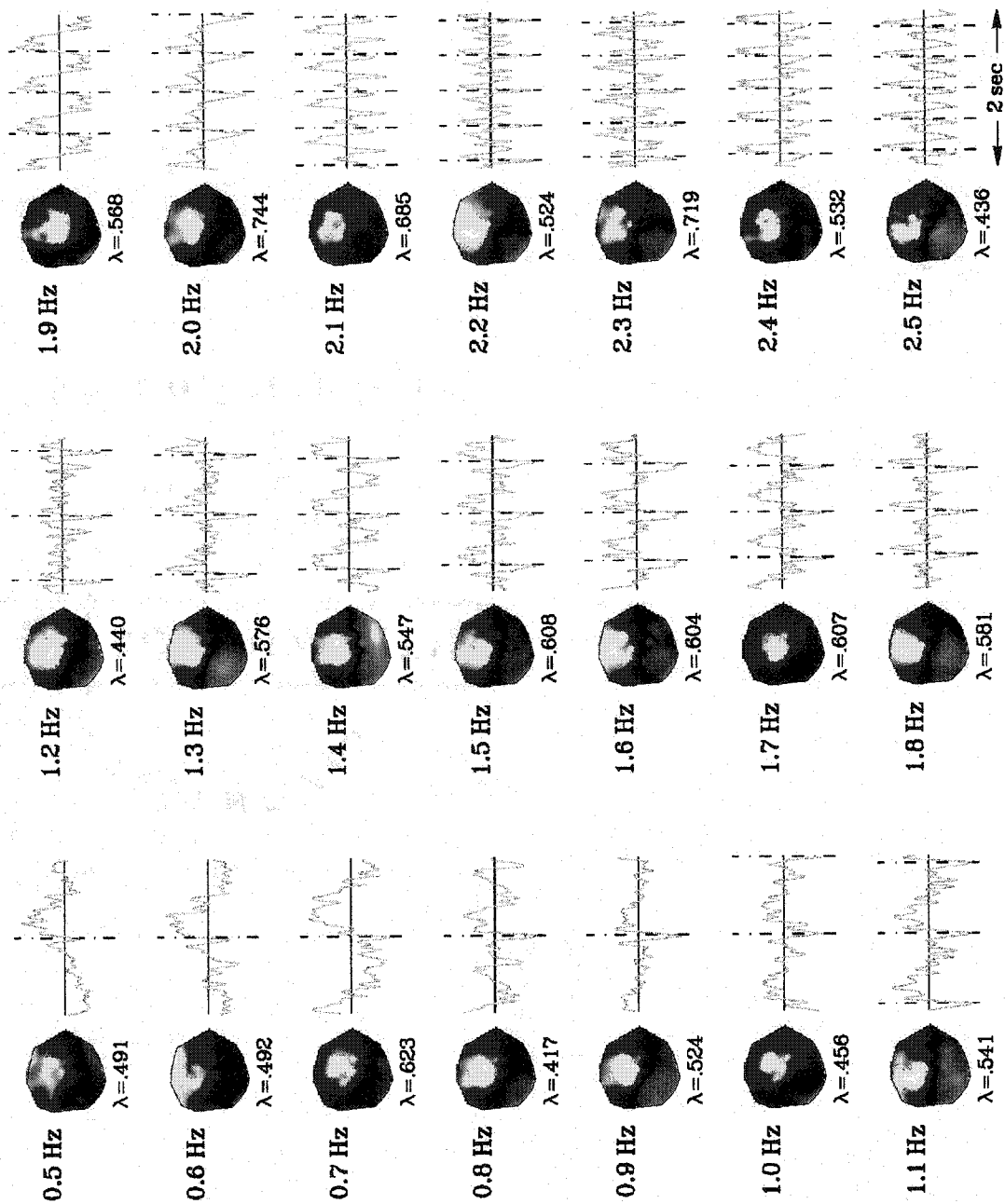


Figure 3.2c

S4

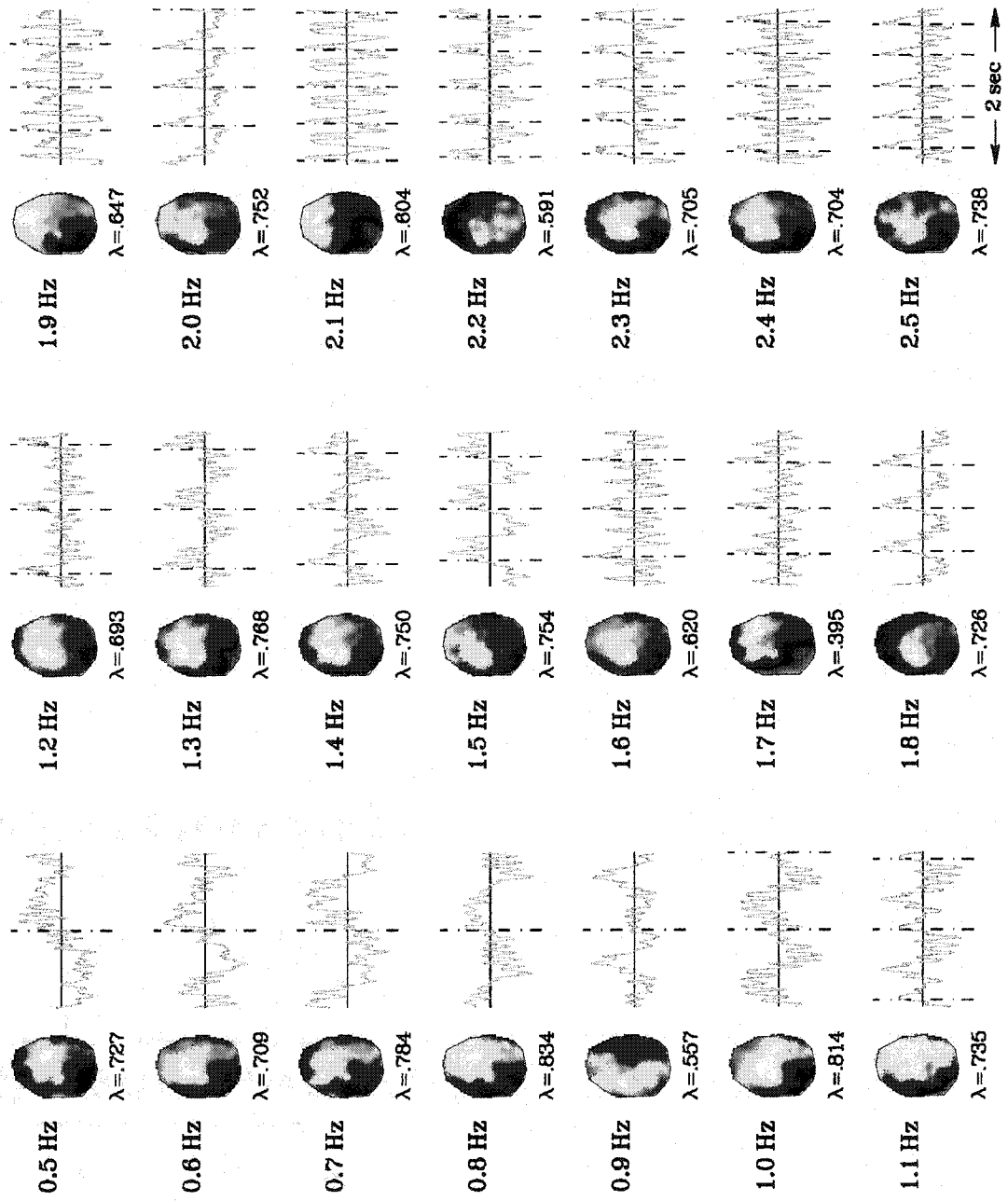


Figure 3.2d

amount of variance at each rate are displayed along with their eigenvalues. Red/yellow color indicates positive potential and blue/light-blue is negative potential. The top mode accounted for more than 40% of the variance at all rates, with some as high as 80%. Plotted to the right of each spatial pattern (or eigenvector) is the time series of activation of the pattern for an interval of two seconds. At rates above 0.5Hz, the time series are appended to each other in order to fill the entire interval. Each time series is centered at the peak of finger flexion, indicated by the dashed line. Additional movement peaks are shown at rates above 1Hz because more than one movement cycle fits in the two-second window. The amplitude scale is the same for each rate in arbitrary units.

In terms of the spatial activity pattern of the dominant response, no clear trend of rate dependence emerges across subjects. However, the associated time series of the response do exhibit a systematic reorganization. For all subjects, the temporal pattern at low rates is a combination of slow-wave oscillation throughout the two-second window, and fast spikes of activity near the peak of the movement. In addition, subject four (figure 3.2d) shows an overlapping 10Hz oscillation throughout the movement cycle. At higher movement rates for all subjects, the slow-wave activity has disappeared, and the response is dominated by faster potential oscillations at or above the movement rate. Despite the decrease in slow-wave activity, the overall amplitude of the response remains approximately constant for all rates.

3.3.3. *Separate Response Components*

Independent components analysis was applied to the concatenated dataset in order to determine if the transition from slow to fast wave activity seen in figures 3.2a-d

resulted from differential activation of separate components of the movement-related response. The resulting movement-related components for all subjects fit into two categories.

The first type of response (Type I) is shown in figure 3.3 for all subjects. The percent of variance accounted for in the original time series was 34%, 23%, 23%, and 13% for subjects 1-4, respectively. Plotted at left is the spatial pattern of the response component. For three out of four subjects, the activity is predominantly contralateral to the side of finger movement. The time series in red at bottom shows one second of the temporal activation pattern of the response averaged over all stimulation rates. Peak finger flexion is indicated by the vertical axis; a sample movement profile at 1Hz is shown in blue. The main feature of the temporal activation pattern is a positive peak just prior to peak flexion, which occurs approximately 100ms past movement onset. In three out of four subjects (1-3) the positive peak is followed by smaller negative and positive deflections occurring after peak finger flexion. At top-right for each subject is an interpolated color plot of the temporal response pattern at all stimulation rates, with movement rate increasing along the vertical axis. For all subjects the component peaks at the same latencies across rates. In addition, the amplitude of the response is relatively independent of movement rate.

The second type of component (Type II) found in all subjects is shown in figure 3.4. The percent of variance accounted for in the original time series is 3%, 16%, 19%, and 10% for subjects 1-4, respectively. For all subjects, the spatial pattern of the type II response exhibits a positive peak over central electrodes. The average time series of the response shows negative activation peaking before the movement and positive activation

Figure 3.3. Type I ICA component for all subjects. Left for each subject: Topographic image of the component. Red/yellow represents positive potential; blue/light-blue indicates negative potential. Right-top: Color-coded rate-latency plot of the activation time series of the component at all required movement rates centered at peak flexion, with amplitude in arbitrary units. Bottom: Average of the activation time series across rate shown in red, and an average 1Hz movement profile shown in blue.

Figure 3.4. Same as figure 3.3 for the type II component

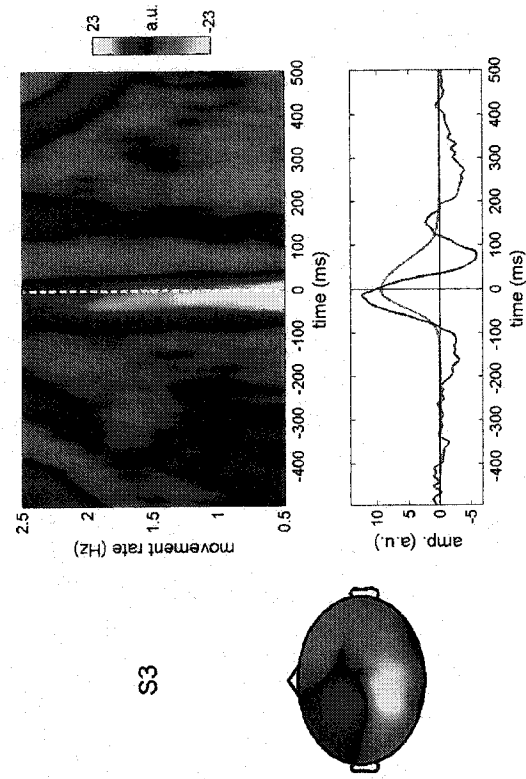
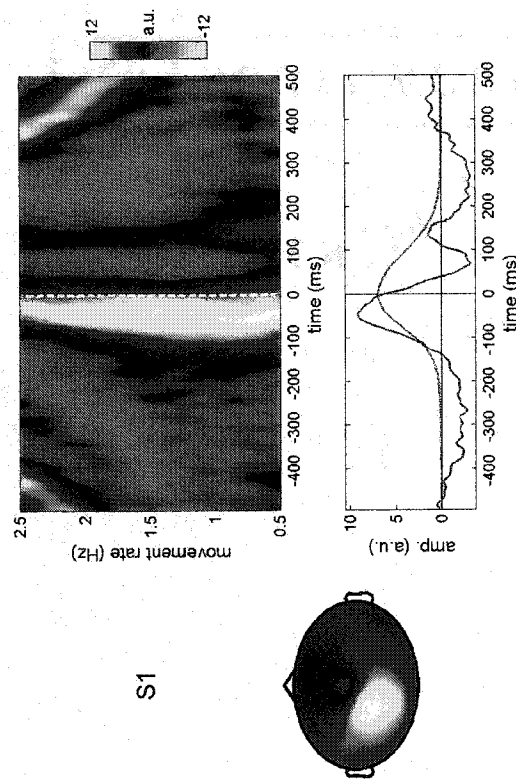
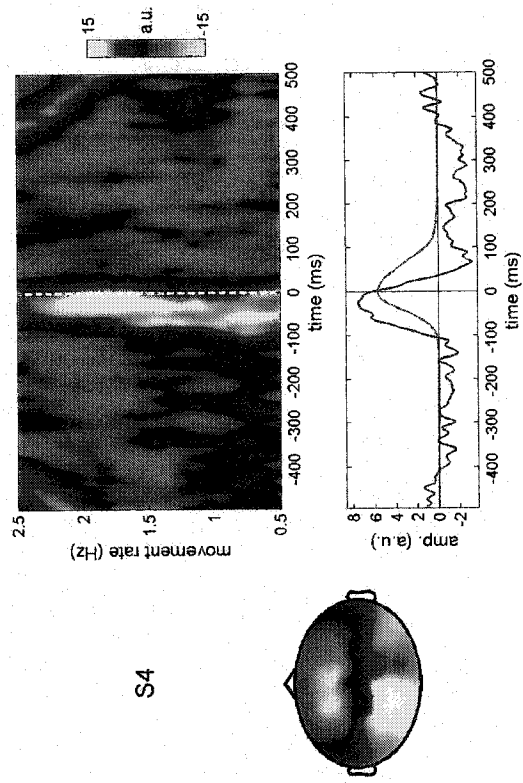
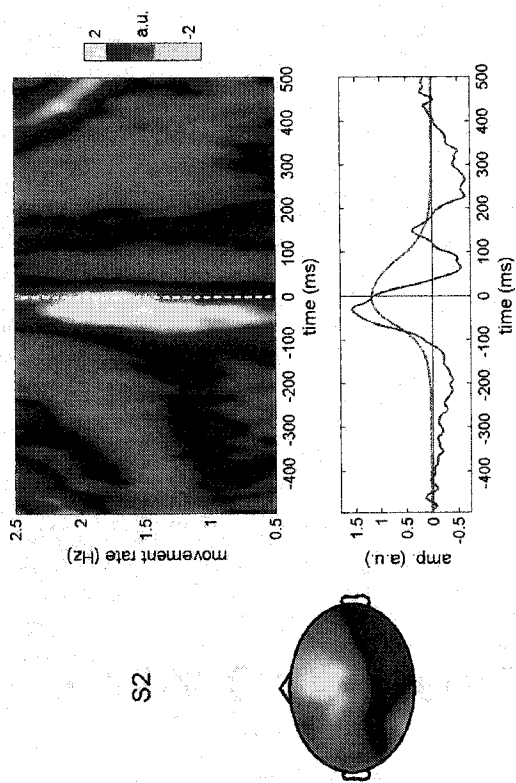


Figure 3.3

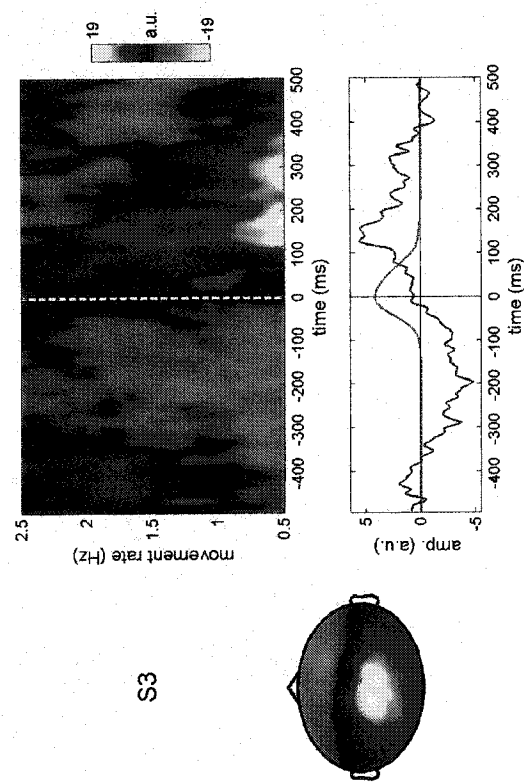
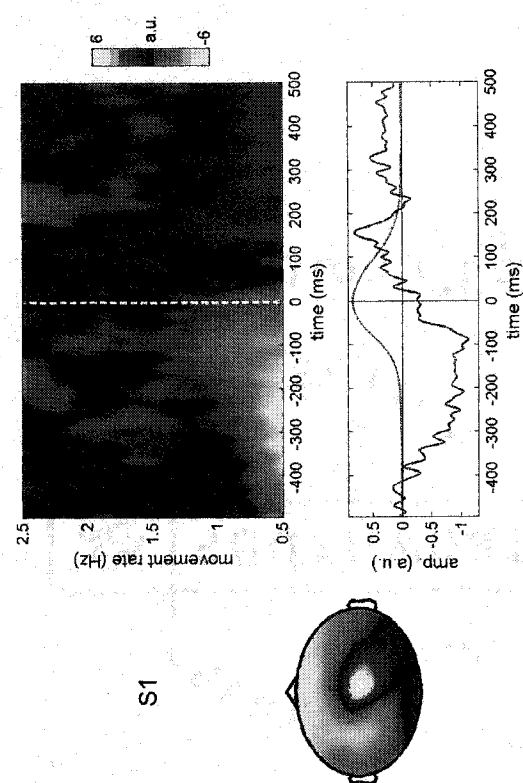
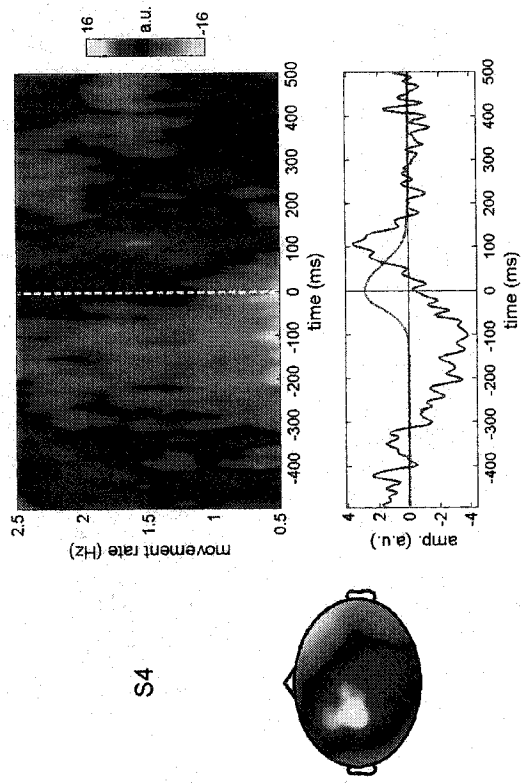
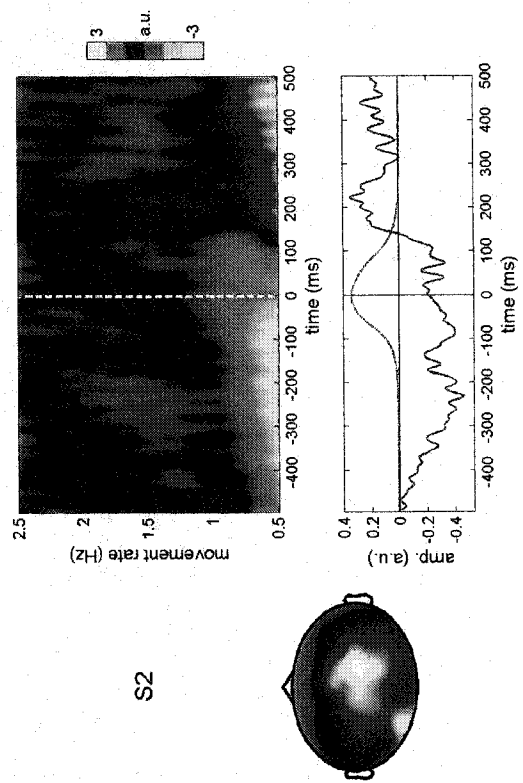


Figure 3.4

post-movement. Overall, the response is distinct from the type I component in two respects. The first is the slow-wave nature of the average time series, with a minimum before and a maximum after the movement. This contrasts with the type I response, which displayed sharp amplitude spikes during the movement. In addition, the amplitude of the type II response exhibits a strong dependence on movement rate, with its highest amplitude at low rates, whereas the amplitude of type I is relatively independent of rate. For all subjects, the type II response is practically nonexistent at rates above 1Hz, suggesting that the main contribution to movement-related activity at high rates is from the type I response only.

3.4. Discussion

The goal of this experiment was to determine the rate dependence of the movement-related responses in EEG over a broad range of rhythmic movement rates. For this purpose, we used a continuation paradigm to elicit self-paced movements at 21 rates from 0.5 to 2.5Hz. The neural correlates of self-paced movement were hypothesized here to undergo a fundamental transition from a discrete transient response at low rates to a continuous steady-state response at high rates. Our objective was to characterize this transition with the intent of providing insight into known rate-dependent behavioral differences seen over these rates (e.g. Fraisse, 1982; Kelso, 1984). We used KL decomposition of the average responses to reveal the dominant spatiotemporal pattern of the neural activity at each rate. The response was found to be dominated by slow-wave activity at low rates, and fast-wave activity at high rates. ICA decomposition revealed that the origin of this difference was attenuation of a slow-wave component of

the event-related response at high rates. A separate fast-wave component had the same amplitude at all rates, and was the main contributor to the overall response at rates above 1Hz.

The first type of ICA component (Type I) is distinguished by fast oscillation of the potential during the movement, with a large positive peak just prior to the point of maximum finger flexion followed by two smaller negative and positive peaks during the extension phase of the movement. A large amplitude peak at the latency of the first positive peak seen here has previously been observed in both EEG and MEG studies of voluntary movement (Shibasaki et al., 1980; Kelso et al., 1998). Because it occurs after movement onset, this peak is referred to as a movement-evoked potential or field, depending on the recording technology, and is thought to arise from cutaneous and proprioceptive feedback elicited by the movement (Kristeva-Feige et al., 1996). The relationship to sensory feedback was confirmed by Cheyne, Endo, Takeda, and Weinberg (1997) who showed that cooling of the arm delayed the latency of the first magnetic field evoked by finger movement. The delay was presumably caused by increases in conduction times along afferent pathways from the finger. The first large amplitude peak of the type I response was followed by two smaller negative and positive deflections in three out of four subjects. These likely correspond to the second and third movement-evoked potentials/fields seen in previous studies of voluntary movement. The source of the second response is still under debate, although it has been hypothesized to relate to activity in primary motor cortex associated with the command for the extension phase of the movement (Kristeva, Cheyne, & Deecke, 1991). The third movement-evoked response is thought to result from sensory feedback from the extension phase of the

movement. This was confirmed in a study by Holroyd, Endo, Kelso, and Takeda (1999) in which subjects performed synchronized finger flexion with an auditory metronome. In some conditions, the subjects performed normal flexion and extension movements as used in the present study; in others, the subjects flexed on the beat and then left their finger in a flexed position until the next beat at which they extended. The result was that a third movement-evoked response was only observed when a full flexion and extension movement was performed.

The second type of response revealed by the ICA procedure (Type II) is distinct from the type I response in that activation extended from well before to well after the actual movement. This type of component has been termed movement-related as opposed to movement-evoked in previous studies because activity is present before movement onset (Cheyne & Weinberg, 1989). Slow-wave activity prior to movement onset has been seen in a large body of EEG and MEG studies of voluntary movement using IRIs over two seconds (see for example Cheyne et al., 1995; Deecke et al., 1976; Deecke, Weinberg, & Brickett, 1982). First reported by Kornhuber and Deecke (1965), slow-wave activity preceding voluntary movement is referred to as the Bereitschaftspotential (BP) in EEG, and the Bereitschaftsmagnetfeld in MEG. The BP begins between 2 and .5 seconds before movement onset depending on the experimental context, and is believed to relate to processes underlying motor preparation and planning, although the exact origin is still under debate (Deecke et al., 1976; Praamstra, Stegman, Horstink, Brunia, & Cools, 1995). Contributions to the BP originate from areas typically associated with motor planning, such as the supplementary motor area and the pre-motor cortex (Erdler et al., 2000; Deecke & Kornhuber, 1978; Praamstra et al., 1996). Deecke

et al. (1976) divided the response into three phases, the first two of which are characterized by diffuse bilateral activity. The last phase is referred to as the motor potential (MP) and is thought to relate to the outgoing motor command from primary motor cortex. In support of this idea, the BP becomes less symmetric and more dominated by contralateral activity just prior to movement onset, suggesting activity in contralateral motor cortex (Cheyne et al., 1995). In contrast to the BP, post-movement activity has not received as much experimental attention. Kristeva et al. (1991) reported one such response after the movement-evoked fields in MEG. The authors suggested that it has the same origin as the Bereitschaftsmagnetfeld. This idea is supported by the present results, which show pre- and post-movement activity associated with the same independent component. Because we were able to separate temporally overlapping components, we found that the slow-wave components do not cease at movement onset, but instead continue throughout and after the movement.

In addition to distinct time courses at individual rates, the type I and type II responses exhibit markedly different patterns of rate dependence. In all subjects, the type I response is remarkably consistent in latency and amplitude across rate, while the type II response is primarily active at rates of 1Hz and below. In fact, beyond 2Hz, the response is non-existent for all subjects. The distinct rate dependence of the two response types explains the slow to fast wave transition in the top mode of the KL decomposition performed at each rate (figures 3.2a-d). Mayville et al. (submitted) observed a similar pattern of rate dependence in an MEG continuation experiment. The authors used KL decomposition to separate spatiotemporal components similar to the type I & II responses observed here. They employed the same stimulation rates as in the present study and

showed that the type II slow-wave activity also disappears for rates faster than 1Hz. We have associated the type II activity pattern with the pattern observed during movement preparation in previous studies of voluntary movement with long IRIs. The fact that this slow-wave preparatory activity drops out as movement rate increases indicates a fundamental reorganization of the control of a rhythmic movement. At rates above 1Hz the main contribution to the average response originates from the type I movement-evoked potentials, which represent sensory feedback from the physical properties of the movement. The drop out of the type II response suggests that individual movements are no longer planned and executed in a discrete sequential fashion. Instead, the cortex appears to be simply monitoring feedback from a continuous sustained oscillation where individual movements are grouped as part of a single rhythmic process. A transition from discrete 'one-at-a-time' control to maintenance of a continuous oscillation could be related to rate-dependent transitions in sensorimotor coordination tasks observed at rates from 1-2Hz, such as a shift from reaction to anticipation in synchronization (Engström et al., 1996) and a transition from anti-phase to in-phase timing when coordinating with a metronome (Kelso et al., 1990). More work needs to be done to determine if a similar drop out of pre-movement activity occurs during metronome-paced movements as used in the above behavioral experiments. The ICA procedure employed here did not separate components of the movement-related response during synchronization as effectively as for continuation, possibly due to interference from overlapping auditory evoked activity.

A main purpose of the present study was to characterize the onset of the movement-related steady-state response recorded previously by Gerloff et al. (1997, 1998) at a movement rate of 2Hz. Our intent was to shed light on the composition of the

response by observing its evolution with increased movement rate. Gerloff et al. (1997) proposed that a steady-state paradigm is a better way to observe the movement-evoked responses in clinical applications because collection times are faster. The present results support this idea; the steady-state response at 2Hz is a simpler response, without the slow-wave pre- and post-movement activity apparent at low rates. In addition, the type I movement-evoked responses were remarkably consistent across movement rate, showing no large-scale changes in amplitude or latency. Gerloff et al. (1997) observed two primary responses, a motor potential just before movement onset, and a movement-evoked potential approximately 90ms after movement onset. The movement-evoked potential likely corresponds to the large initial spike of the type I response observed in the present study. However, we did not observe a distinct motor potential just prior to movement onset, which is in agreement with Kopp, Kunkel, Müller, Mühlnickel, and Flor (2000) who performed a steady-state experiment at 1Hz and also did not report a significant motor potential. As stated above, the MP is generally considered to be the last part of the slow-wave *Bereitschaft* activity leading up to movement onset (Cheyne et al., 1995). Thus, it may have been a part of the slow-wave type II component that we associated with the *Bereitschaft* potential and which disappeared with the rest of the component at a movement rate of 1Hz.

Here we have shown that a continuation paradigm can be an effective method for studying neural correlates of rhythmic movements over a broad parameter range. Recent results from fMRI studies, however, suggest caution in treating continuation movements as purely 'self-paced' context independent oscillations. The neural organization of the continuation movements may depend on the type of metronome or coordination task

employed in the pacing phase of the paradigm. For instance, Jäncke, Loose, Lutz, Specht, and Shah (2000) showed differences in activation of cortical and subcortical areas during continuation depending on whether the subject initially synchronized with an auditory or visual metronome. Jantzen et al. (2002) performed an fMRI continuation study using either synchronization or syncopation with an auditory metronome during the pacing phase. They showed that differences in the activity patterns seen during the two pacing phases persist into the continuation phase, suggesting a strong context dependence for the organization of the continuation movements. EEG and MEG experiments using a variety of metronome and coordination conditions should be performed in order to assess whether context-dependence also has an effect on the movement-related steady-state response.

Experiment 4: Spatiotemporal Analysis of Neuromagnetic Activity

Underlying Rhythmic Movements: Development of the Movement-related Steady-state Response

4.1. Introduction

In studies of rhythmic movement, transitions in the ability to maintain specific coordinative relationships are known to occur at specific movement rates (e.g. Engström, Kelso, & Holroyd, 1996; Fraisse, 1982). For instance, when subjects perform rhythmic bimanual coordination in an anti-phase pattern, they spontaneously switch to in-phase movement with increased rate (Kelso, 1984). Such transitions typically occur near 2Hz. Interestingly, a similar behavioral transition occurs when subjects are asked to coordinate the oscillation of a single effector with an auditory metronome. When subjects flex their index finger between successive tones (syncopate), they find the task more and more difficult as the stimulation rate is increased, and beyond a critical point they switch spontaneously to a movement synchronized with the metronome (Kelso, DelColle, & Schöner, 1990). Again, this transition typically occurs when movement rates approach 2Hz. In non-linear oscillator models of the above phenomena, coupling of either two effectors or an effector and a metronome can model coordinative transitions at similar movement rates (Haken, Kelso, & Bunz, 1985; Kelso et al., 1990). The similarity of transitions in coordinating an effector with either another effector or a metronome is striking, and suggests a common timing mechanism in the two contexts.

Previous EEG and MEG studies have found significant alterations in ongoing cortical dynamics associated with the above behavioral transitions at rates near 2Hz (Fuchs, Kelso, & Haken, 1992; Jantzen, Fuchs, Mayville, Deecke, & Kelso, 2001; Kelso et al, 1992; Mayville, Bressler, Fuchs, & Kelso, 1999; Wallenstein, Kelso, & Bressler, 1995). However, analysis of the movement-related activity patterns in these studies can be complicated by the potential for overlap between activity associated with successive movements. Gerloff et al. (1997, 1998) referred to the neural correlates of either metronome-paced or self-paced movement at fast rates (~2Hz) as the movement-related steady-state response. In general, a steady-state response is characterized by continuous cortical activation between separate stimulus or movement events (Regan, 1982). The continuous activity can be related to overlap of transient activity patterns seen at low rates (see Carver, Fuchs, Jantzen, & Kelso, 2002), although it could also be the result of new sources becoming active (Regan, 1989).

Traditional EEG and MEG studies of voluntary movements produce transient movement-related responses because the activity associated with each movement is allowed to return to baseline before the next movement starts (e.g. Cheyne & Weinberg, 1989; Deecke, Grözing, & Kornhuber, 1976). In EEG, voluntary movements separated by several seconds are preceded by a slow-wave of negative potential over central electrodes known as the readiness potential or Bereitschaftspotential (BP). This deflection can start a second or more before EMG onset, and is thought to derive from sources involved in the preparation for movement such as the supplementary motor area (SMA) and pre-motor cortex (Deecke & Kornhuber, 1978; Erdler et al., 2000; Praamstra, Stegman, Horstink, & Cools, 1996). The corresponding Bereitschaftsmagnetfeld (BM) in

MEG is more difficult to observe and is typically of shorter duration than the BP in EEG, possibly due to field cancellation caused by bilateral SMA activity across the central fissure (Lang et al., 1991). The end of the BM is marked by a motor field (MF) occurring just before movement onset, which is thought to relate to the outgoing motor command from primary motor cortex. Following the BM/MF complex is a series of fast field oscillations beginning just after movement onset. These responses are believed to relate to proprioceptive and cutaneous feedback from the movement, and have been localized to primary sensorimotor cortex (Kristeva, Cheyne, & Deecke, 1991). Because of their relation to sensory feedback they are referred to as movement-evoked fields. The first movement-evoked field is the most consistently observed of the evoked responses, with peak latencies ranging from 50 to 100ms after movement onset (Cheyne & Weinberg, 1989; Hoshiyama et al., 1997). Kelso et al. (1998) showed a correspondence between the first movement-evoked field and proprioceptive features of the movement by demonstrating a tight coupling of the activation profile of the response and velocity of finger movement. Two additional movement-evoked fields follow the first, although these are not observed in all subjects. Taken together, the entire sequence of cortical activity associated with a single movement can last well over one second.

In a recent EEG continuation study (Chapter 3) we assessed the relationship between the movement-related transient and steady-state responses by employing a systematic exploration of a parameter space of rhythmic movement from 0.5 to 2.5Hz with an inter-rate interval of 0.1Hz. This afforded observation of the development of the steady-state response and direct comparison to the transient response at low rates. The results did not indicate new sources of activity at high rates. On the contrary, the steady-

state response represented a simplification of the response pattern seen at low rates due to the attenuation of pre-movement slow-wave activity associated with activation of motor planning areas. The primary contribution to the response came from the movement-evoked potentials, which peak during the movement. The attenuation of pre-movement slow-wave activity suggested a fundamental reorganization of the movement-related response characterized by a reduction in separate cortical planning and control for each movement. Mayville et al. (submitted) found similar results in an MEG study of self-paced movement at rates from 0.5 to 2.5Hz. In both studies, the disappearance of motor planning activity occurred at movement rates between 1 and 2Hz, suggesting a relationship to the above mentioned transitions in bimanual and sensorimotor coordination seen at similar movement rates (e.g. Engström et al., 1996; Kelso, 1984).

A continuation paradigm (Wing & Kristofferson, 1973) was employed in the Chapter 3 and Mayville et al. (submitted) studies in order to investigate the neural correlates of self-paced movement over a wide range of movement rates. Each trial in a continuation paradigm begins with a pacing phase during which subjects synchronize some aspect of movement such as peak finger flexion with an auditory or visual metronome. After a certain period, the metronome ceases and subjects continue moving at the same rate. The continuation phase provides movements at set rates without metronome interference. Here we seek to confirm and extend the results of previous continuation studies in an MEG experiment with 21 movement rates ranging from 0.5 to 2.5Hz in 0.1Hz steps. Independent components analysis (ICA) is used to determine the component structure of the continuation and synchronization averages, with the goal of

determining whether a similar rate-dependent reorganization of the motor-related responses occurs in self-paced and metronome-paced movements.

4.2. Methods

4.2.1. Subjects

Four right-handed subjects (one female and three males) participated in the experiment. A small number of subjects were used because of the large datasets involved and a desire to analyze subject's responses on an individual basis. The experiment was conducted in compliance with all standards of human research outlined in the Declaration of Helsinki as well as by the Institutional Review Board. Informed consent was obtained from each participant prior to MEG recording. No subject reported motor or hearing deficits.

4.2.2. Procedure

Subjects were seated inside a magnetically shielded room (Vacuum Schmelze, Hanau) with their heads held firmly within the dewar. Auditory stimulation (1kHz tones, 60ms duration) was delivered binaurally through plastic headphones at a volume that the subjects reported to be comfortable. Subjects were asked to fix their gaze at a point two meters in front of them and to minimize all extraneous eye or body movements during the trials. Movement was recorded in the form of pressure changes in an air pillow placed beneath the right index finger. Subjects were instructed to synchronize right index finger flexion with the auditory metronome for twenty pacing tones and to continue flexing their finger at the same rate after the tones stopped until they heard a long beep indicating the

end of the trial. The time span for the continuation phase was the same as for the pacing. Subjects were asked to maintain contact with the pillow throughout the synchronization and continuation phases of each trial. The trials were conducted at rates from 0.5 to 2.5Hz in 0.1Hz steps, with trial order randomized for each subject. Each rate was presented in five or six separate trials, thus providing 100 or more continuation movements for averaging. The experiment lasted approximately 2 hours.

4.2.3. Data Acquisition

MEG activity was recorded using a full-head magnetoencephalograph (CTF Inc., Port Coquitlam, BC) comprised of 143 SQUID (superconducting quantum interference device) sensors distributed homogeneously across the scalp. A coordinate system for each subject's head was defined with respect to three fiducial points: the nasion, and left and right preauricular points. The three-dimensional locations of these points in the sensor coordinate system were measured prior to each experiment. Conversion to third-order gradiometers was performed in firmware using a set of reference coils (Vrba, Cheung, Taylor, & Robinson, 1999). MEG signals were band-pass (0.3-80Hz) and notch filtered (50 and 100Hz: the European line frequency and its harmonic). Digitization was performed at a rate of 312.5Hz. Movements were recorded using a pressure sensitive pillow and digitized along with the MEG signal at 312.5Hz.

4.2.4. Data Processing

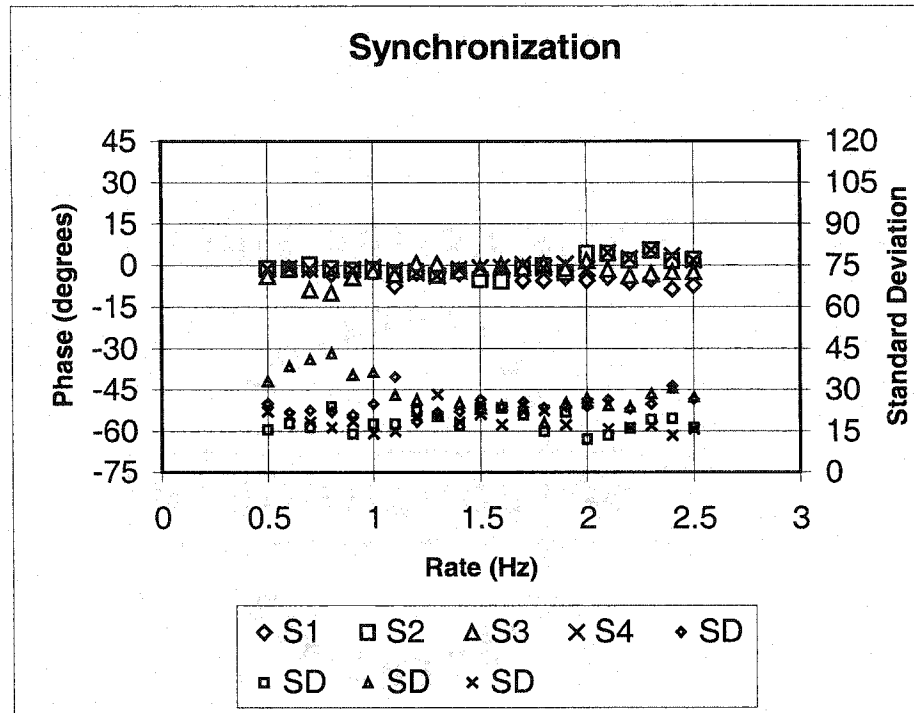
Separate averages of movement-related neural activity were produced for the synchronization and continuation phases at each stimulation rate. Before averaging, the

times of peak finger flexion for each movement were analyzed to determine if the subjects adequately performed the synchronization and continuation tasks. For the synchronization phase, movements were kept for averaging if they fell within a 60° phase relation to the nearest tone onset. In the continuation phase, movements with inter-response intervals (IRIs) deviating by less than two standard deviations from the mean IRI were included in the final average. Each movement cycle for averaging was centered at peak movement amplitude, and the duration of the cycle was equal to the required inter-response interval. Prior to averaging, the MEG signals were manually inspected for eye-blink or movement artifacts, and any cycle with contaminations was discarded. The first two movements in the continuation phase from each trial were excluded from the final averages in order to avoid transients. Topographical mapping of the resulting event-related fields was performed by a polar projection of the three-dimensional sensor coordinates into two-dimensional space. A spline of 3rd order was used to interpolate activity between sensor positions.

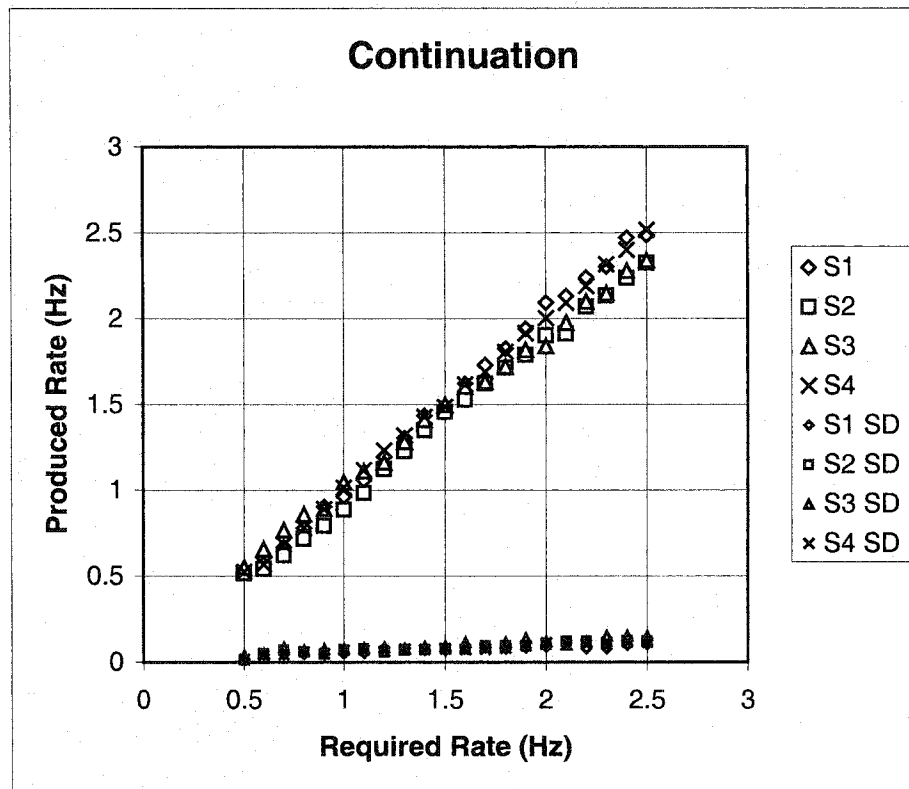
4.2.5. Data Analysis

In order to separate the movement-related responses from the synchronization and continuation averages into distinct spatiotemporal patterns, an independent components analysis (ICA) procedure (Makeig et al., 2002) was used to analyze the average data across all stimulation rates. The procedure uses the InfoMax algorithm from Bell and Sejnowski (1995) to separate the multi-channel signal into statistically independent time series, each with a distinct spatial pattern at the sensors. Separate continuation and synchronization datasets were formed for each subject by concatenating the averages at

each rate. The ICA algorithm was applied to each dataset in order to track the evolution of separate response components across movement rates. One of the assumptions of the InfoMax algorithm is that there are as many independent components in the data as there are sensors. This can be an overestimation of the number of sources contributing to the evoked response if the number of sensors is relatively large compared to the number of time points. In order to avoid this problem, KL decomposition was applied to the datasets to reduce the dimension of the sensor space. The top few modes of the decomposition were used as an orthogonal basis for the data, and new time series in each principal direction were found by projecting the original data onto the new basis. The resulting ICA decompositions for each subject produced several components that related to residual noise in the averaged data, determined by lack of temporal consistency across stimulation rate and by spatial patterns that suggested eye movement and muscle artifacts as well as occipital alpha activity. We discuss here only those types of the remaining motor-related components that were found in all subjects. The percent of original variance accounted for by each component was estimated by calculating the mean variance of the component and dividing by the mean variance in the original data. Spatial and temporal correlations were used to assess the similarity of components found in the synchronization and continuation conditions. The significance of the separate spatial and temporal correlations was assessed using a t -statistic: $t = \frac{r\sqrt{N-2}}{\sqrt{1-r^2}}$, where r is the correlation coefficient and N is the sample size.



a) Average relative phase and standard deviation during synchronization in degrees.



b) Produced versus required rate and standard deviation for the continuation phase.

4.3. Results

4.3.1 Behavior

Figure 4.1 presents the average behavioral performance of each subject during the synchronization and continuation phases at all rates. All subjects were able to synchronize with the auditory metronome at all rates, producing an averaged phase relation with the metronome of 20 degrees or less (figure 4.1a). Figure 4.1b shows the mean and standard deviation of the actual rate produced during the continuation phase across rates. All subjects produced a mean movement rate close to that required, indicating that they were able to perform the continuation task.

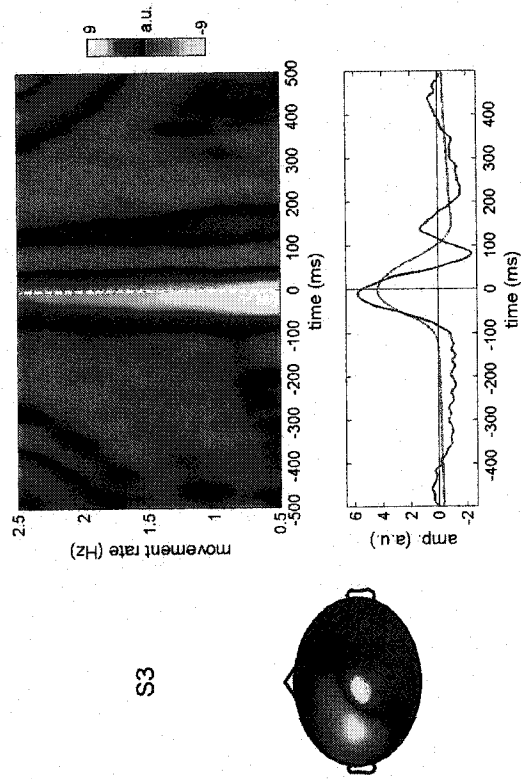
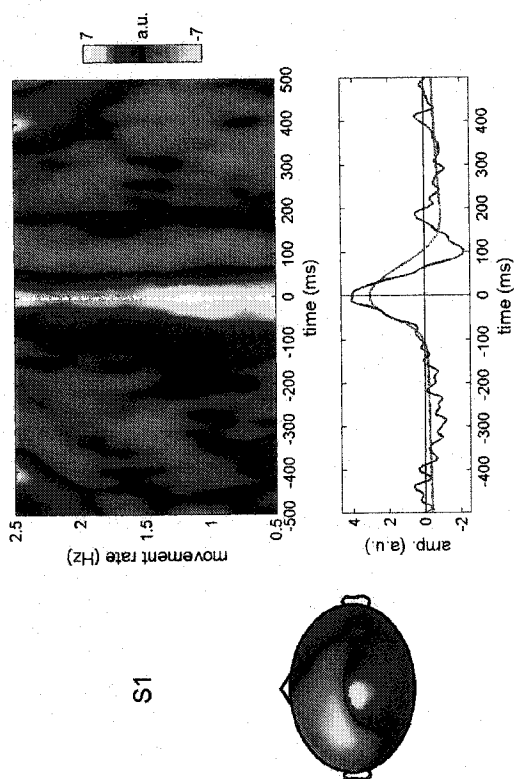
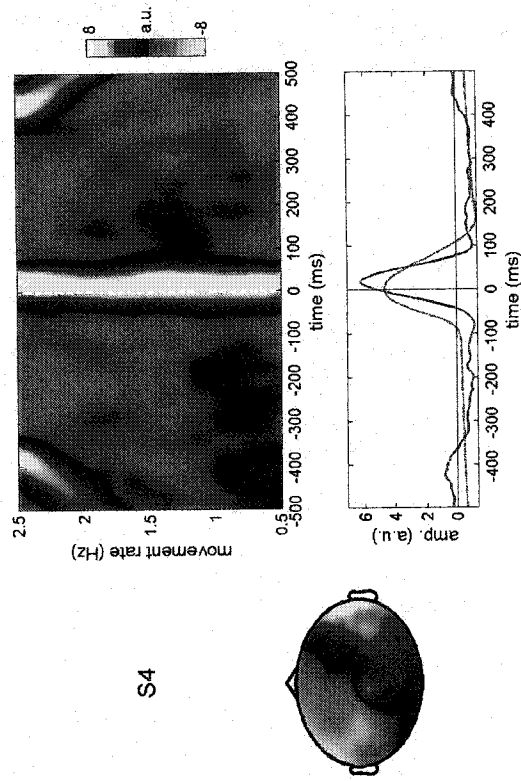
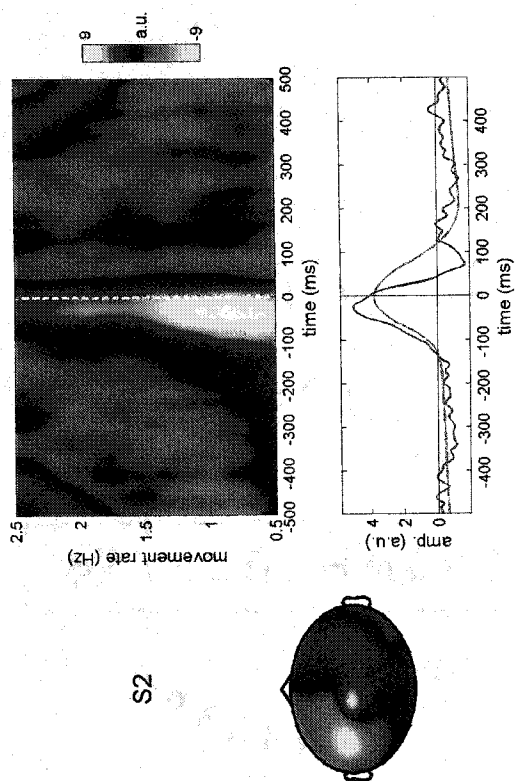
4.3.2. Continuation

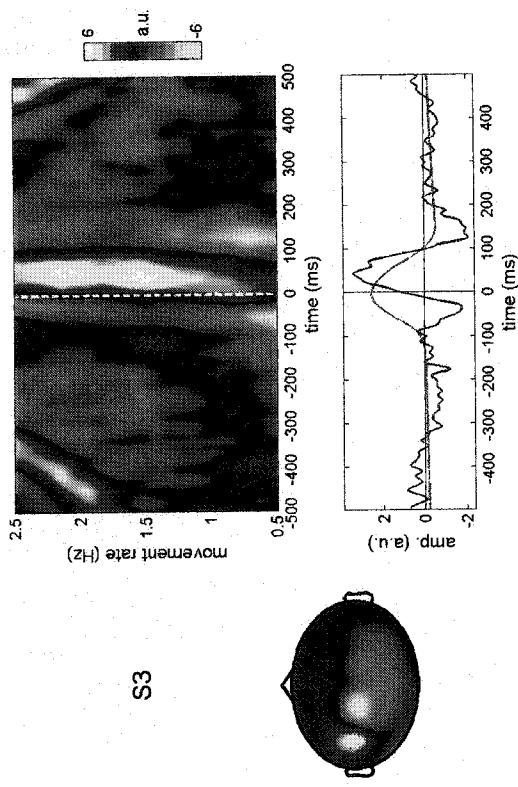
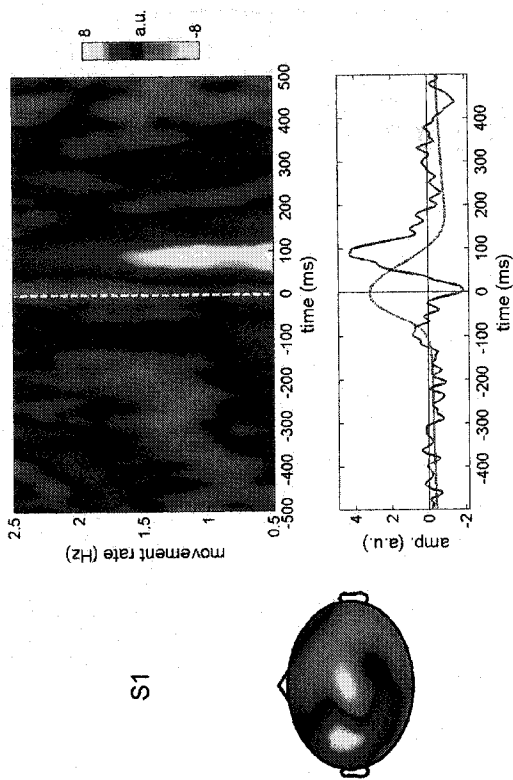
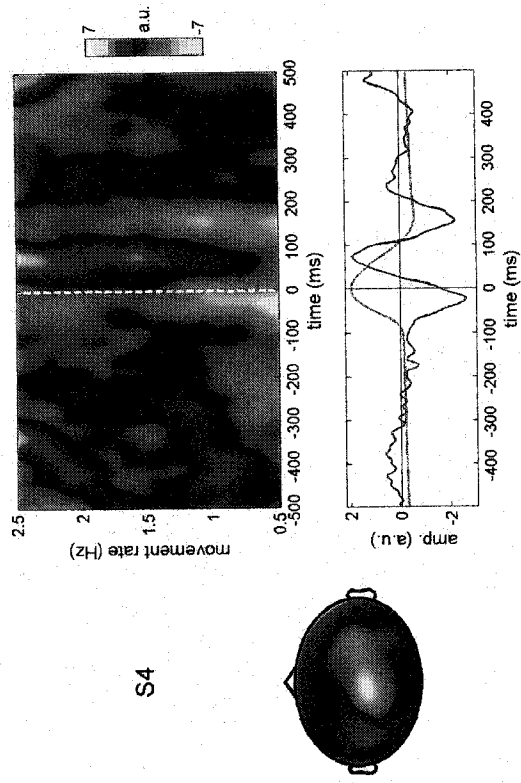
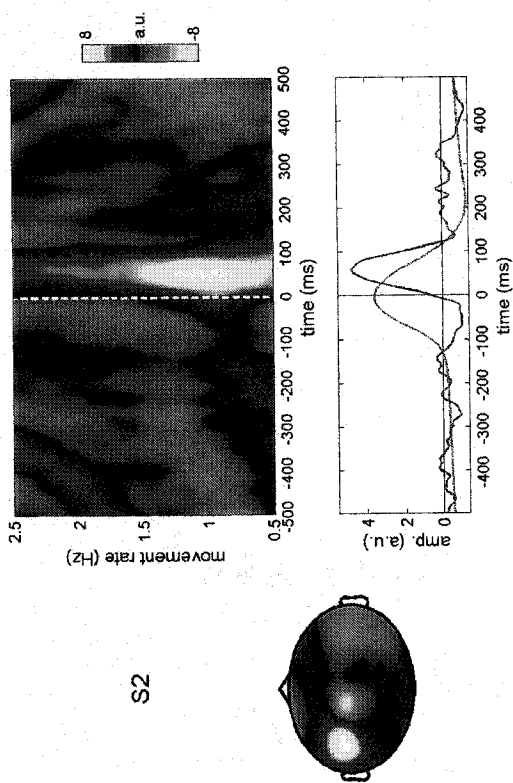
The continuation averages were analyzed first in order to provide a comparison with previous studies. For each subject, the averages at all rates were concatenated together, and ICA decomposition was performed on the entire dataset. Three main types of components were found for all subjects. The first type (type I) is shown in figure 4.2. The main characteristic of the spatial pattern of this component, shown at left for each subject in figure 4.2, is activity primarily on the side of the cortex contralateral to that of the movement. In addition, the response exhibits a dipolar pattern indicative of current flow parallel to the surface of the skull within left central cortex in a posterior-lateral direction. The plot at right-top for each subject shows the color-coded amplitude of this component at all rates for one second of data centered at peak finger flexion in arbitrary units. At bottom is the average of the activation pattern at all rates (red line) superimposed with an average movement profile at 1Hz (blue line). The main temporal

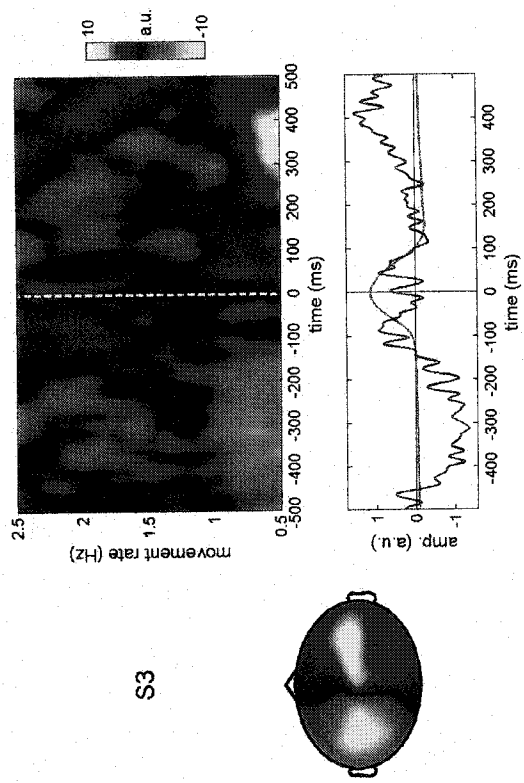
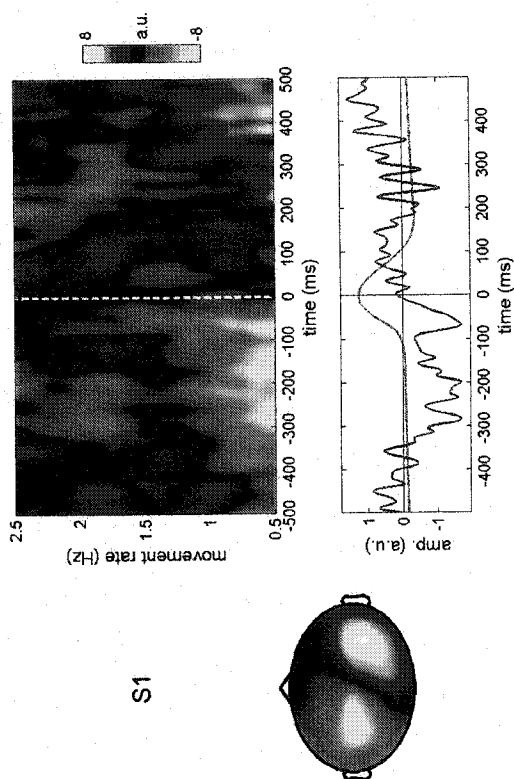
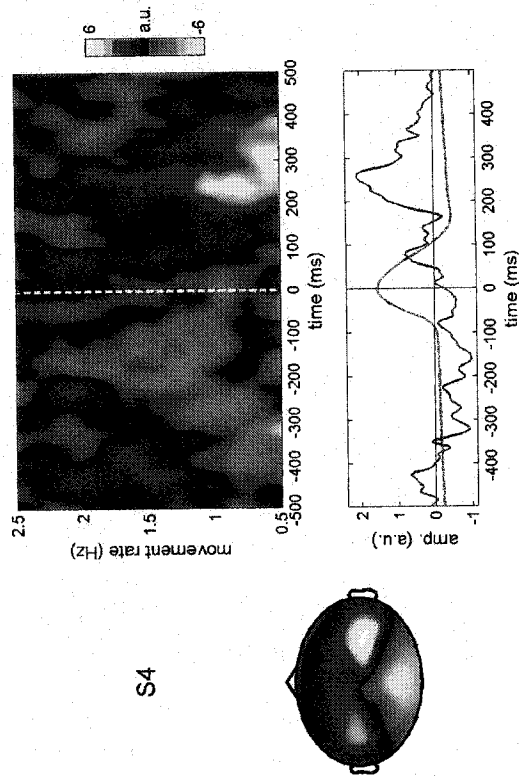
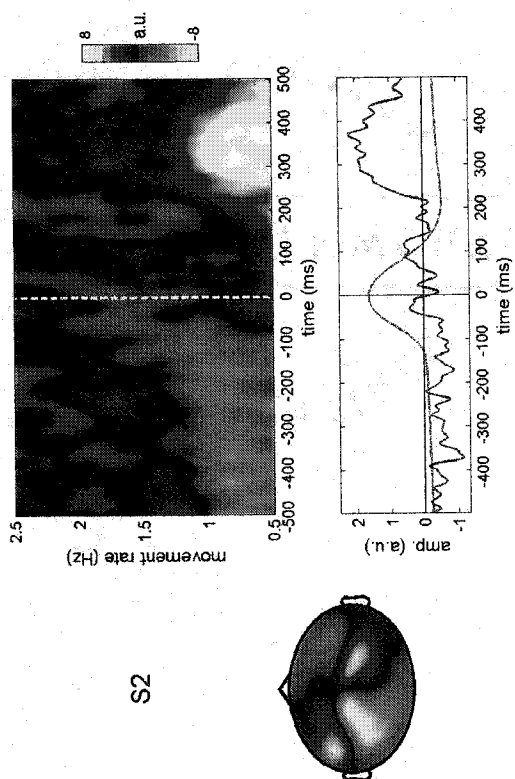
Figure 4.2. Type I ICA component from the continuation averages for all subjects. Left for each subject: Topographic image of the component. Red/yellow represents exiting field; blue/light-blue indicates entering field. Right-top: Color-coded rate-latency plot of the activation time series of the component at all movement rates. Latency is centered at peak flexion; amplitude is in arbitrary units. Bottom: Average of the activation time series across rate shown in red, and an average 1Hz movement time series shown in blue.

Figure 4.3. Same as figure 4.2 for the type II continuation component.

Figure 4.4. Same as figure 4.2 for the type III continuation component.







characteristic of this component in all subjects is a strong positive peak that occurs approximately 100ms after movement onset. In three out of four subjects (1-3), the main peak is followed by a second smaller positive deflection near movement offset. In all subjects, the amplitude of this response is almost independent of movement rate. The percent of variance accounted for by this, and all other components, is presented in table 4.1. The second type of component (type II) observed in all subjects is qualitatively similar to the type I response. As shown for the first component, the type II response is characterized by a dipolar pattern at the sensors over left-central cortex (figure 4.3). Underlying current flow is in an anterior direction in this case, opposite to the direction indicated for the type I response. The time series of the response exhibits a fast field oscillation during the movement, which is similar to the type I response, although the primary peak is during the extension phase of the movement. Amplitude stays at a near constant level at all rates, indicating a component independent of the rate of rhythmic movement.

Table 4.1.

Percent of mean variance accounted for by each ICA component

| Subject | Continuation | | | Synchronization | | |
|---------|--------------|---------|----------|-----------------|---------|----------|
| | Type I | Type II | Type III | Type I | Type II | Type III |
| 1 | 14% | 8% | 15% | 9% | 7% | 14% |
| 2 | 34% | 11% | 7% | 26% | 15% | 9% |
| 3 | 53% | 4% | 7% | 29% | 3% | 5% |
| 4 | 35% | 6% | 8% | 29% | 7% | 6% |

Figure 4.4 shows the last type of response (type III) that is consistently found in all subjects. The type III response is defined by three main characteristics that distinguish it from the previous two responses. The first is a diffuse bilateral pattern of activity spread over both sides of the cortex, which is less localized than the patterns for the first two types of responses. The second difference is a slower wave of temporal activation that peaks primarily pre- and post-movement. Lastly, unlike the previous two responses, the type III component exhibits a pronounced pattern of rate-dependence. For all subjects, the component is highest in amplitude at low rates, and practically disappears at rates between 1 and 2Hz.

4.3.3. Synchronization

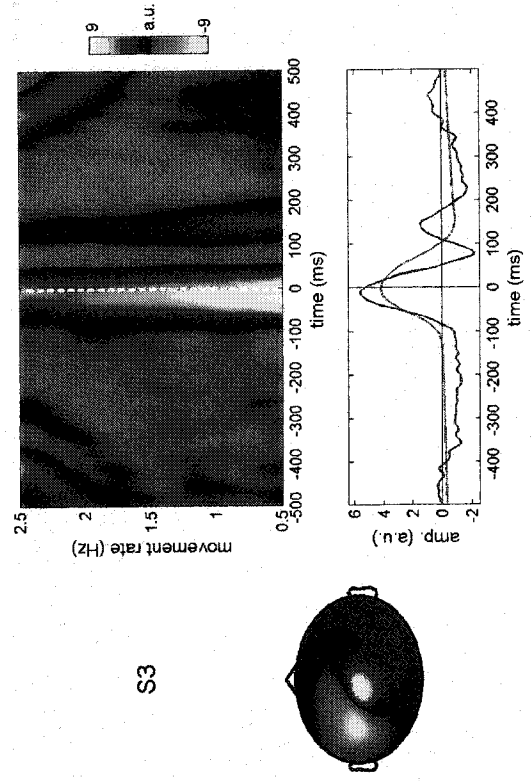
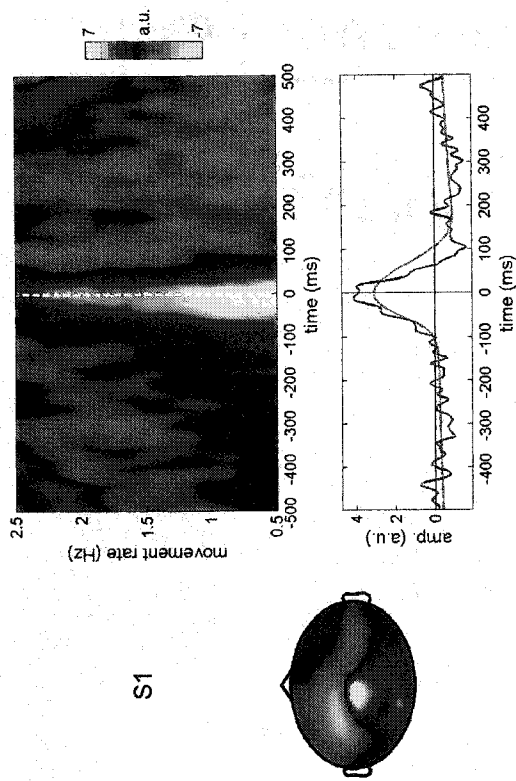
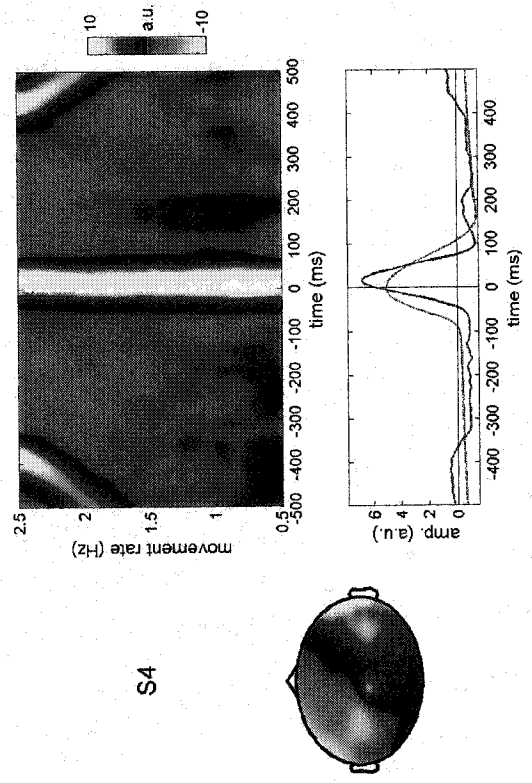
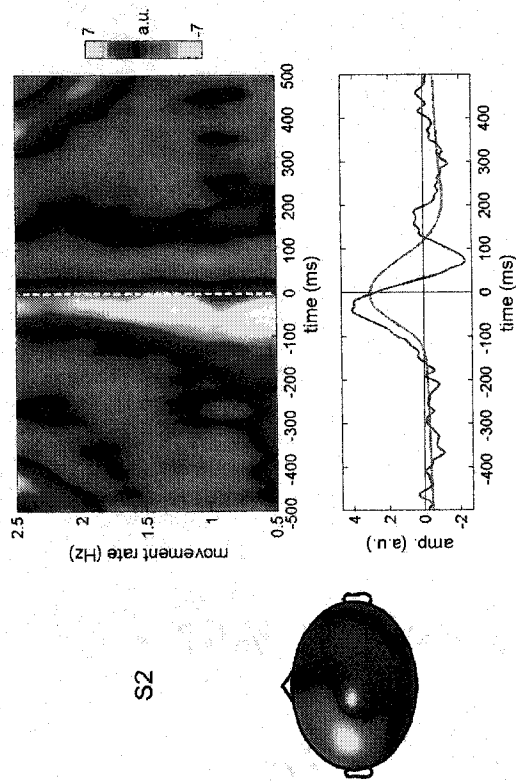
We applied the same ICA procedure to the averages from the synchronization phase at all rates with the intent to compare the component structure of the synchronization and continuation movement-related responses. No major differences were found. All subjects exhibited a motor component similar to the type I component presented above in figure 4.2. The defining characteristic of this response is a large amplitude peak near the peak of finger flexion. Figure 4.5 shows the type I synchronization component for all subjects. Just as above, the spatial pattern of the response is dominated by a dipolar structure over contralateral cortex, and the response is largely independent of movement rate. All subjects also show a component similar to the type II response revealed in the continuation condition (figure 4.6). The main feature is an amplitude peak just after peak flexion. Once again, the dipolar structure of the response is primarily contralateral to the side of movement and nearly opposite in

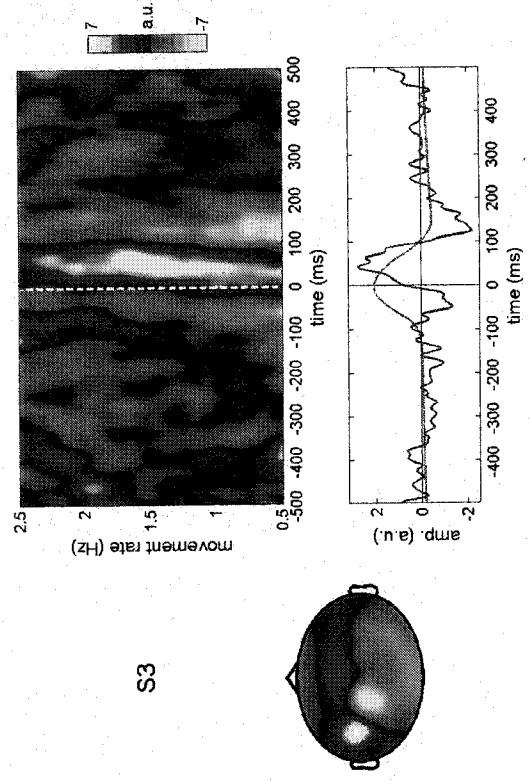
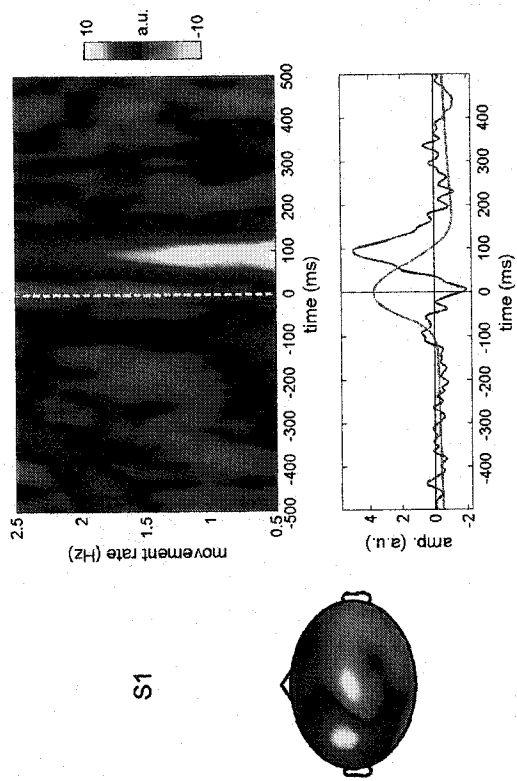
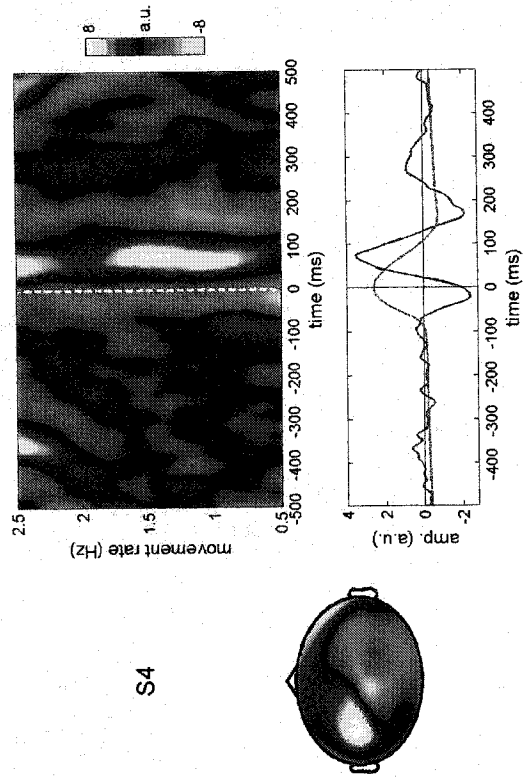
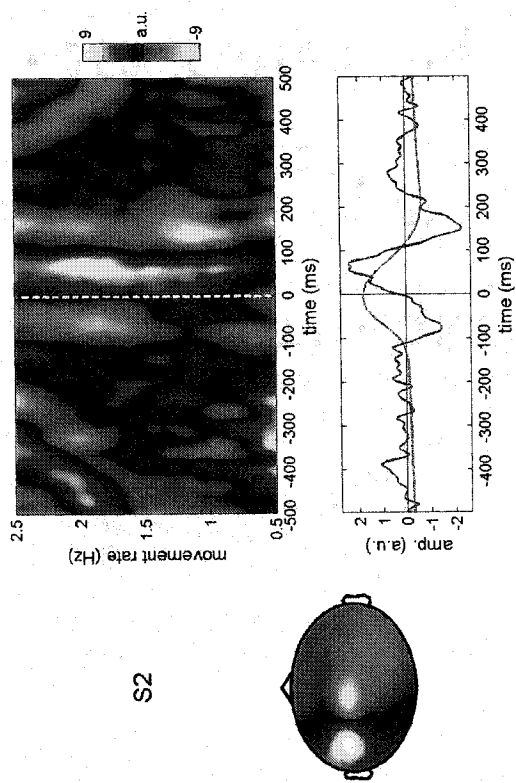
Figure 4.5. Same as figure 4.2 for the type I synchronization component.

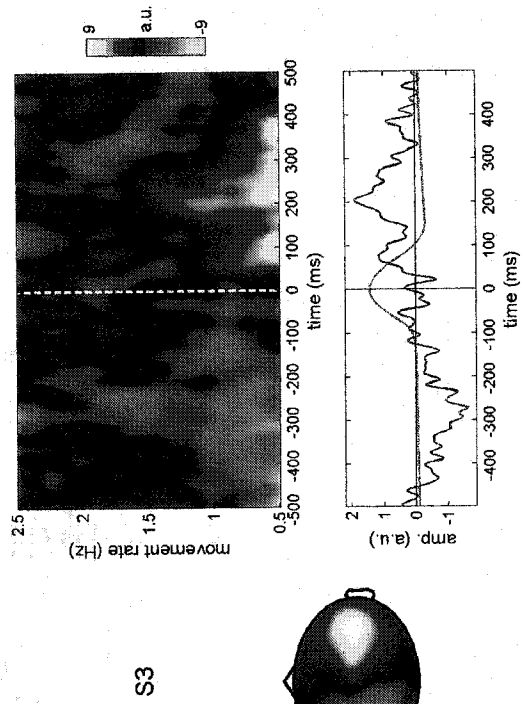
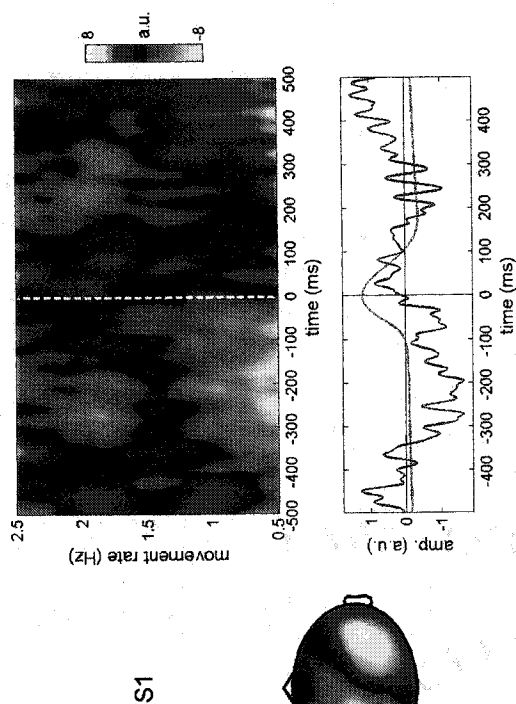
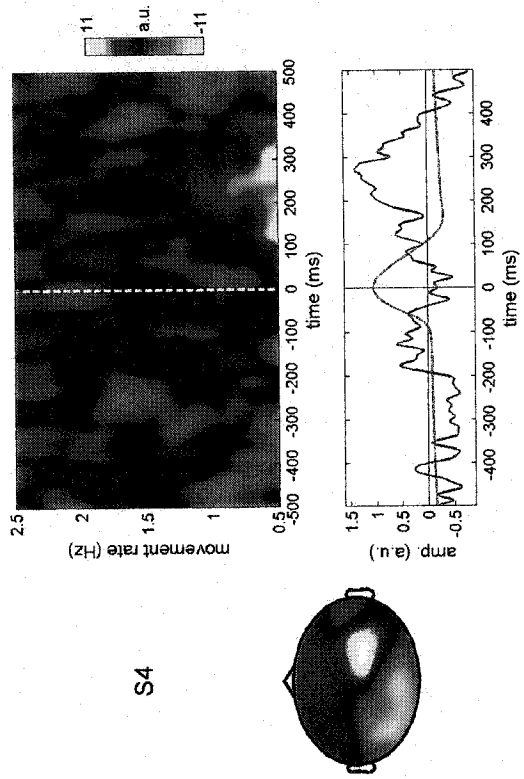
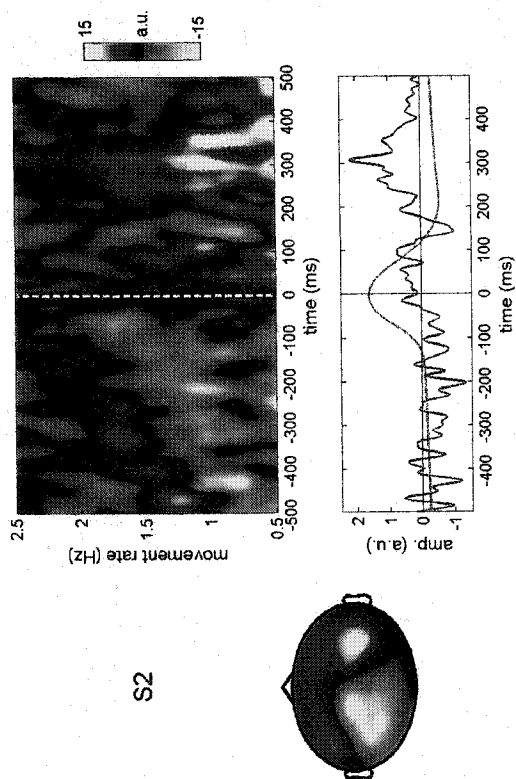
Figure 4.6. Same as figure 4.2 for the type II synchronization component.

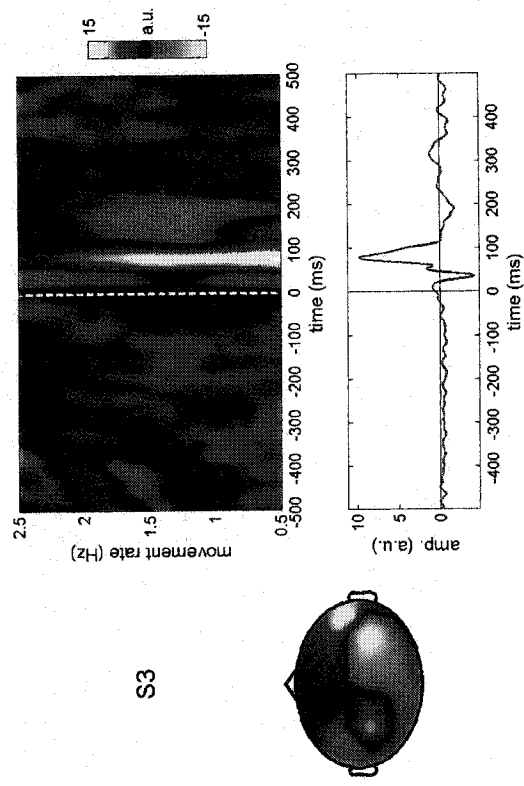
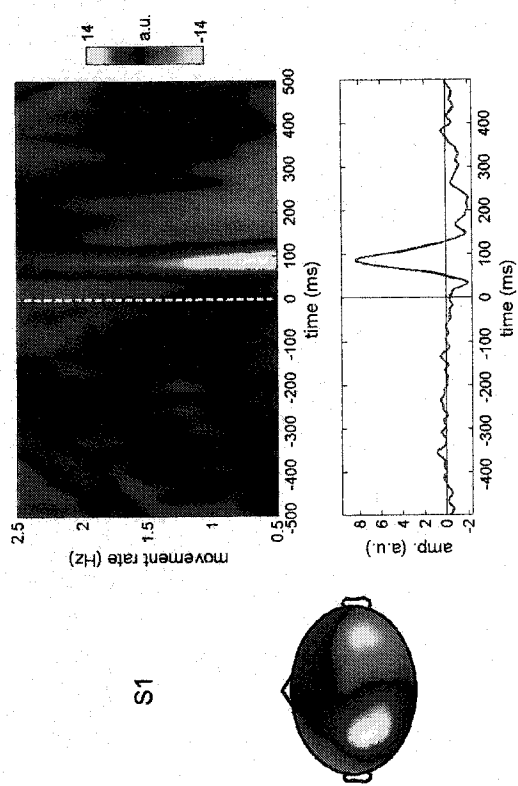
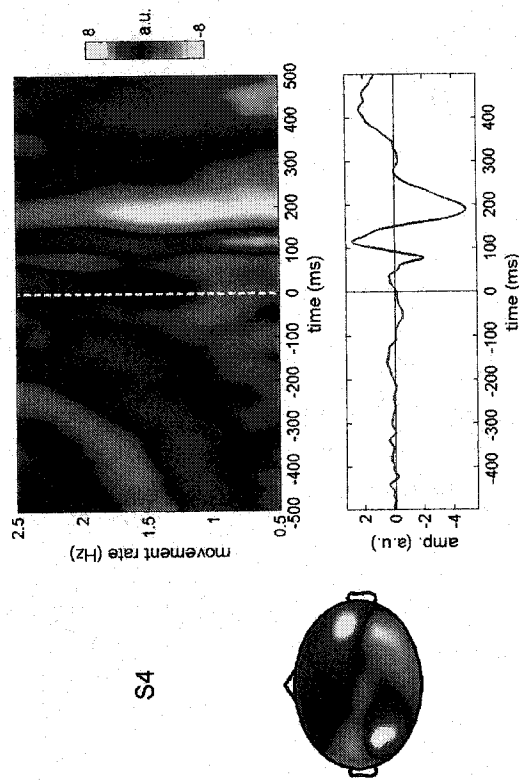
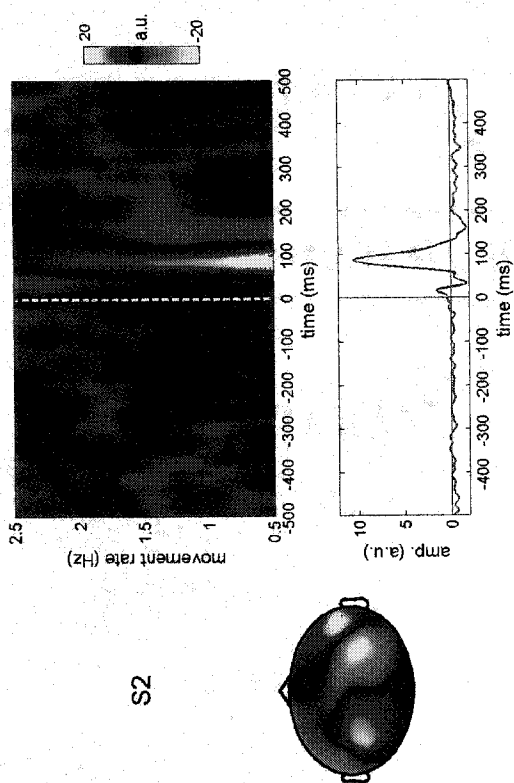
Figure 4.7. Same as figure 4.2 for the type III synchronization component.

Figure 4.8. Same as figure 4.2 for the synchronization N1m component. Latency is centered at tone onset.









orientation to the type I response. The slow-wave type III component found during continuation was also evident in the synchronization averages (figure 4.7). The spatial and temporal patterns of the components are remarkably similar in the two conditions. The primary features are bilateral activity and strong activation only at low stimulation rates. As in the continuation phase, the activity associated with this component peaks pre- and post-movement. Spatial and temporal correlations were performed in order to assess the correspondence between the similar response types in the continuation and synchronization conditions. The results are presented in table 4.2. All response types were significantly correlated between conditions, indicated by p -values less than .001 when the correlations were converted to t -tests. The similar temporal patterns of each component indicate not only a similar time course, but a similar rate dependence as well since the activation time series are appended together across rate.

A significant feature of the synchronization results is a lack of components corresponding to the typical auditory evoked responses. This includes the high amplitude N1m response, which should be visible at least at the lower stimulation rates used in this study (see Carver et al., 2002). An obvious explanation for this result is that the synchronization phases at each rate were averaged with respect to the peak of the movement. Each movement peak was not precisely timed with respect to tone onset; thus the N1m fell at slightly different latencies with respect to the movement and was averaged out of the time series. In order to test whether auditory evoked responses do occur during the synchronization phase we re-averaged the data at each rate with respect to tone onset and decomposed the results with the same ICA procedure as above. The components of the decomposition reveal a typical N1m auditory evoked response for

each subject (figure 4.8). As expected for the N1m, the component peaks in amplitude near 100ms latency. The spatial patterns of the responses show twin dipolar fields over both temporal cortices. For subject 4 the component captures an additional response of opposite polarity near 200ms latency.

Table 4.2.

Spatial and temporal correlations between continuation and synchronization components

| Subject | Component | Spatial | Temporal |
|---------|-----------|---------|----------|
| | | r | r |
| 1 | Type I | 0.926 | 0.728 |
| | Type II | 0.956 | 0.802 |
| | Type III | 0.982 | 0.747 |
| 2 | Type I | 0.990 | 0.769 |
| | Type II | 0.852 | 0.352 |
| | Type III | 0.760 | 0.378 |
| 3 | Type I | 0.998 | 0.954 |
| | Type II | 0.782 | 0.563 |
| | Type III | 0.935 | 0.575 |
| 4 | Type I | 0.997 | 0.942 |
| | Type II | 0.753 | 0.554 |
| | Type III | 0.744 | 0.347 |

4.4. Discussion

A major goal with this study was to compare the neural correlates of metronome-paced and self-paced movements over a broad range of rhythmic movement rates. For this purpose, we determined the component structure of the average neuromagnetic signals from the synchronization and continuation phases of a continuation paradigm.

The results revealed no large-scale difference in the cortical organization of synchronization versus continuation. This may be somewhat surprising given the different modes of coordination involved; however, the current findings are compatible with recent fMRI studies of continuation. For instance, Jäncke, Loose, Lutz, Specht, and Shah (2000) showed similar activation patterns for synchronization and continuation, but only if synchronization was performed with an auditory metronome as opposed to visual. This suggests that timing with an auditory metronome and self-paced timing both employ same cortical and subcortical network. Our finding of a similar component structure during the different coordinative modes is also supported in an fMRI continuation study by Jantzen, Steinberg, & Kelso (2002). The authors report no difference in the motor areas involved in synchronization vs. continuation. Activation was found in ventral premotor cortex, primary sensorimotor cortex, and SMA during both conditions. However, the authors do show that the activation pattern is highly context dependent; when subjects syncopated instead of synchronized during the pacing phase the increased activation produced by syncopation persisted into the continuation phase.

The decomposition of the synchronization and continuation averages revealed three major response types for all subjects. In our previous EEG continuation experiment (Chapter 3) we observed two components of the evoked response, which were similar in time course and rate dependence to the type I and III components seen here. The same ICA decomposition procedure was used in the EEG study, which implies that the greater number of components observed in the present study relates to differential sensitivities of the two recording technologies. An MEG continuation study by Mayville et al. (submitted) also reported only two components of the movement-related response.

However, the authors employed KL decomposition instead of ICA, which may account for the greater number of components found here. Although ICA is more commonly employed for artifact rejection and analysis of raw data (e.g. Makeig et al., 2002), we have shown that the procedure can be effective for finding task-related components in averaged data. Crucial to the current approach were analysis of a large dataset and reduction of the space using KL decomposition. Both factors increased the ratio of sample size to the number of channels, which can be an important factor in the success of the InfoMax algorithm (Bell & Sejnowski, 1995).

The first two components of the decompositions for each subject exhibited short amplitude peaks in close proximity to peak finger flexion. We have referred to these types of components as movement-evoked fields (MEFs) because they occur just after movement onset. In an MEG study by Kristeva et al. (1991) the authors found three such evoked fields with peaks at 100, 225 and 320ms after movement onset. The first of these responses (MEF1) likely corresponds to the initial peak of the type I response recorded here, which also peaks near 100ms after movement onset. EEG and MEG studies commonly report a large amplitude peak at a similar latency past movement onset (Cheyne & Weinberg, 1989; Hoshiyama et al., 1997; Shibasaki, Barrett, Halliday, & Halliday, 1980). The response has been localized to primary somatosensory cortex and is thought to arise from cutaneous and proprioceptive feedback elicited by the movement (Kristeva-Feige et al., 1996). The spatial pattern of the type I response in this study is consistent with activity in primary somatosensory cortex. All subjects show a clear dipolar pattern of activity over left central cortex, contralateral to the movement.

The second and third movement-evoked responses are not observed in all studies of voluntary movements. In the case of the second response, this fact has been suggested to relate to overlap from the high amplitude MEF1 (Kristeva et al., 1991). Here we overcame the problem of response overlap through the use of the independent components analysis procedure which separated overlapping time series based on their distinct spatiotemporal patterns of activity. This analysis revealed a second movement-evoked component (type II) that overlapped in time with the type I response. The primary feature of the type II response is a temporal peak in activity just after the peak of the movement, which is at a latency consistent with the second movement-evoked field (MEF2). The source of the MEF2 is not clear from previous studies, although Kristeva et al. (1991) state that the MEF2 and the motor field occurring just before movement onset exhibit similar spatial patterns of activity at the sensors. The motor field has been localized to primary motor cortex along the anterior wall of the central sulcus, and is associated with the outgoing motor command (Cheyne, Kristeva, & Deecke, 1991). Thus the MEF2 could represent activity associated with the outgoing motor command for the extension phase of the movement arising within primary motor cortex. The motor cortex receives direct and indirect sensory innervation, so the MEF2 could also be the result of sensory feedback from the movement.

The third movement-evoked field (MEF3) is thought to result from sensory feedback from the extension phase of the movement (Holroyd et al., 1999). In our previous EEG continuation study we observed that the first and the third movement-evoked potentials were associated with the same independent component (Chapter 3). The same is found here for two out of four subjects who show a second positive peak in

the time series of the type I response at a latency associated with the MEF3. This indicates that the spatial pattern of the MEF1 and MEF3 are the same, which is expected given that both responses are hypothesized to represent sensory feedback from the finger, and presumably innervate similar areas of cortex.

The third type of component revealed by the ICA procedure is distinct from the previous two in that activation extended from well before to well after the actual movement. Because it is not directly related to sensory feedback arising during the movement, this type of component has been termed movement-related as opposed to movement-evoked (Cheyne & Weinberg, 1989). In MEG studies, slow-wave activity observed prior to movement onset is referred to as the readiness field, or the Bereitschaftsmagnetfeld (BM), and follows a similar time course as the readiness potential observed in EEG (Deecke, Weinberg, & Brickett, 1982; Hari et al., 1983). The spatial pattern of the slow-wave activity observed here is very similar to the BM observed in previous studies. The response consists of diffuse bilateral activity with field exiting the head on the left, and entering on the right. This pattern reflects bilateral activity in a distributed set of areas in motor cortex typically associated with motor planning and execution, such as the supplementary motor area and the pre-motor cortex (Erdler et al., 2000; Lang et al., 1991). The major difference between the present results and those of previous studies is that here the slow-wave components do not cease at movement onset, but instead continue throughout and after the movement. In fact all subjects show a field reversal after the movement. This pattern of field reversal was likely not observed in previous studies due to overlap from the high amplitude movement-evoked fields. Post movement activity may also have been more pronounced in the present results due to an

experimental context distinct from previous studies of voluntary movement. These studies typically involve isolated voluntary movements requiring no precise timing relative to a metronome or to neighboring movements (e.g. Cheyne & Weinberg, 1989). In the present study subjects were required to perform finger flexion at a set rate, which could produce more post-movement processing of sensory information necessary to assess the timing of the just performed movement.

The amplitude of the type III response is highly dependent on movement rate, which contrasts with the relatively constant amplitude of the type I and II responses. A slow-wave component observed in previous continuation studies showed a similar pattern of rate dependence (Chapter 3, Mayville et al., submitted). As discussed above, SMA is a primary contributor to slow-wave activity preceding voluntary movements (Erdler et al., 2000). A PET study by Sadato et al. (1996) showed attenuation of SMA activation with increased movement rate, which supports the present finding of a rate-dependent decrease in pre-movement activity. The differential rate dependence of the response components observed here has significant implications for our understanding of the control of rhythmic movements. Slow-wave activity prior to movement onset is associated with the planning and preparation of voluntary movements. Because this activity disappears between 1 and 2Hz, it may reflect a transition in the mode of coordination away from one in which each movement is individually planned and controlled. At higher rates the only movement-related cortical activity is the simple evoked responses elicited by the physical parameters of the movement. This suggests a transition into a mode of coordination in which the cortex is monitoring a sustained oscillatory process instead of controlling individual movements. The transition from a discrete to a continuous mode of

coordination may in turn relate to transitions in sensorimotor coordination known to occur between 1 and 2Hz (e.g. Engström et al., 1996; Kelso et al., 1990). Future investigation employing both the present paradigm and the transition paradigms in previous studies is needed to show whether the precise rate of cortical reorganization is associated with a rate of behavioral transition.

One reason for performing the present continuation experiments was to characterize the onset of the movement-related steady-state response recorded previously by Gerloff et al. (1997, 1998) at a movement rate of 2Hz. Our intent was to shed light on the origin of the response by observing its evolution with increased movement rate. Since movement-related cortical activity can last well over a second, the steady-state response observed at 2Hz could be affected by the overlap of activity associated with successive movements. By systematically studying a range of movement rates we stood a better chance of observing the effect of response overlap as IRI decreased to a length where overlap could occur. However, the present analyses revealed no evidence of significant interference between successive responses. At slow rates, the duration of the slow-wave responses was over a second, but as rate increased the slow-wave activity reduced, and was essentially non-existent beyond rates of 1.5Hz. This left the movement-evoked responses as the only remaining source of cortical activity at higher rates. The MEFs were remarkably consistent across movement rate, showing no large-scale changes in amplitude or latency. This result supports the Gerloff et al. (1997, 1998) suggestion that the steady-state paradigm is a faster method for observing the movement-evoked responses in clinical applications.

In the Gerloff et al. (1997) EEG study, the authors used a metronome to pace finger movement; however, they report no evidence of auditory evoked responses in the movement-related averages. Here, we found the same to be true when the synchronization averages were centered at the peak of the movement. However, when averaged around tone onset we found the N1m auditory components. Due to their short time course and the lack of temporal precision of the movement, these components were presumably attenuated when the averages were timed with the movement instead of the tone. The lack of auditory components in the movement centered synchronization averages, and the similarity of the component structure of synchronization and continuation suggest that in the steady-state paradigm it is not necessary to employ continuation in order to observe the movement-evoked responses.

General Discussion

The experiments in this thesis were aimed at the question of how humans perceive and produce rhythms. By performing a thorough investigation of the neuromagnetic and neuroelectric responses to auditory stimulation and movement as a function of rate we were able to identify correlates in the neural activity patterns that allow for a better understanding of the mechanisms underlying rhythm perception and production. Additionally, through a systematic variation of stimulus and movement rate in small steps across a wide range of rates we found transition-like phenomena in the brain activity at rates that have been identified as functionally significant in earlier behavioral studies. Employing both EEG and MEG in almost identical experimental settings we took advantage of the complementary information provided by these neurophysiological measures, which lead to a more comprehensive picture of neural activity than could be obtained from a single imaging technology. Moreover, we developed and applied sophisticated data analysis and visualization methods that allow for a representation of large datasets in a compressed fashion.

Rate Dependence of the Transient Responses

In all four studies presented here we found components of the event-related brain responses that exhibit a strong dependence on the rate of auditory stimulation or movement. In the auditory experiments (Chapters 1 & 2), evidence of a rate-dependent

reorganization of the transient responses was found in a systematic decrease of N1/N1m amplitude with decreasing ISI. This response is believed to reflect changes in the auditory environment; in fact, an N1 is elicited by the offset of a tone if the tone lasts over 500ms (Näätänen, & Winkler, 1999). The reduction of the N1/N1m components with increased stimulation rate found by us and others may reflect the fact that as stimuli come closer together each new tone represents less of a change in the environment. From this point of view, the predicted disappearance of the response near a stimulation rate of 10Hz then indicates the border beyond which tones are no longer clearly distinct. This finding is in accordance with perceptual evidence indicating that rhythm perception is only possible for ISIs from ~120 to 1800ms (Fraisse, 1982). At the high end of the range of ISIs, separate tones are no longer grouped as a rhythmic pattern and the next stimulus can no longer be anticipated. Despite this fact, the amplitude of the N1/N1m is known to be dependent on stimulation rate for rates below 0.1Hz (Hari, Kaila, Katila, Tuomisto, & Varpula, 1982), suggesting that the reminiscence of tone stimulation represented by N1/N1m attenuation does not reflect the onset of rhythm perception at low rates. So what are the possible signs of the beginning of rhythm perception in the cortical evoked potentials? One candidate is the broad 500ms response discussed in Chapter 1. A component at this latency has not been observed in previous studies of transient responses with longer inter-stimulus intervals than the ones used here (e.g. Picton, Hillyard, Krausz, & Galambos, 1974), indicating that it can only be observed above a certain stimulation rate. Moreover, responses at such long latencies have been associated with higher order cognitive processing; for example, the P300 elicited in an auditory oddball paradigm (McCarthy & Donchin, 1981; Polich & Kok, 1995). Further

experiments are needed to discover under what conditions the 500ms response is elicited in order to determine its possible connection to rhythm perception.

In the continuation studies (Chapters 3 & 4), the pre-movement Bereitschaftspotential/Bereitschaftsmagnetfeld (BP/BM) was found to disappear above a movement rate of 1Hz. Pre-movement activity of this kind is commonly reported in studies employing self-initiated movements separated by several seconds, and is indicative of motor planning and control activity in regions such as supplementary motor area and premotor cortex (Deecke, Weinberg, & Brickett, 1982; Erdler et al., 2000; Hari et al., 1983; Lang et al., 1991). Studies of this kind typically employ self-paced movements; however, here it was shown that pre-movement slow-wave activity occurs with metronome pacing as well (Chapter 4). The loss of motor planning activity at rates above 1Hz suggests a change in the control of the rhythmic movement from a discrete “one-at-a-time” initiation of separate movements, towards maintaining a sustained oscillation of the effector where movements are controlled as a single rhythmic process. This transition suggests that at least two forms of organization of a series of rhythmic movements exist, with rate being the control parameter that drives the transition. This transition may also relate to known rate-dependent differences in coordinative abilities that occur within parameter ranges employed here (e.g. Engström, Kelso, & Holroyd, 1996; Kelso, 1984). At rates near 2Hz subjects lose the ability to syncopate with a metronome (Kelso, DelColle, & Schöner, 1990). Syncopation as compared to synchronization is known to require more direct control of individual movements, which may lead to an inability to perform syncopation when inter-response intervals are too short to separately plan each movement (Mayville, Jantzen, Fuchs, Steinberg, & Kelso,

2002). The reduction in motor planning activity seen here supports this idea by indicating that at high rates the cortex no longer directly controls individual movements. The disappearance of pre-movement activity occurs at rates just above 1Hz, which is well below rates typically associated with the transition from syncopation to synchronization. However, in the relatively simple task employed here subjects may switch to a mode of monitoring a sustained oscillation before the highest rate at which they still have the capacity to control movements individually. In other words, subjects may be able to maintain separate planning of each movement at higher rates during a more demanding task such as syncopation. An experiment to test this idea would employ syncopation and synchronization over the same movement rates in order to determine if the attempt to maintain syncopation results in a delay of the decrease in motor planning activity relative to synchronization.

Transition into the Steady-state

The experiments in this thesis were designed to characterize the transition from discrete transient evoked activity at low stimulus and movement rates to a continuous steady-state response at high rates. For the auditory responses, earlier experiments have focused on determining the origin of steady-state activity, although typically using higher stimulation rates than employed here (Azzena et al., 1995; Gutschalk et al., 1999; Hari, Hämäläinen, & Joutsiniemi, 1989). In the MEG study presented in Chapter 1 it was found that continuous steady-state activity begins at a stimulation rate of 2Hz and is associated with an overlap between successive transient responses, i.e. an interaction between the 500ms response and a 50ms P1m response to the next tone. In the auditory

EEG study (Chapter 2) the onset of the steady-state response at 2Hz was also associated with the beginning of large-scale oscillations of the evoked response at low multiples of the stimulation rate, indicating a resonant-like response to the rhythmic stimulation. The origin of oscillatory activity at 2Hz is an open question; however, the onset of overlap between successive transient responses at the same stimulation rate suggests that the two phenomena are related. The fact that oscillatory activity appears at a stimulation rate of 2Hz may also be significant for the understanding of known perceptual phenomena, such as a preference for listening to a metronome near this rate (Fraisse, 1982), and an increased ability to perceive the difference between two metronome rates if they are both near 2Hz (Drake & Botte, 1993). Perceptual phenomena such as these lead Drake and Bertrand (2001) to refer to rates near 2Hz as a 'zone of optimal processing' for rhythm perception, which suggests that the cortical resonances seen here mark a period of perceptual resonance as well.

A major finding of the above experiments was that transients are imbedded in the steady-state in both the auditory and motor domains. In each case, the onset of a continuous steady-state response with increased stimulation and movement rates did not represent a fundamental reorganization of the response in which transients died out and a new continuous oscillation appeared from a new source. In the auditory experiments the steady-state response began at a stimulation rate of 2Hz, but transient responses such as the N1m and the 40Hz response continued into higher stimulation rates. This juxtaposition of continuous steady-state activity and discrete transient responses suggests a possible coexistence of continuous and discrete representations of the series of tones. A similar combination of transient and steady-state activity occurred in the studies of

rhythmic movements. As movement rate increased, pre-movement activity associated with motor planning and initiation disappeared, implying that individual movements were no longer planned and controlled separately, but instead the series of movements were controlled as a single rhythmic process. However, this transition did not lead to a disappearance of separate evoked responses associated with each movement. Just as with the auditory experiments, the cortex appears to have access to both continuous and discrete aspects of the train of movements.

The possible coexistence of continuous and discrete representations in both the auditory and motor rhythmic responses is in agreement with past work indicating multiple representations of rhythm at different time scales and in distinct brain regions (Chen, Ding, & Kelso, 1997, 2001; Jantzen, Steinberg, & Kelso, 2002; Lashley, 1951; Mayville, Jantzen, Fuchs, Steinberg, & Kelso, 2002; Nair, Purcott, Fuchs, Steinberg, & Kelso, 2003; Rao et al., 1997). Instead of being single stand-alone processes, rhythm perception and production appear to rely on a dynamic interplay between representations at different levels of organization. From this perspective, rate-dependent differences in perceptual and coordinative abilities may depend on which aspect of the representation is dominant at certain rates (e.g. Drake and Botte, 1993; Kelso, DelColle, & Schöner, 1990). In addition, preferences for listening to tones and producing movements at a rate of 2Hz (Fraisse, 1982) might relate to a balance between discrete and continuous representations near the border between transient and steady-state activity.

Interaction of Spontaneous and Evoked Activity

In addition to the analysis based on averaged brain data, we also studied the relationship between spontaneous and evoked 40Hz gamma activity (chapter 2) in unaveraged single trial signals. We found first, that the evoked gamma response is generated by phase resetting of ongoing gamma activity, and second that the amplitude of the evoked response depends on the phase of the ongoing spontaneous activity. Similar phase-resetting behavior has been seen in the alpha and theta frequency bands with visual stimulation, suggesting that phase resetting is a common mechanism in brain function (Makeig et al., 2002; Tesche & Karhu, 2000). These results highlight the importance of investigating non-phase locked activity in studies of event-related responses, as the process of averaging can lead to the false assumption that evoked responses represent an increase in cortical activity, when instead they may be generated by phase resetting of ongoing rhythms. The cortex is shown here to possess its own internal dynamics, and it is the interplay between this ongoing activity and incoming sensory information that creates the evoked response.

The functional significance of the auditory gamma resetting observed here remains an open question. Synchronous gamma activity has been related to functional binding of separate cortical areas (for a review see Lee, Williams, Breakspear, & Gordon, 2003). In this context, phase resetting of ongoing rhythms by an incoming stimulus may serve as a mechanism for synchronizing separate neural ensembles. Also, attention to auditory stimuli is known to increase the amplitude of evoked gamma activity (Tiitinen et al., 1993). The present results suggest that the amplitude increase may relate to increased pre-stimulus gamma activity that is reset by the stimulus to form a larger evoked

response. In support of a relationship between pre-stimulus gamma activity and attention, Makeig and Jung (1996) showed that increased amplitude of pre-stimulus gamma activity was correlated with better performance in a target detection task. In addition, Snyder and Large (submitted) showed an increase in non phase-locked gamma activity in expectation of tone stimulation that was then reset by the stimulus, suggesting that modulation of gamma activity is associated with focused attention.

Additional studies are needed to determine if the same phase resetting behavior occurs with shorter inter-stimulus intervals when evoked 40Hz responses begin to overlap. In other words, does the phase of the previous evoked response affect the amplitude of the response to the present tone? If the phase-amplitude relation holds, it may be important for understanding the origins of the large amplitude steady-state response observed with stimulation at 40Hz (Galambos, Makeig, & Talmachoff, 1981). According to the present results, the 40Hz SSR could be the product of resonance between successive evoked gamma responses that overlap at the correct phase, instead of mere linear summation of overlapping responses at the sensors as has been previously hypothesized (Hari, Hämäläinen, & Joutsiniemi, 1989). In addition, phase resetting of overlapping evoked gamma responses may relate to perceptual binding of neighboring auditory stimuli (see Sauvé, 1999). Joliot, Ribary, and Llinas (1994) showed that differences in cortical gamma activity relate to whether two click stimuli in close proximity are perceived as distinct. If the clicks were separated by less than 13ms they were perceived as a single event. This boundary was also associated with the existence of one or two evoked gamma responses; below 13ms only the gamma response to the first stimuli was observed. The phase/amplitude relation observed here may contribute

to the reduction of the second response by suppressing new activation that comes within a particular phase of the first gamma response.

References

- Alain, C., Woods, D. L., & Ogawa, K. H. (1994). Brain indices of automatic processing. *Neuroreport*, 6, 140-144.
- Aldenderfer, M. S., & Blashfield, R. K. (1984). *Cluster analysis*. Newbury Park: Sage Publications.
- Azzena, G. B., Conti, G., & Santarelli, R., Ottaviani, F., Paludetti, G., & Maurizi, M. (1995). Generation of human auditory steady-state responses (SSRs). I: Stimulus rate effects. *Hearing Research*, 83, 1-8.
- Barrett, G., Shibasaki, N., & Neshige, R. (1986). Cortical potentials preceding voluntary movement: evidence for three periods of preparation in man. *Electroencephalography and Clinical Neurophysiology*, 63, 327-339.
- Başar, E. (1980). *EEG-brain dynamics: Relations between EEG and brain evoked potentials*. New York: Elsevier.
- Başar, E., Rosen, B., Başar-Eroglu, C., & Greitschus, F. (1987). The associations between 40 Hz-EEG and the middle latency response of the auditory evoked potential. *International Journal of Neuroscience*, 33, 103-17.
- Başar-Erglu, C., Strüber, D., Schürmann, M., Stadler, M., & Başar, E. (1996). Gamma-band responses in the brain: a short review of psychophysiological correlates and functional significance. *International Journal of Psychophysiology*, 24, 101-112.
- Bell, A. J., & Sejnowski, T. J. (1995). An information-maximization approach to blind

- separation and blind deconvolution. *Neural Computation*, 7, 1129-1159.
- Brandt, M. E., Jansen, B. H., & Carbonari, J. P. (1991). Pre-stimulus spectral EEG patterns and the visual evoked response. *Electroencephalography and Clinical Neurophysiology*, 80, 16-20.
- Bressler, S. L., Coppola, R., & Nakamura, R. (1993). Episodic multiregional cortical coherence at multiple frequencies during visual task performance. *Nature*, 366, 153-156.
- Carver, F. W., Fuchs, A., Jantzen, K. J., & Kelso, J. A. S. (2002). Spatiotemporal analysis of neuromagnetic activity associated with rhythmic auditory stimulation. *Clinical Neurophysiology*, 113, 1921-1931.
- Carver, F. W., Fuchs, A., Mayville, J. M., Davis, S. W., & Kelso, J. A. S. (1999). Systematic investigation of the human brain's response to rhythmic auditory stimulation [Abstract]. *Dynamical Neuroscience VII*.
- Chen, Y., Ding, M., & Kelso, J. A. S. (1997). Long memory process (1/f) type in human coordination. *Physical Review Letters*, 79, 4501-4504.
- Chen, Y., Ding, M., & Kelso, J. A. S. (2001). Origins of timing errors in human sensorimotor coordination. *Journal of motor behavior*, 33, 3-8.
- Cheyne, D., Endo, H., Takeda, T., & Weinberg (1997). Sensory feedback contributes to early movement-evoked fields during voluntary finger movements in humans. *Brain Research*, 771, 196-202.
- Cheyne, D., & Weinberg, H. (1989). Neuromagnetic fields accompanying finger movements. *Experimental Brain Research*, 78, 604-612.
- Cheyne, D., Kristeva, R., & Deecke, L. (1991). Homuncular organization of human

- motor cortex as indicated by neuromagnetic recordings. *Neuroscience Letters*, 122, 17-20.
- Cheyne, D., Weinberg, H., Gaetz, W., & Jantzen, K. J. (1995). Motor cortex activity and predicting side of movement: Neural network and dipole analysis of pre-movement magnetic fields. *Neuroscience Letters*, 188, 81-84.
- Deecke, L., Grözing, B., & Kornhuber, H. H. (1976). Voluntary finger movement in man: Cerebral potentials and theory. *Biological Cybernetics*, 23, 99-119.
- Deecke, L., & Kornhuber, H. H. (1978). An electrical sign of participation of the mesial 'supplementary' motor cortex in human voluntary movement. *Brain Research*, 159, 473-476.
- Deecke, L., Weinberg, H., & Brickett, P. (1982). Magnetic fields of the human brain accompanying voluntary movement: Bereitschaftsmagnetfeld. *Experimental Brain Research*, 48, 144-148.
- Drake, C., & Bertrand, D. (2001). The quest for universals in temporal processing in music. *Annals of the New York Academy of Sciences*, 930, 17-27.
- Drake, C., & Botte, M. C. (1993). Tempo sensitivity in auditory sequences: Evidence for a multiple-look model. *Perception & Psychophysics*, 54, 277-286.
- Engström, D. A., Kelso, J. A. S., & Holroyd, T. (1996). Reaction-anticipation transitions in human perception-action patterns. *Human Movement Science*, 15, 809-832.
- Erdler, M., Beisteiner, R., Mayer, D., Kaindl, T., Edward, V., Windischberger, C., et al. (2000). Supplementary motor area activation preceding voluntary movement is detectable with a whole-scalp magnetoencephalography system. *Neuroimage*, 11, 697-707.

- Erwin, R. J., & Buchwald, J. S. (1986). Midlatency auditory evoked responses: Differential recovery cycle characteristics. *Electroencephalography and Clinical Neurophysiology*, 64, 417-423.
- Fraisse, P. (1982). Rhythm and tempo. In D. Deutsch (Ed.), *The psychology of music* (pp. 149-180). New York: Academic Press.
- Fuchs, A., Kelso, J. A. S., & Haken, H. (1992). Phase transitions in the human brain: Spatial mode dynamics. *International Journal of Bifurcation and Chaos*, 2, 917-939.
- Galambos, R., Makeig, S., & Talmachoff, P. J. (1981). A 40-Hz auditory potential recorded from the human scalp. *Proceedings of the National Academy of Sciences*, 78, 2643-2647.
- Gerloff, C., Toro, C., Uenishi, N., Cohen, L. G., Leocani, L., & Hallett, M. (1997). Steady-state movement-related cortical potentials: A new approach to assessing cortical activity associated with fast repetitive finger movements. *Electroencephalography and Clinical Neurophysiology*, 102, 106-113.
- Gerloff, C., Uenishi, N., Nagamine, T., Kunieda, T., Hallett, M., & Shibasaki, H. (1998). Cortical activation during fast repetitive finger movements in humans: Steady-state movement-related magnetic fields and their cortical generators. *Electroencephalography and Clinical Neurophysiology*, 109, 444-453.
- Gilden, D. L., Thornton, T., & Mallon, M. W. (1995). 1/f noise in human cognition. *Science*, 267, 1837-1839.
- Gray, C. M., & Singer, W. (1989). Stimulus-specific neuronal oscillations in orientation columns of cat visual cortex. *Proceedings of the National Academy of Sciences*,

86, 1698-1702.

Gura, T. (2001) Rhythm of life. *New Scientist*, 171, 32-35.

Gutschalk, A., Mase, R., Roth, R., Ille, N., Rupp, A., Hähnel S., et al. (1999).

Deconvolution of 40 Hz steady-state fields reveals two overlapping source activities of the human auditory cortex. *Clinical Neurophysiology*, 110, 856-868.

Haken, H. (1977). *Synergetics: An Introduction*. Springer Verlag, Berlin.

Haken, H., Kelso, J. A. S., & Bunz, H. (1985). A theoretical model of phase transitions in human hand movements. *Biological Cybernetics*, 51, 347-356.

Hari, R., Antervo, A., Katila, T., Poutanen, T., Seppänen, M., Toumisto, T., et al. (1983). Cerebral magnetic fields associated with voluntary limb movements. *Il Nuova Cimento*, 2D, 484-494.

Hari, R., Hämäläinen, M., & Joutsiniemi, S. L. (1989). Neuromagnetic steady-state responses to auditory stimuli. *The Journal of the Acoustical Society of America*, 86, 1033-1039.

Hari, R., Kaila, K., Katila, T., Tuomisto, T., & Varpula, T. (1982). Interstimulus interval dependence of the auditory vertex response and its magnetic counterpart: Implications for their neural generation. *Electroencephalography and Clinical Neurophysiology*, 54, 561-569.

Hari, R., Pelizzzone, M., Makela, J. P., Hallstrom, J., Leinonen, L., & Lounasmaa, O. V. (1987). Neuromagnetic responses of the human auditory cortex to on- and offsets of noise bursts. *Audiology*, 26, 31-43.

Holroyd, T., Endo, H., Kelso, J. A. S., & Takeda, T. (1999). Dynamics of the MEG recorded during rhythmic index-finger extension and flexion. In T. Yoshimoto, M.

- Kotani, S. Kuriki, N. Nakasato, & H. Karibe (Eds.), *Recent advances in biomagnetism: Proceedings of the 11th international conference on biomagnetism* (pp. 446-449). Sendai: Tohoko University Press.
- Hoshiyama, M., Kakigi, R., Berg, P., Koyama, S., Kitamura, Y., Shimojo, M., et al. (1997). Identification of motor and sensory brain activities during unilateral finger movement: spatiotemporal source analysis of movement-associated magnetic fields. *Experimental Brain Research*, 115, 6-14.
- Huottilainen, M., Winkler, I., Alho, K., Escera, C., Virtanen, J., Ilmoniemi, R. J., et al. (1998). Combined mapping of human auditory EEG and MEG responses. *Electroencephalography and Clinical Neurophysiology*, 108, 370-379.
- Ivry, R. B., & Keele, S. W. (1989) Timing functions of the cerebellum. *Journal of Cognitive Neuroscience*, 1, 136-152.
- Jäncke, L., Loose, R., Lutz, K., Specht, K., & Shah, N. J. (2000). Cortical activation during paced finger-tapping applying visual and auditory pacing stimuli. *Cognitive Brain Research*, 10, 51-66.
- Jantzen, K. J., Fuchs, A., Mayville, J. M., Deecke, L., & Kelso, J. A. S. (2001). Neuromagnetic activity in alpha and beta bands reflect learning-induced increases in coordinative stability. *Clinical Neurophysiology*, 112, 1685-1697.
- Jantzen, K. J., Steinberg, F. L., & Kelso, J. A. S. (2002). Neural mechanisms of timing depend on situational context [Abstract]. *Society for Neuroscience Abstracts*, #459.6.
- Jirsa, V. K., Friedrich, R., Haken, H., & Kelso, J. A. S. (1994). A theoretical model of phase transitions in the human brain. *Biological Cybernetics*, 71, 27-35.

- Jirsa, V. K., Fuchs, A., & Kelso, J. A. S. (1998). Connecting cortical and behavioral dynamics: bimanual coordination. *Neural Computation*, 10, 2019-2045.
- Jirsa, V. K., & Kelso, J. A. S. (2000). Spatiotemporal pattern formation in neural systems with heterogeneous connection topologies. *Physical Review E*, 62, 8462-8465.
- Joliot, M., Ribary, U., & Llinas, R. (1994). Human oscillatory brain activity near 40 Hz coexists with cognitive temporal binding. *Proceedings of the National Academy of Sciences*, 91, 11748-11751.
- Kelso, J. A. S. (1984). Phase transitions and critical behavior in human bimanual coordination. *American Journal of Physiology*, 246, 1000-1004.
- Kelso, J. A. S. (1995). *Dynamic Patterns: The Self-Organization of Brain and Behavior*. MIT Press, Cambridge, MA.
- Kelso, J. A. S., Bressler, S. L., Buchanan, S., DeGuzman, G. C., Ding, M., Fuchs, A., et al. (1991). Cooperative and critical phenomena in the human brain revealed by multiple SQuIDs. In D. Duke, & W. Pritchard (Eds.), *Measuring chaos in the human brain* (pp. 97-112). Teaneck, NJ: World Scientific.
- Kelso, J. A. S., Bressler, S. L., Buchanan, S., DeGuzman, G. C., Ding, M., Fuchs, A., et al. (1992). A phase transition in human brain and behavior. *Physics Letters A*, 169, 134-144.
- Kelso, J. A. S., DelColle, J. D., & Schöner, G. (1990). Action-perception as a pattern formation process. In M. Jeannerod (Ed.), *Attention and performance XIII*, (pp. 139-169). Hillsdale, NJ: Erlbaum.
- Kelso, J. A. S., Fuchs, A., Lancaster, R., Holroyd, T., Cheyne, D., & Weinberg, H. (1998). Dynamic cortical activity in the human brain reveals motor equivalence.

Nature, 392, 814-818.

Kopp, B., Kunkel, A., Müller, G., Mühlnickel, W., & Flor, H. (2000). Steady-state movement-related potentials evoked by fast repetitive movements. *Brain Topography*, 13, 21-28.

Kornhuber, H. H., & Deecke, L. (1965). Hirnpotentialänderungen bei willkurbewegungen und passiven bewegungen des menschen: Bereitschaftspotential und reafferente potentiale. *Pflügers Archiv*, 284, 1-17.

Kristeva, R., Cheyne, D., & Deecke, L. (1991). Neuromagnetic fields accompanying unilateral and bilateral voluntary movements: Topography and analysis of cortical sources. *Electroencephalography and Clinical Neurophysiology*, 81, 284-298.

Kristeva-Fiege, R., Rossi, S., Pizzella, V., Sabato, A., Tecchio, F., Fiege, B., et al. (1996). Changes in movement-related brain activity during transient deafferentation: A neuromagnetic study. *Brain Research*, 714, 201-208.

Lang, W., Cheyne, D., Kristeva, R., Beisteiner, R., Lindinger, G., & Deecke, L. (1991). Three-dimensional localization of SMA activity preceding voluntary movement. *Experimental Brain Research*, 87, 688-695.

Large, E. W., Fink, P., & Kelso, J. A. S. (2002). Tracking simple and complex sequences. *Psychological Research*, 66, 3-17.

Large, E. W., & Jones, M. R. (1999). The dynamics of attending: how people track time-varying events. *Psychological Review*, 106, 119-159.

Lashley, K. (1951). The problem of serial order in behavior. In L. A. Jeffress (Ed.), *Cerebral mechanisms in behavior* (pp. 123-147). New York: Wiley.

- Lee, T., Girolami, M., & Sejnowski, T. J. (1999). Independent components analysis using an extended infomax algorithm for mixed subgaussian and supergaussian sources. *Neural Computation, 11*, 417-441.
- Lee, K., Williams, L. M., Breakspear, M., & Gordon, E. (2003). Synchronous gamma activity: a review and contribution to an integrative neuroscience model of schizophrenia. *Brain Research Reviews, 41*, 57-78.
- Loveless, N., Levänen, S., Jousmäki, V., Sams, M., & Hari, R. (1996). Temporal integration in auditory sensory memory: Neuromagnetic evidence. *Electroencephalography and Clinical Neurophysiology, 100*, 220-228.
- Lü, Z. L., Williamson, S. J., & Kaufman, L. (1992). Human auditory primary and association cortex have differing lifetimes for activation traces. *Brain Research, 572*, 236-241.
- Makeig, S., & Jung, T. P. (1996). Tonic, phasic, and transient EEG correlates of auditory awareness in drowsiness. *Cognitive Brain Research, 4*, 15-25.
- Makeig, S., Westerfield, M., Jung, T. P., Enghoff, S., Townsend, J., Courchesne, E., et al. (2002). Dynamic brain sources of visual evoked responses. *Science, 295*, 690-694.
- Mäkelä, J. P., Ahonen, A., Hämäläinen, M., Hari, R., Ilmoniemi, M., Kajola, M., et al. (1993). Functional differences between auditory cortices of the two hemispheres revealed by whole-head neuromagnetic recordings. *Human Brain Mapping, 1*, 48-56.
- Mäkelä, J. P., Hämäläinen, M., Hari, R., & McEvoy, L. (1994). Whole-head mapping of middle-latency auditory evoked magnetic fields. *Electroencephalography and*

- Clinical Neurophysiology*, 92, 414-421.
- Martin, J. D. (1972). Rhythmic (hierarchical) versus serial structure in speech and other behaviors. *Psychological Review*, 79, 487-509.
- Mayville, J. M., Bressler, S. L., Fuchs, A., & Kelso, J. A. S., (1999). Spatiotemporal reorganization of electrical activity in the human brain associated with a timing transition in rhythmic auditory-motor coordination. *Experimental Brain Research*, 127, 371-381.
- Mayville, J. M., Fuchs, A., Ding, M., Cheyne, D., Deecke, L., & Kelso, J. A. S. (2001). Event-related changes in neuromagnetic activity associated with syncopation and synchronization timing tasks. *Human Brain Mapping*, 14, 65-80.
- Mayville, J. M., Fuchs, A., & Kelso, J. A. S. (submitted). Neuromagnetic motor fields accompanying self-paced rhythmic finger movement of different rates.
- Mayville, J. M., Jantzen, K. J., Fuchs, A., Steinberg, F. L., & Kelso, J. A. S. (2002). Cortical and subcortical networks underlying syncopated and synchronized coordination revealed using fMRI. *Human Brain Mapping*, 17, 214-229.
- McCarthy, G., & Donchin, E. (1981). A metric for thought: a comparison of P300 latency and reaction time. *Science*, 211, 77-80.
- Näätänen, R., & Picton, T. W. (1987). The N1 wave of the human electric and magnetic response to sound: A review and an analysis of the component structure. *Psychophysiology*, 24, 375-425.
- Näätänen, R., & Winkler, I. (1999). The concept of auditory stimulus representation in cognitive science. *Psychological Bulletin*, 125, 826-859.
- Nair, D. G., Purcott, K. L., Fuchs, A., Steinberg, F. L., & Kelso, J. A. S. (2003). Cortical

- and cerebellar activity of the human brain during imagined and executed unimanual and bimanual action sequences: a functional MRI study. *Cognitive Brain Research*, 15, 250-260.
- Nunez, P. L. (1981) *Electric Fields of the Brain: The Neurophysics of EEG*. University Press, New York, NY.
- Pantev, C., Bertrand, O., Eulitz, C., Verkindt, C., Hampson, S., Schuirer, G., et al. (1995). Specific tonotopic organizations of different areas of the human auditory cortex revealed by simultaneous magnetic and electric recordings. *Electroencephalography and Clinical Neurophysiology*, 94, 26-40.
- Pantev, C., Eulitz, C., Hampson, S., Ross, B., & Roberts, L. E. (1996). The auditory evoked "off" response: sources and comparison with the "on" and the "sustained" responses. *Ear and Hearing*, 17, 255-65.
- Pantev, C., Makeig, S., Hoke, M., Galambos, R., Hampson, S., & Gallen, C. (1991). Human auditory evoked gamma-band magnetic fields. *Proceedings of the National Academy of Sciences*, 88, 8996-9000.
- Pantev, C., Roberts, L. E., Elbert, T., Roß, B., & Wienbruch, C. (1996). Tonotopic organization of the sources of human auditory steady-state responses. *Hearing Research*, 101, 62-74.
- Picton, T. W., Champagne, S. C., & Kellett, A. J. C. (1992). Human auditory evoked potentials recorded using maximum length sequences. *Electroencephalography and Clinical Neurophysiology*, 84, 90-100.
- Picton, T. W., Hillyard, S. A., Krausz, H. I., & Galambos, R. (1974). Human auditory evoked potentials. I: Evaluation of components. *Electroencephalography and*

- Clinical Neurophysiology*, 36, 179-190.
- Picton, T. W., Skinner, C. R., Champagne, S. C., Kellett, A. J. C., & Maiste, A. C. (1987). Potentials evoked by the sinusoidal modulation of the amplitude or frequency of a tone. *Journal of the Acoustical Society of America*, 82, 165-178.
- Polich, J., & Kok, A. (1995). Cognitive and biological determinants of P300: an integrative review. *Biological Psychology*, 41, 103-146.
- Povel, J. D., & Essens P. J. (1985). Perception of temporal patterns. *Music Perception*, 2, 411-440.
- Praamstra, P., Stegman, D. F., Horstink, M. W. I. M., Brunia, H. M., & Cools, A. R. (1995). Movement-related potentials preceding voluntary movement are modulated by the mode of movement selection. *Experimental Brain Research*, 103, 429-439.
- Praamstra, P., Stegman, D. F., Horstink, M. W. I. M., & Cools, A. R. (1996). Dipole source analysis suggests selective modulation of the supplementary motor areas contribution to the readiness potential. *Electroencephalography and Clinical Neurophysiology*, 98, 468-477.
- Rao, S. M., Harrington, D. L., Haaland, K. Y., Bobholz, J. A., Cox, R. W., & Binder, J. R. (1997). Distributed neural systems underlying the timing of movements. *Journal of Neuroscience*, 14, 5528-5535.
- Regan, D. (1982) Comparison of transient and steady-state methods. *Annals of the New York Academy of Sciences*, 388, 5-71.
- Regan, D. (1989). *Human brain electrophysiology: Evoked potentials and evoked magnetic fields in science and medicine*. New York: Elsevier.

- Repp, B. H. (2001). Processes underlying adaptation to tempo changes in sensorimotor synchronization. *Human Movement Science, 20*, 277-312.
- Roß, B., Picton, T. W., & Pantev, C. (2002). Temporal integration in the human auditory cortex as represented by the development of the steady-state magnetic field. *Hearing Research, 165*, 68-84.
- Sadato, N., Ibanez, V., Deiber, M. P., Campbell, G., Leonardo, M., & Hallett, M. (1996). Frequency-dependent changes of regional cerebral blood flow during finger movements. *Journal of Cerebral Blood Flow Metabolism, 16*, 23-33.
- Sams, M., Hari, R., Rif, J., & Knuutila, J. (1993). The human auditory sensory memory trace persists about 10 sec: Neuromagnetic evidence. *Journal of Cognitive Neuroscience, 5*, 363-370.
- Santarelli, R., Maurizi, M., Conti, G., Ottaviani, F., Paludetti, G., & Pettorossi, V. E. (1995). Generation of human auditory steady-state responses (SSRs). II: Addition of responses to individual stimuli. *Hearing Research, 83*, 9-18.
- Sauvé, K. (1999). Gamma-band synchronous oscillations: recent evidence regarding their functional significance. *Consciousness and Cognition, 8*, 213-224.
- Schubotz, R. I., Friederici, A. D., & Yves von Cramon, D. (2000). Time perception and motor timing: A cortical and subcortical basis revealed by fMRI. *Neuroimage, 11*, 1-12.
- Shibasaki, H., Barrett, G., Halliday, E., & Halliday, A. M. (1980). Components of the movement-related cortical potential and their scalp topography. *Electroencephalography and Clinical Neurophysiology, 49*, 213-226.
- Snyder, J. S., & Large, E. W. (submitted). Finding the beat: a neural correlate of rhythm

expectancy in the gamma band.

Stapells, D. R., Linden, D., Suffield, J. B., Hamel, G., & Picton, T. W. (1984). Human auditory steady-state potentials. *Ear and Hearing*, 5, 105-113.

Sukov, W., & Barth, D. S. (1998). Three-dimensional analysis of spontaneous and thalamically evoked gamma oscillations in auditory cortex. *Journal of Neurophysiology*, 79, 2875-2884.

Sukov, W., & Barth, D. S. (2001). Cellular mechanisms of thalamically evoked gamma oscillations in auditory cortex. *Journal of Neurophysiology*, 85, 1235-1245.

Talon-Baudry, C., Bertrand, O., Delpuech, C., & Pernier, J. (1996). Stimulus specificity of phase-locked 40 Hz visual responses in humans. *The Journal of Neuroscience*, 16, 4240-4249.

Tesche, C. D., & Karhu, J. (2000). Theta oscillations index human hippocampal activation during a working memory task. *Proceedings of the National Academy of Sciences*, 97, 919-924.

Tiitinen, H., Sinkkonen, J., Reinikainen, K., Alho, K., Lavikainen, J., & Näätänen, R. (1993). Selective attention enhances the auditory 40-Hz transient response in humans. *Nature*, 364, 59-60.

Tuller, B., Case, P., Ding, M., & Kelso, J. A. S. (1994). The nonlinear dynamics of speech categorization. *Journal of Experimental Psychology: Human Perception and Performance*, 20, 3-16.

Virtanen, J., Ahveninen, J., Ilmoniemi, R. J., Näätänen, R., & Pekkonen, E. (1998). Replicability of MEG and EEG measures of the auditory N1/N1m-response. *Electroencephalography and Clinical Neurophysiology*, 108, 291-298.

- Vorberg, D. & Wing, A. M. (1996). Modeling variability and dependence in timing. In H. Heuer & S. W. Keele (Eds.), *Handbook of Perception and Action* (pp. 181-262). New York: Academic Press.
- Vrba, J., Cheung, T., Taylor, B., & Robinson, S. E. (1999). Synthetic higher-order gradiometers reduce environmental noise, not the measured brain signals. In T. Yoshimoto, M. Kotani, S. Kuriki, H. Karibe, & N. Nakasato (Eds.), *Recent advances in biomagnetism* (pp. 105-108). Sendai: Tohoku University Press.
- Wallenstein, G. V., Kelso, J. A. S., & Bressler, S. L. (1995). Phase transitions in spatiotemporal patterns of brain activity and behavior. *Physica D*, 20, 626-634.
- Wing, A. M. (1977). Effects of type of movement on temporal precision of response sequences. *British Journal of Mathematical and Statistical Psychology*, 30, 60-72.
- Wing, A. M. & Kristofferson, A. B. (1973). The timing of inter-response intervals. *Perception and Psychophysics*, 13, 455-460.
- Woods, D.L. (1995). The component structure of the human auditory evoked potential. *Electroencephalography and Clinical Neurophysiology, supplement 44*, 102-109.
- Yoshiura, T., Ueno, S., Iramina, K., & Masuda, K. (1996). Human middle latency auditory evoked magnetic fields. *Brain Topography*, 8, 291-296.

Curriculum Vitae

Frederick W. Carver

Date of Birth: 9/9/70
Citizenship: USA
Current Address: MEG Core Facility
National Institute of Mental Health
Bldg. 10, Rm. 4S 235
9000 Rockville Pike
Bethesda, MD 20892-1059
Phone: (301) 402-2378
FAX: (301) 480-7795
E-mail: carverf@intr.nimh.nih.gov

Research Interests

Sensorimotor coordination, Self-organization of brain and behavior, Perception-action coupling in rhythmic movements and music, Development of spatiotemporal analysis techniques for EEG and MEG.

Education

1997-2003: Ph.D. candidate, Center for Complex Systems and Brain Sciences
Florida Atlantic University (Boca Raton, FL)
Co-advisors: Dr. Armin Fuchs & Dr. J. A. Scott Kelso

1988-1992: B.S., Bates College (Lewiston, ME)
Mathematics major, Computer Science minor

Honors and Awards: Barry M. Goldwater Scholarship for research, 1990-1992
Magna Cum Laude
Phi Beta Kappa
Sigma Xi
Institutional NRSA training grant, 1998-2001
Newell Doctoral Fellowship, 2000-2002

Work Experience

- 2003-Present: Postdoctoral Researcher, MEG Core Facility
National Institute of Mental Health (Bethesda, MD)
- 1994-1997: Mathematics Teacher, 7-12th grades
Porter-Gaud School (Charleston, SC)
- 1992-1993: Research Assistant, U.S. Army Corps of Engineers
Cold Regions Research & Engineering Laboratory (Hanover, NH)

Publications

Articles:

- Carver, F.W., Fuchs, A., Jantzen, K.J., & Kelso, J.A.S. (2002). Spatiotemporal Analysis of Neuromagnetic Activity Associated with Rhythmic Auditory Stimulation. *Clinical Neurophysiology*, 113, 1921-1931.

Abstracts:

- Carver, F.W., Fuchs, A., & Kelso, J.A.S. Neuroelectric and Neuromagnetic Brain Activity Underlying Rhythmic Movements: Separation of Responses using Independent Components Analysis and Projection onto the Cortical Surface. *Society for Neuroscience Abstracts* 2002, #459.5
- Carver, F.W., Fuchs, A., & Kelso, J.A.S. Neuroelectric and Neuromagnetic Activity of Evoked Responses to Rhythmic Movements: Response Separation using Independent Components Analysis. *Coordination Dynamics*, Delray Beach, FL, May 2002.
- Carver, F.W., Fuchs, A., Jirsa, V.K., & Kelso, J.A.S. Neuromagnetic Activity of Evoked Responses to Rhythmic Auditory Stimulation: Amplitude Dependence and Interference. *Society for Neuroscience Abstracts* 2001, #512.19
- Carver, F.W., Fuchs, A., Jantzen, K.J., & Kelso, J.A.S. Neuromagnetic Activity of Evoked Responses to Rhythmic Auditory Stimulation as revealed by MEG: Amplitude Dependence on Rate and Pattern Interference. *Helsinki Summer School in Cognitive Neuroscience*, Helsinki, Finland, September 2001.
- Carver, F.W., Fuchs, A., Mayville, J.M., Davis, S.W., & Kelso, J.A.S. Systematic Investigation of the Human Brain's Response to Rhythmic Auditory Stimulation. *Dynamical Neuroscience VII: Integration across Multiple Imaging Modalities*, Delray Beach, FL, October 1999.
- Brown, L.E., Carver, F.W., & Kelso, J.A.S. How Learning may overcome Intrinsic Biophysical Differences among Individual Effectors in a Coordination Task. *Medicine and Science in Sports and Exercise* 31(5S):S206, 1999.